



Thesis for the degree
Doctor of Philosophy

עבודת גמר (תזה) לתואר
דוקטור לפילוסופיה

Submitted to the Scientific Council of the
Weizmann Institute of Science
Rehovot, Israel

מוגשת למועצה המדעית של
מכון ויצמן למדע
רחובות, ישראל

By
Ehud Zigmond

מאת
אהוד זיגמונד

תפקיד התאים החד גרעיניים של הלמינה פרופריה המבטאים
CX₃CR1 בבקרה על הומאוסטזיס ובמצבי דלקת במערכת העיכול
The role of CX₃CR1^{pos} lamina propria mononuclear phagocytes in
homeostasis and in gastrointestinal inflammatory conditions

Advisor:
Prof. Steffen Jung

מנחה:
פרופ' סטפן יונג

september 2013

תשרי תשע"ד

TABLE OF CONTENTS

List of abbreviations -----	3
Abstract -----	4
Introduction -----	5 - 12
Study hypothesis and research goals -----	12 - 13
Methods -----	14 - 20
Results	
• Chapter 1 - Ly6C ^{hi} monocytes in the inflamed colon give rise to proinflammatory effector cells and migratory antigen-presenting cells -----	21 - 39
• Chapter 2 - Macrophage restricted IL-10 receptor -, but not IL-10 deficiency causes severe spontaneous colitis -----	40 - 51
• Chapter 3 - Utilization of Murine Colonoscopy for Orthotopic Implantation of Colorectal Cancer --	52 - 56
Discussion -----	57 - 64
Literature -----	65 - 77
List of Publications during PhD studies -----	78
Student Declaration -----	79
Acknowledgements -----	80

ABBREVIATIONS

AOM – Azoxymethane, BATF3 - Basic leucine zipper transcription factor 3,
BM – Bone Marrow, CCL5 - Chemokine (C-C motif) Ligand 5,
CCR7 - C-C chemokine receptor type 7, CD – Crohn’s Disease, cDC – classical
Dendritic Cells, CDP – Common Dendritic cells Precursor,
cMoP - Common Monocyte Progenitor, CRC – Colo-Rectal Cancer,
DC – Dendritic cells, DSS – Dextran Sodium Sulphate,
DTR – Diphtheria Toxin Receptor, DTx - Diphtheria Toxin, GALT - Gut Associated
Lymphoid Tissue, GFP - Green Fluorescent Protein, GM-CSF - Granulocyte
Macrophage Colony-Stimulating Factor, IBD – Inflammatory Bowel Diseases,
ID2 - Inhibitor of DNA-binding protein 2, IFN – Interferon, IL – Interleukin,
IL10R – Interleukin-10 Receptor, iNOS – inducible Nitric Oxide Synthase,
IRF8 - Interferon Regulatory Factor 8, LN – Lymph node, LP – Lamina propria,
LPS – Lipopolysaccharide, M-CSF - Macrophage Colony-Stimulating Factor,
MDP - Macrophage and DC Precursor, MF – Macrophages, MHC - Major
Histocompatibility Complex, MLN – Mesenteric Lymph Node,
MP – Mononuclear Phagocytes, NOD - Nucleotide-binding Oligomerization Domain-
containing protein, PGE₂ - Prostaglandin E2, RFP – Red Fluorescent Protein, SAA3 -
Serum amyloid A3, TAMs – Tumor Associated Macrophages,
TCR – T cell Receptor, TH – T Helper cell, TLR – Toll-Like Receptor,
TNF – Tumor Necrosis Factor, TREM - Triggering Receptor Expressed on Myeloid
cells, UC – Ulcerative colitis, VEGF - Vascular Endothelial Growth Factor, Zbtb46 -
Zinc finger and BTB domain containing 46

ABSTRACT

Inflammatory Bowel Diseases are complex disorders that arise as a result of the interaction of environmental and genetic factors. Recent studies highlighted the role of the mononuclear phagocytes system in intestinal homeostasis as well as in inflammatory conditions. Using an acute innate model of colitis, we demonstrated that infiltrating Ly6C^{hi} monocytes acquire in the inflamed colonic lamina propria two functionally distinct fates. Rather than giving rise - as in the healthy colon - to resident CX₃CR1^{hi} MFs, the monocyte infiltrate initially differentiates into CX₃CR1^{int}Ly6C^{hi} effector cells that sense bacterial products via TLR/NOD2 receptors and critically promote inflammation through the production of pro-inflammatory mediators, such as IL6, IL23, VEGFa and iNOS. With time the monocyte infiltrate gives rise to a phenotypically and functionally distinct CX₃CR1^{int}Ly6C^{lo} population displaying migratory DC hallmarks including the uptake and processing of orally acquired antigens and priming of naive CD4⁺ T cells, as well as CCR7 expression that endows it with the capacity to emigrate from the colonic lamina propria towards the tissue-draining lymph nodes. To investigate the physiological importance of macrophage-derived IL10, the consequence of IL10 exposure of macrophages, as well as the possible existence of an IL10-based autocrine loop, we generated mice that harbor macrophage-restricted IL10 or IL10R1 mutations. Strikingly, CX₃CR1^{Cre}IL10R^{fl/fl} mice, but not CX₃CR1^{Cre}IL10^{fl/fl} mice, whose macrophages are impaired in IL10 production, developed severe spontaneous gut inflammation. These data highlight the central role IL10 plays in the continuous and active silencing of macrophages to maintain gut homeostasis. We established intestinal macrophages as critical component for the maintenance of gut homeostasis. Specifically, these cells have to be exposed to IL10, most likely produced by T cells to maintain a characteristic non-inflammatory gene expression profile.

Together, the two studies mentioned above shed new light on the fate and function of monocyte-derived cells in intestinal inflammation. Thus, our findings contribute to the overall understanding of gut physiology and IBD pathogenesis. As such our findings might assist the development of novel IBD therapies.

Finally, we established a new murine Colo-Rectal Cancer model that provides significant advantages over existing models. Our approach is minimally invasive, highly repetitive and enables absolute control of tumor number and growth rate. This model allows studying tumor interactions with the native environment, yet avoids collateral damage and inflammation seen in many other models. Importantly, this model makes it possible to compare several distinct tumors side by side in the same organism avoiding the variability between animals and microbiota context and significantly reducing animal numbers needed to gain significant results.

INTRODUCTION

The intestinal landscape and its challenge

The intestinal tract is the largest surface of the human body, covering an area of approximately 100 m², lined by a single layer of columnar epithelial cells, which forms the barrier between the gut lumen and the host connective tissue. In addition to its constant exposure to dietary and environmental antigens, the intestine harbors an estimated 10¹⁴ commensal bacteria, comprising around 1000 different species (Savage 1977). The unique architecture and the highly dynamic and occasionally hostile environment in the gut creates special challenge for the intestinal immune system. A critical feature of the gut landscape is ongoing tissue renewal, with the single epithelial cell layer being replaced every five days from crypt-resident stem cells (Van der flier et al., 2009) and an equally dynamic immune cell composition (Hapfelmeier et al., 2010, Lathrop et al., 2012). Coevolution of the host immune system and the microbiome with symbiotic interactions has generated a mutually beneficial environment for both sides. Yet, this scenario poses a unique challenge, as the organism has to tolerate the foreign symbionts and constant exposure to their products. Moreover, rather, than remaining unresponsive, the host actively controls the microbiota composition by secretion of anti-microbial peptides and immunoglobulins (Bevins and Salzman, 2011; Peterson et al., 2007). Conversely, defined intestinal commensals, such as *Clostridiae*, have recently been shown to critically shape the gut associated immune system, e.g. the prevalence of distinct helper and regulatory T cell populations (Atarashi et al., 2011; Ivanov et al., 2009). While actively engaging the commensal microbial challenge, the organism has to remain sensitive to deviations from this "primed homeostasis" and rapidly respond to invading entero-pathogens or injuries causing epithelial damage. Failure to maintain this exquisite balance and hyper-responsiveness in genetically predisposed individuals is likely associated with the development of chronic inflammatory bowel disorders (IBD), such as Crohn's disease and Ulcerative colitis (Cho, 2008).

One of the major arms of the innate immune system in the gut is the intestinal mononuclear phagocytes (MPs), comprising of macrophages (MFs), dendritic cells (DCs) and monocytes. These cells are strategically positioned in the intestine, residing in the gut associated lymphoid tissue (GALT) and are also dispersed throughout the

sub-epithelial lamina propria. Recent findings have indicated that intestinal MPs are crucial for maintaining intestinal homeostasis.

Intestinal mononuclear phagocytes

Tissue resident dendritic cells (DCs) and macrophages (MFs) are key players in the control of innate and adaptive immune reactions. Historically categorized by their anatomic locations and surface marker profiles, DC and MF definitions have more recently been extended to include differential growth and transcription factors requirements, subset-specific gene expression signatures and distinct ontogenies (Hashimoto et al., 2011). Moreover, emerging evidence for unique contributions of DCs and MFs to the initiation and control of intestinal innate and adaptive immune responses has lend support to the notion of distinct functional entities (Varol et al., 2010).

Several pioneering studies have elucidated DC lineage commitment in the bone marrow (BM). Lymphoid organ-resident classical DC (cDC), plasmacytoid DC, and monocytes are now known to share a common progenitor called the macrophage and DC precursor (MDP) identified in the BM as lineage^{neg} CD117^{hi} CX3CR1^{pos} CD115^{pos} cells (Fogg et al., 2006). In the BM MDPs give rise to a CD117^{lo} CD115^{pos} CD135^{pos} common DC precursor (CDP) that differentiates into plasmacytoid DC and pre-cDC, a cDC-restricted progenitor that has lost plasmacytoid DC differentiation potential. Pre-cDC circulate through the blood to localize to lymphoid organs such as the spleen and LNs where they give rise to cDC (Liu et al., 2009). Intestinal CX₃CR1^{hi} macrophage were shown by our lab and others to be generated from directly from monocytes (Varol et al., 2009, Bogunovic et al., 2009). Recently a clonogenic, monocyte- and macrophage-restricted progenitor cell derived from the MDP was identified in the bone marrow and the spleen. This common monocyte progenitor (cMoP) can be identified as CD117^{pos}CD115^{pos}CD135^{neg}Ly6C^{pos}CD11b^{neg} (Hettinger et al., 2013) (Scheme 1).

Monocytes: These plastic cells are continuously generated in the bone marrow (BM) from dedicated MF/DC precursors (MDPs) via an cMoP intermediate and released to the circulation (Varol et al., 2007; Hettinger et al., 2013). Discrete expression levels of CX₃CR1/GFP in CX₃CR1^{gfp} animals led to the identification of two monocyte subsets in mice as CX₃CR1^{int} Ly6C^{hi} and CX₃CR1^{hi} Ly6C^{lo} cells (Palframan et al.,

2001; Geissmann et al., 2003;). CX₃CR1^{hi} Ly6C^{lo} “patrolling” monocytes – the correlate of human CD14^{dim} CD16⁺ cells (Cros et al., 2010) - have been shown to adhere and crawl along the luminal vessel surfaces of endothelial cells (Auffray et al., 2007). CX₃CR1^{int} Ly6C^{hi} monocytes, the correlate of human CD14⁺ CD16⁺ and CD14⁺ CD16⁻ monocytes (Cros et al., 2010), are poised to traffic to sites of infection and inflammation (Geissmann et al., 2003; Serbina and Pamer, 2006). CX₃CR1^{int} Ly6C^{hi} monocytes have a short circulation half-life (Liu et al., 2009) and tend to differentiate in steady state by default into CX₃CR1^{hi} Ly6C^{lo} cells (Varol et al., 2007). In contrast under inflammation, CX₃CR1^{int} Ly6C^{hi} monocytes are by virtue of their expression of the chemokine receptor CCR2 efficiently recruited to the sites of insult where they can transiently complement resident MF populations (Ajami et al., 2011). Notably, the intestinal MF compartment is unique in that it continuously recruits monocytes in homeostasis for its replenishment - most likely due to tonic low-grade inflammation caused the microbiota exposure of this tissue. In addition to the MF fate, Ly6C^{hi} monocytes have been shown to give rise to a distinct population of TNF/iNOS-producing inflammatory monocyte-derived DC, as well as cells that share other functional features of classical DC, although functional contributions of these cells remain less well defined (Cheong et al., 2010; Serbina et al., 2003).

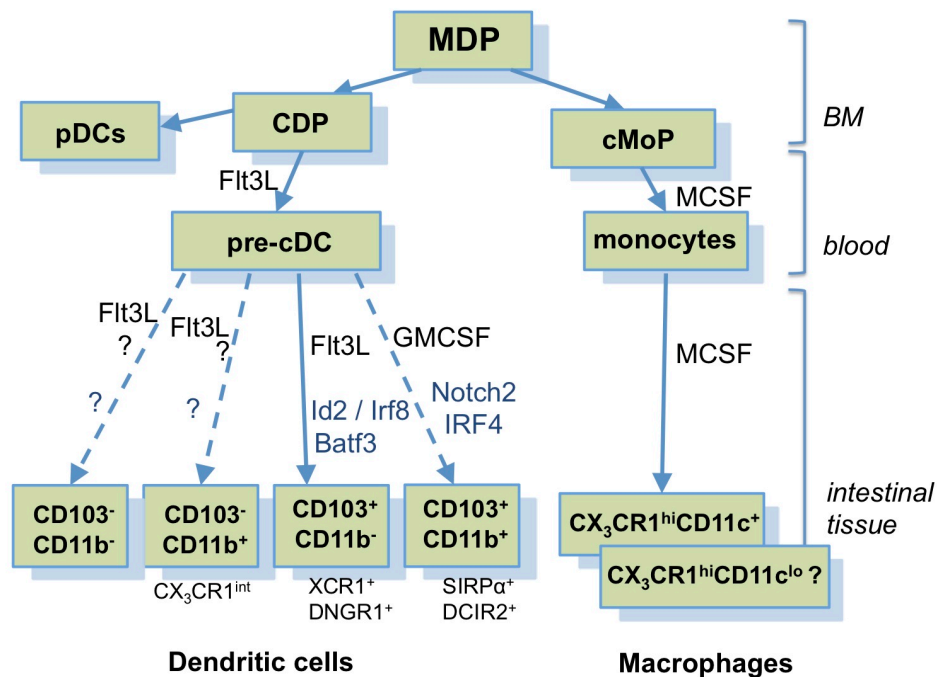
Gut Dendritic cells: The intestinal steady state mononuclear phagocyte compartment comprises at least four types of DC. CD103^{pos}CD11b^{neg}, CD103^{pos}CD11b^{pos}, CD103^{neg}CD11b^{pos} and CD103^{neg}CD11b^{neg} DC. CD103^{pos}CD11b^{neg} DC are generated without a monocytic intermediate from pre-cDC, driven by the growth factor Flt3L. Some evidence suggests that other DC are generated from pre-cDC as well, however further research is required to resolve this issue (Persson et al., 2013). CD103^{pos}CD11b^{pos} cells development further requires GM-CSF, whereas CD103^{pos}CD11b^{neg} cells develop independently of this growth factor (Bogunovic et al., 2009). Interestingly, the generation of CD11b^{neg}CD103^{pos} cells is uniquely affected by deficiencies in the transcription factors ID2, IRF8 and BATF3 (Bogunovic et al. 2009, Edelson et al., 2010). CD103^{pos} CD11b^{pos} DC populate especially the small bowel lamina propria where as sentinels they can capture antigen and migrate in a CCR7-dependent manner to the draining lymph nodes (LNs) to prime T cell responses. Moreover, CD103^{pos} DC can promote the generation of inducible regulatory T cell and the expression of the gut

homing receptors CCR9 and $\alpha 4\beta 7$ integrin by producing retinoic acid and transforming growth factor- β (Jaensson et al., 2008; Johansson-Lindbom et al., 2005; Sun et al., 2007; Worbs et al., 2006). It was recently demonstrated that CD103^{pos} CD11b^{pos} DCs are recruited from the lamina propria to the intraepithelial region in a toll-like receptor dependent manner; there they can efficiently phagocytosed luminal bacteria using intraepithelial dendrites (Farache et al., 2013). All four types of DCs express the chemokine receptor CCR7, possess migratory capacity and indeed can be identified in lymph. (Cerovic et al., 2013). CD103^{neg}CD11b^{neg} DCs were found to be reduced in the lymph and LP of ROR γ t^{-/-} mice indicating that the majority of these DCs may derive from organized intestinal lymphoid tissues, and not from the LP. Interestingly, CD103^{neg}CD11b^{pos} DCs were shown to have better capacity to induce differentiation of IFN γ and IL-17-producing T cells (Cerovic et al., 2013).

Gut macrophages: In addition to the short-lived DC, the lamina propria harbors a major population of resident MF, which are marked by prominent surface expression of F4/80 (EMR1) and the CX₃CR1 chemokine receptor. CX₃CR1^{hi} MF represent the most abundant mononuclear phagocytes in the steady state lamina propria of the intestine and constitute in fact the largest reservoir of macrophages of the body (Lee et al., 1985). Recent studies showed that most tissue macrophages are established pre-birth and subsequently maintain themselves through longevity and limited self-renewal (Ginhoux et al., 2010, Schulz et al., 2012, Yona et al., 2013). In contrast, intestinal lamina propria macrophages rely on the constant recruitment of blood monocytes in a M-CSF dependent pathway, potentially attracted by the tonic low-grade inflammatory stimulus present in the gut (Bogunovic et al., 2009; Varol et al., 2009). Shortly after arrival, these monocytes acquire in the gut, likely under the influence of the microbiota-exposed epithelium, a distinct non-inflammatory gene expression profile (Rivollier et al., 2012). CX₃CR1^{hi} MF are considered to critically contribute to the maintenance or local expansion of T effector or regulatory cells in the lamina propria (Hadis et al., 2011). They have been shown to gain access to the gut lumen by virtue of trans-epithelial dendrites (Niess et al., 2005; Rescigno et al., 2001) and are believed to contribute to gut homeostasis by production of IL10 (Denning et al., 2007; Hadis et al., 2011). CX₃CR1^{hi} MF can be divided into CD11c⁺ and CD11c^{lo} subsets, although the functional significance of these populations

remains unclear. These two subsets express largely similar baseline gene expression (Rivollier et al., 2012) and could represent different levels of activation and/or maturity of the same cells.

Scheme 1



Scheme 1. Schematic representation of developmental origin, as well as growth and transcription factor requirements of intestinal lamina propria dendritic cells and macrophages

A common precursor, the macrophage and dendritic-cell precursor (MDP), gives rise to common DC precursor (CDP) that differentiates into plasmacytoid DCs and pre-cDC and common monocyte progenitor (cMoP) that gives rise to monocytes. pre-cDC and monocytes exit the bone marrow, enter the blood circulation and home to the gut. Locally, pre-cDC give rise to CD103^{pos}CD11b^{neg} lamina propria DC and potentially additional DC populations. Ly6C^{hi} monocytes differentiate locally into CX3CR1^{hi} lamina propria macrophages comprising several yet to be defined subsets. Generation of these cells depends on the presence of M-CSF.

Interleukin-10 signaling in the intestine: Interleukin-10 (IL-10) was first identified as a factor produced by Th2 cells that inhibited cytokine production by Th1 cells (Fiorentino et al., 1989). In both mouse and human systems, IL-10 is produced by many cell types, including T cell subsets, B cells, mast cells, eosinophils, macrophages, and DCs, as well as by non-hematopoietic cells (O'Garra et al., 1990; Thompson-Snipes et al., 1991; Boonstra et al., 2006; Maloy et al., 2003). The main role for IL-10 appears to be as an immunosuppressive cytokine with broad anti-

inflammatory properties, in particular by its inhibition of macrophage and DC functions. This includes the production of pro-inflammatory cytokines, expression of co-stimulators, MHC class II molecules and general APC functions (Moore et al., 2001). IL-10 is a potent suppressor of macrophage activation in vitro. It inhibits the production of inflammatory cytokines such as IL-1, IL-6, and TNF. Moreover, it also suppresses the ability of macrophages to stimulate the production of IFN γ and other cytokines by Th1 cells (Moore et al., 2001).

The first convincing evidence for an implication of IL-10 in intestinal immune regulation came from IL-10 null mice, which spontaneously develop entero-colitis (Kuhn et al., 1993). A pro-inflammatory role for mononuclear phagocytes in this model is suggested by the finding that depletion of intestinal mononuclear phagocytes by rectal administration of cytotoxic microspheres prevents colitis in IL-10- deficient mice (Watanabe et al., 2003). However, intestinal mononuclear phagocytes possess also crucial IL-10 mediated immunoregulatory roles, as intestinal CD11c⁺CD11b⁺F4/80⁺ cells (which are probably CX₃CR1^{hi} lamina propria MFs) have been shown to be an important source of IL-10 in the gut (Murai et al., 2009). IL-10 produced by these cells in the intestinal lamina propria and mesenteric lymph nodes maintains FoxP3 expression by T reg's and is sufficient to prevent colitis induced by the adoptive transfer of CD4⁺CD45RB^{hi} T cells (Murai et al., 2009).

The IL-10 receptor (IL-10R) is composed of an IL-10-specific ligand-binding component, known as IL-10R1, and a β -chain, which is essential for signal transduction (IL-10R2). IL-10R2 is shared by at least three other class II cytokine receptors (Moore et al., 2001). IL-10R2 expression can be found on most cell types, while IL-10R1 is constitutively expressed only on hematopoietic cells and is inducible on several non-hematopoietic cells (Moore et al., 2001). Recently, IL-10R1 knock-out mice were generated and have been shown to replicate the phenotype of IL-10 null mice regarding the susceptibility to develop DSS-induced colitis (Pils et al., 2010). Moreover, also mice harboring specific disruption of the Stat3 gene in macrophages and neutrophils develop chronic entero-colitis (Takeda et al. 1999). Taken together, these results suggest an IL-10-based self-regulatory loop in macrophages, as a possible mechanism for the initiation of an overt inflammatory reaction against the microbiota. Importantly, IL-10 / IL-10R signaling have also been shown to be involved in human IBDs. Thus, a large-scale genome-wide association study (GWAS) identified IL-10 as a susceptibility gene for UC (Franke et al., 2008). Moreover, in

another clinical study, loss-of-function mutations in either IL10RA or IL10RB were found in patients with early-onset colitis (Glocker et al., 2009). Allogeneic stem-cell transplantation resulted in disease remission thus establishing that in these cases IL-10 acted primarily on hematopoietic cells (Glocker et al., 2009).

Colo-rectal cancer models: Colo-rectal cancer (CRC) is the second leading cause of cancer mortality in many industrialized countries (Jemal et al., 2006). A variety of available CRC animal models have provided important tools for investigating the complex development and pathogenesis of CRC. These models can be used to gain insights into the etiologic and pathophysiologic mechanisms as well as the treatment of human CRC. A number of spontaneous CRC mouse strains have been developed that replicate human cancer syndrome, such as hereditary nonpolyposis colorectal cancer (HNPCC) (Edelmann et al., 2004), and familial adenomatous polyposis (FAP) (Moser et al., 1990). These mouse models allowed observation of the effects of known genetic alteration. Moreover, they have been proven invaluable in understanding disease course and evaluating new therapies. Of note, many of these mouse models form adenomas primarily in the small intestine, typically with slow growth rate and high variability between individual mice. Another strategy for the induction of CRC in mice is the use of different carcinogenic compounds. Although these tumors share many of the histopathological characteristics of human CRC, the latency period for tumor development is with about 30 weeks very long, and induction of neoplasms in other tissues have been described (Reddy et al., 1981). The combination of carcinogenic compound with chronic inflammation, such as in the case of the AOM/DSS model has proven to shorten the latency time observed in the classical model to about 10 weeks (Neufert et al., 2007). This advantage as well as high potency, simple mode of application, and relative cost efficiency, has made this model very common in CRC research (Neufert et al., 2007). However, it is important to mention that in this model tumors develop under the environmental influences of chronic inflammation, a condition that does not mimic the situation in most human CRC cases. In addition, and similarly to the above-described models, the AOM/DSS system also suffers from its inherent inability to control tumor numbers, location, size, and growth kinetics. Alternatively, heterotopic s.c. implantation of tumor cell lines is widely used as a research tool, especially for the assessment of cytostatic therapeutic compounds. But, heterotopic implantation ignores the complexity of the native

unique environmental characteristics of the colon. It is well established that the incongruent host stroma can affect tumorigenicity and cell cycle regulation compared to implantation in the native tissue bed (White et al., 1982; Fare et al., 2002). Several orthotopic murine CRC models have been described (Alencar et al., 2005; Cespedes et al., 2007), most of which require an operative approach and a surgical incision for injection / implantation of the cancer cells into the colon layers. The surgical trauma and the immune reactions it triggers severely limit the value of this system to study innate and adaptive anti-tumor immune responses. Another important practical limitation of orthotopic transplants is the complexity of the surgical procedure involved.

In humans, endoscopic examination of the colon is the most important method for the discovery and follow-up care of CRC. Recently, *in vivo* murine colonoscopy has been developed (Becker et al., 2006). This endoscopic procedure allows high resolution imaging of the colon in living mice, enabling researchers to directly visualize pathologic tissue changes in the gut. (Becker et al., 2006; Neurath et al., 2010).

Study hypothesis and research goals

In recent years our understanding of the mononuclear phagocyte system of the intestinal tract has progressed dramatically with the identification of different types of cells based on their origin and function. Yet, most of these studies focused on steady state conditions avoiding the complexity accompanying the inflammatory process. Our overall aim was to understand the contribution of the intestinal MPs to the pathogenesis of gut inflammation. More specifically, we wished to define the alteration in MP composition and function under inflammatory conditions and to identify key molecules and pathway associated with the role of MPs in intestinal inflammation. Inflammation is associated with a massive accumulation of inflammatory monocytes in the inflamed lamina propria. Our hypothesis was that in inflammatory settings the differentiation process of monocyte in the lamina propria is distorted, and that monocyte derived cells might contribute to the inflammatory process. Utilizing model of acute intestinal inflammation we focused on differential fates of these cells and the differentiation process they undergo to reveal task division between the inflammatory infiltrate and resident tissue MFs.

Interleukin 10 is a pleiotropic cytokine whose activity aims to limit inflammatory responses. IL-10 knockout mice develop spontaneous colitis resembling human UC. Importantly, large-scale genome wide association studies identified the IL-10 axis to be highly associated with IBD pathogenesis, especially the UC type. IL10 is produced and sensed by most hematopoietic cells, and has been reported also in non-hematopoietic cells, including the colonic epithelium. Recent observations including our preliminary data pointed at lamina propria MFs as an important source of IL10 in the colon. Interestingly, colonic MFs also exhibit high expression level of the IL10 receptor, implying an autocrine mode of action of the cytokine in these cells. Our hypothesis was that IL10 signaling in colonic lamina propria MFs is important for intestinal homeostasis. We wished to explore *in-vivo* effects of IL10 on the phenotype and activity of the gut resident MFs, as well as its importance in IBD pathogenesis. We believed that this approach could reveal new insights about the early events initiate IBD and hence could pave the road for novel therapeutic interventions.

Colorectal-cancer (CRC) is the second leading cause of cancer mortality in many industrialized countries. Small animal CRC models are important tools for investigating the underlying etiologic and pathophysiologic mechanisms of CRC development and for the preclinical assessment of novel therapeutic modalities. However, existing murine CRC models tumor have several limitations including long latency period, slow growth rate, considerable inter-animal variability in tumor numbers and size and lack of invasiveness. Moreover, results can be confounded by side effects of chronic inflammatory environment, a condition that mimics IBD-associated CRC but not the much more common sporadic human CRC. Our goal was to create a minimal invasive, orthotopic murine CRC model by utilizing the murine endoscopic system. We believe that this approach could provide an easy and straightforward solution to the technical limitations associated with existing CRC models. We wish to take advantage of this model in order to investigate tumor associated macrophages (TAMs) biology in CRC.

METHODS

Mice

C57BL/6 CD45.2 mice were purchased from Harlan. C57BL/6 CD45.1, OT-II TCR transgenic mice harboring OVA-specific CD4⁺ T cells (Barnden et al., 1998), *Cx3cr1^{gfp/+}* mice (Jung et al., 2000), *CD11c-DTR* transgenic mice (B6.FVB-Tg [Itgax-DTR/GFP] 57Lan/J) (Jung et al., 2002), and *Ccr2^{-/-} Cx3cr1^{gfp/+}* mice were bred at the Weizmann animal facility. *Myd88^{-/-} Ticam1^{-/-}* mice were kindly provided by E. Elinav (Yale University). *Thr2^{-/-}* (Travassos et al., 2004) and *Nod2^{-/-}* (Kobayashi et al., 2005) mice were bred at the Institute Pasteur animal facility. *Zbtb46^{gfp/+}* (BTBD4) mice (Satpathy et al., 2012) served as BM donors. *IL10^{-/-}* mice (Kuhn et al., 1993) were crossed to *Cx3cr1^{gfp}* mice to obtain *IL10^{-/-} Cx3cr1^{gfp/+}* mice. *Cx3cr1^{cre}* mice (Yona et al., 2013) were crossed to *IL-10^{fl}* and *IL10Rα^{fl}* mice (Roers et al., 2004, Pils et al., 2011) to obtain *Cx3cr1^{cre}IL-10^{fl/fl}* and *Cx3cr1^{cre}IL-10Rα^{fl/fl}* mice. All mice were backcrossed against a C57BL/6 background.

BM chimeras were generated as reported (Varol et al., 2007). After BM transfer, the recipients were allowed to rest for 8 weeks before use. All mice were maintained under specific-pathogen-free conditions and handled according to protocols approved by the Weizmann Institute and the Institute Pasteur Animal Care Committee as per international guidelines. For chapter 3 experiments, 8–10 week-old males C57BL/6, Balb C and A-thymic nude mice were obtained from Harlan biotech (Rehovot, Israel). 8–10 week-old males NOD SCID mice were kindly provided by Prof. Tsvee Lapidot (Weizmann Institute of Science, Rehovot, Israel). A-thymic nude mice were sub-lethally irradiated (450 rad) before the orthotopic implantation of human CRC cell lines to eliminate immuno-rejection. The study was approved by the Tel Aviv Sourasky Medical Center ethical committee. Animals had unrestricted access to food and water, were housed in temperature and humidity controlled rooms, and were kept on a 12-hour light/dark cycle.

Cell Isolation, Flow Cytometry Analysis, and Sorting of Phagocyte Subsets

Isolation of colonic lamina propria cells was performed by following a method established previously with slight modifications (Varol et al., 2009). In brief, extra-intestinal fat tissue and blood vessels were carefully removed and colons were then flushed of their luminal content with cold PBS, opened longitudinally, and cut into 0.5 cm pieces. Epithelial cells and mucus were removed by 40 min incubation with HBSS (without Ca²⁺ and Mg²⁺) containing 5% FBS, 2 mM EDTA, and 0.15 mg/ml (1 mM) DTT (Sigma) at 37°C shaking at 250 rpm. Colon pieces were then digested in PBS^{+/+} containing 5% FBS, 1 mg/ml Collagenase VIII (Sigma), and 0.1 mg/ml DNase I (Roche) for 40 min at 37°C shaking at 250 rpm. The digested cell suspension was then washed with PBS and passed sequentially through 100 and

40 mm cell strainers. Antibodies used for colonic lamina propria staining included: CD45 (30-F11), CD45.2 (104), CD45.1 (A20), Ly6C (HK1.4), CD11c (N418), CD11b (M1/70), IAb (AF6-120.1), CD86 (GL-1), CD14, CD64 (54-5/7.1), CD24 (M1/69), CD40 (3/23) CD3 (145-2C11), TCRb (H57-597), CD4 (GK1.5), CD25 (PC61) and CD8 (53-6.7) (all from BioLegend), CD103 (M290) and CCR7 (4B12) (BD Bioscience), F4/80 (CI:A3-1) (Serotec), Trem1 (174031) R&D and FoxP3 (FJK-165) eBioscience. For intracellular staining of FoxP3 fixation and permeabilization was done using BD Cytotfix/Cytoperm kit according to manufacturer's protocol. BM cells were harvested from the femora and tibiae of *CD45.1 Cx3cr1^{gfp/+}* or *CD45.2 Ccr2^{-/-} Cx3cr1^{gfp/+}* mice and enriched for mononuclear cells on a Ficoll density gradient. Ly6C^{hi} monocytes were then sorted by gating on cells positive for CD115, CD11b, CX3CR1-GFP, and Gr1 (Ly6C/Ly6G) and negative for CD117 (cKit). Spleens of *Cx3cr1^{gfp/+}* mice were mashed through 100 and 40 mm cell strainers, lysed with ACK (0.15 M NH₄Cl, 0.1 M KHCO₃, 1 mM EDTA in PBS), and enriched for monocytes by magnetic cell separation (MACS) with biotinylated-conjugated CD115 antibody (AFS98) followed by streptavidin MACS beads (Miltenyi Biotec GmbH). Ly6C^{hi} monocytes were then sorted by gating on cells positive for CD115, CD11b, CX3CR1-GFP, and Gr1 (Ly6C/Ly6G). Other antibodies used in the studies: Gr1 (RB6-8C5) (BioLegend), and Valpha 2 TCR (B20.1) (Invitrogen). Cells were analyzed with LSRFortessa flow cytometer (BD) or sorted with a FACSAria machine (BD). Flow cytometry analysis was done with the FlowJo software.

DSS-Induced Colitis Model and Murine Colonoscopy

Mice received one cycle (7 days) of dextran sulfate sodium salt (DSS) (MP Biomedicals, C-160110) treatment 2% in drinking water. To monitor and score colitis severity, we used a high-resolution murine video endoscopic system, consisting of a miniature probe (1.9 mm outer diameter), a xenon light source, a triple chip HD camera, and an air pump ("Coloview," Karl Storz) to achieve regulated inflation of the mouse colon. Digitally recorded video files were processed with Windows Movie Maker software (Microsoft). Endoscopic quantification of colitis was graded as previously described (Becker et al., 2006). The researcher who performed the colonoscopies was blinded to the genotype of the mice.

Histology and Immunohistochemistry

Tissues were fixed in 2% paraformaldehyde overnight at 4°C and next impregnated in 30% sucrose for 48 hr. Sequentially, the colonic tissues were rapidly frozen in O.C.T. (Tissue-Tek) in isopentane cooled with liquid nitrogen and then cut with cryostat to 12 mm thick sections. Slides were observed with a Zeiss Axioscope II fluorescent microscope and image acquisition was conducted with simple PCI software. Alternatively, for images in figures 12 & 13, Tissues were fixed in 4% paraformaldehyde overnight at 4°C, embedded in paraffin, serially

sectioned and stained with hematoxylin and eosin. For immunohistochemistry, paraffin embedded sections after antigen retrieval were stained for CD3 (SP7, abcam) and Ly6G (1A8, biolegend) overnight in 4°C. Alexa-fluor 488-conjugated donkey anti-rabbit and Alexa-fluor 594-conjugated donkey anti-rat (Jackson ImmunoResearch) secondary antibodies were added for 1 hour. Nuclei were stained with Hoechst. Slides were evaluated using an Olympus BX51 microscope, and image acquisition was conducted with the Olympus DP70 camera and DP-Manager software.

Microarray Analysis

Total RNA was extracted from freshly isolated flow cytometry-sorted cells. Total RNA was extracted with the miRNeasy Mini or Micro Kit (Qiagen). RNA purity was assessed with ND-1000 Nanodrop (Peqlab) and BioAnalyzer 2100 (Agilent). The cDNA was prepared, labeled, and hybridized to Affymetrix GeneChip, mouse gene 1.0 ST according to standard manufacturer protocols. Hybridized chips were stained and washed and were scanned with the Affymetrix GeneChip 3000 7G plus scanner. Affymetrix Gen- eChip Operating Software (GCOS v1.4, <http://www.affymetrix.com/estore>) was used for the initial analysis of the microarray data to convert the image files to cell intensity files (CEL). Transcriptome analysis (processing of raw data, clustering, and creating correlation matrices) was carried out with Partek Genomic Suite 6.5 (St. Charles, MO; <http://www.partek.com>). The raw probe intensities were adjusted based on the number of G and C bases in the probe sequence, before any probe correction. Preprocessing was performed with the Robust Microarray Averaging algorithm (Irizarry et al., 2003). Genes expressed below background levels in all examined conditions were removed from further analyses.

Real-Time PCR

Total RNA was extracted from sorted cells with RNeasy Micro Kit (Qiagen) and from murine colons with PerfectPure RNA Tissue Kit (5 PRIME). RNA was reverse transcribed with a mixture of random primers and oligo-dT with a High-Capacity cDNA Reverse Transcription Kit (Applied Biosystems). PCR was performed with SYBR Green PCR Master Mix kit (Applied Biosystems). Quantification of the PCR signals of each sample was performed by comparing the cycle threshold values (Ct), in duplicate, of the gene of interest with the Ct values of the TATA-binding protein (TBP) housekeeping gene.

Colon explant culture

Colons were flushed with RPMI and opened along the longitudinal axis. Thereafter, 3 mm² punch biopsies were obtained from the distal colon and incubated for 24hrs in RPMI supplemented with 10% FCS and antibiotics (one punch biopsy per 100µl medium).

Supernatants were collected and kept in -20°C until assessed.

Cytokine and PGE₂ measurement

The production of the cytokines IL-10, IL-6, TNF α , IL-1 β , and IFN- γ in BM macrophage culture medium or colon explant was assessed with the DuoSet ELISA kit (R&D Systems). In chapter 2 experiments, cytokine levels in sera and colon explant supernatants were assessed by Milliplex map mouse Cytokine/Chemokine Panel (Millipore), according to the manufacturer's instructions. PGE₂ levels in colon explant supernatants were assessed with Prostaglandin E₂ EIA Kit- Monoclonal (Cayman chemical company) according to the manufacturer's instructions.

Two-Photon Microscopy

To visualize cells in the intestinal lymphatics, we modified a protocol described before (Schulz et al., 2009). To label both lymphatic and blood vessels, 200 μl Evans blue (0.2%; Sigma) was injected i.v. 30 min before sacrifice. This dye leaks from blood vessels into the extracellular fluid and gathers in lymphatics where it can be visualized based on its red fluorescence. To distinguish blood vessels, we further i.v. injected the mice with high-MW dextran (MW 500,000; Sigma) labeled with FITC 2 min before sacrifice. Mice were then anesthetized with ketamine/xylazine 100/20 mg/kg. Laparotomy was performed, and the intestinal lymphatics were ligated with a suture close to the MLN. Mice were sacrificed and a 3–4 cm long intestinal segment corresponding to the cecum and the proximal colon with its intact vasculature and the MLNs was dissected, glued into a cell culture dish, and submerged in cold PBS. The collecting intestinal lymphatics were imaged with a 2-photon microscope (Ultima Multi-photon; Prairie Technologies) incorporating a pulsed laser (Mai Tai DeepSee Ti-sapphire; Newport Corp.) tuned to 930 nm to simultaneously excite Evans blue, FITC, and GFP. A water-immersed 20 \times (NA 0.95) objective (Olympus) was used. Three-dimensional reconstruction of the lymphatics was performed with Improvision Volocity software.

T Cell Proliferation Assays

CD4⁺ Ova-specific T cells were isolated from spleen and mesenteric lymph node of TCR transgenic OT-II mice via magnetic cell separation technique (MACS) with anti-CD4 magnetic beads (Miltenyi Biotec GmbH). OT-II cells were labeled with CFSE (C-1157, Invitrogen) and cocultured with mononuclear phagocyte subsets sorted from the colonic lamina propria of mice subjected to DSS-induced colitis and immunization with 100 μg OVA (Sigma Aldrich) by gavage the day before ratio of T cell/APC was 2:1. Analysis of T cell proliferation was performed by flow cytometric analysis of CFSE dilution 3.5 days after coculturing.

Endoscopy-Guided Colonic Transplantation

Ly6C^{hi} monocytes were sorted to high purity (>95%) as described before and injected into the colonic lamina propria submucosal layer utilizing a previously described protocol established by our group (Zigmond et al., 2011), which is based on the adaptation of the murine colonoscopy system.

Bone marrow derived macrophages

BM cells were harvested from the femora and tibiae of *Cx3cr1^{gfp/+}*, *Cx3cr1^{cre}IL10^{fl/fl}* or *Cx3cr1^{cre}IL10Rα^{fl/fl}* mice and enriched for mononuclear cells on a Ficoll density gradient. To extract CD115 positive cells, cells were isolated by MACS cell separation by using CD115-biotin (AFS98 Biolegend) and streptavidin-conjugated magnetic beads (Miltenyi). CD115 positive fraction was seeded on 12-well plates in RPMI (Beit Ha'emek industries) complemented with FCS (10%), L-glutamine (1%), Sodium-pyrovate (1%) and pen-strep (1%), in the presence of 10 ng/ml recombinant M-CSF (Peprotech). At day 3, half the medium was replaced and on day 7 cells were either stimulated with 100 ng/ml LPS (Sigma) or 100 ng/ml LPS and 10 ng/ml recombinant IL10 (Peprotech) or left as control.

Histologic analysis

All sections were examined by the same pathologist who was blinded to the genotype of mice. Because intestinal lesions were multifocal and of variable severity, the grades given to any section of intestine took into account the number of lesions, as well as their severity. A score from 0 to 4 was based on the following criteria: (grade 0) no change from normal tissue; (grade 1) one or a few multi-focal mononuclear cell infiltrates in the lamina propria accompanied by minimal epithelial hyperplasia; (grade 2) lesions tended to involve more of the intestine than grade 1 lesions, or were more frequent. Typical changes included several multifocal, mild inflammatory cell infiltrates in the lamina propria composed primarily of mononuclear cells with a few neutrophils. Small epithelial erosions were occasionally present and inflammation rarely involved the sub-mucosa; (grade 3) lesions involved a large area of the mucosa or were more frequent than grade 2 lesions. Inflammation was moderate and often involved the sub-mucosa but was rarely transmural. Inflammatory cells were a mixture of mononuclear cells as well as neutrophils, and crypt abscesses were sometimes observed. Ulcers were occasionally observed; (grade 4) lesions usually involved most of the intestinal section and were more severe than grade 3 lesions. Inflammation was severe, including mononuclear cells and neutrophils, and was sometimes transmural. Crypt abscesses and ulcers were present. Five segments of the intestine (terminal ileum, cecum, proximal colon, medial colon and distal colon-rectum) were given a score based on the criteria described

above and the summation of these scores provided a total colonic disease score per mouse. The disease scores could range from 0 (no change in any segment) to a maximum of 20 (grade 4 lesions in all five segments).

Colo-Rectal tumor cells

Murine C57BL/6 CRC tumor cells (MC38) were kindly provided by Dr. Avi Eisenthal (Tel Aviv Sourasky Medical Center). Luciferase stably- transfected murine CRC tumor cells (CT26) were kindly provided by Prof. Lea Eisenbach (Weizmann Institute of Science Rehovot, Israel). The human CRC tumor cell-lines SW620, SW480 and LS174T were kindly provided by prof. Zelig Eshhar (Weizmann Institute of Science Rehovot, Israel). The HT-29 human CRC cell-line was the generous gift of Dr. Isabel Zvibel (Tel-Aviv Sourasky Medical Center, Tel-Aviv, Israel).

Generation of MC38 CRC tumor cells expressing GFP or RFP

MC38-GFP and MC38-RFP CRC tumor cells were generated by transduction with pCSC-SP-PW-IRES-GFP/RFP lentiviruses designed to express GFP or RFP with M.O.I of 50 (kindly provided by Dr. Alon Chen, Weizmann Institute for science Rehovot, Israel). Subsequently, MC38 cells expressing GFP or RFP were sorted to high purity using a high speed FACSAria II sorter (Beckton-Dickinson).

Orthotopic colonic sub-mucosal implantation of CRC cells

Mice were anesthetized using Ketamine/ Xylazine. Sub-mucosal injections were accomplished using stainless flexible steel; 8 inch long, 30 gauge and 45 degree bevel hypodermic needles custom made according to our specification (Cadence Inc. U.S.A). The needle was inserted through Luer lock (Söllner, GmbH) screwed on the working channel of the scope to avoid air leakage. Subsequently, the scope was inserted into the mouse colon and following its inflation the needle was brought through the working channel to the scope's front. The CRC cell implantation procedure was performed by two coordinated persons; one person was navigating the colonoscopy while the other person was operating the injection maneuver. The injection was performed under observation by a very gentle sub-mucosal penetration with the open side of the bevel heading up in a flat angle. A volume of 50 microliter CRC tumors cells was then injected into the colonic sub-mucosa.

In-vivo imaging of CRC tumors

To follow luciferase-expressing CT26 CRC tumor implantation and growth in BALB/c mice, 50 ml D-Luciferin (30 mg/ml) was i.p injected 10 minutes before and

subsequently mice were inserted into the closed dark chamber of the whole body cooled CCD camera Photon Imager system (Biospace Lab, France). For in-vivo visualization of GFP and RFP positive tumors Leica MZ16F fluorescent stereomicroscopy system was used (Leica Microsystems, Germany).

CRC tumor growth kinetics

C57BL/6 mice were orthotopically sub-mucosal injected with 103, 104, or 105 MC38 cells. The tumor's colonic circumference and developmental stage were monitored over time by colonoscopy every week for 3 weeks following cell implantation. Endoscopic grading was done according to tumor size relatively to the circumference of the colon as established by Becker et al (Becker et al., 2006) In short, tumor size was graded as follows: Grade 1 (just detectable tumor), Grade 2 (tumor covering up to 1/8 of colonic circumference), Grade 3 (tumor covering up to 1/4 of the colonic circumference), Grade 4 (tumor covering up to 1/2 of the colonic circumference) and Grade 5 (tumor covering more than 1/2 of the colonic circumference).

Statistical Analysis

Data were analyzed by ANOVA followed by Bonferroni's Multiple Comparison test or by unpaired, two-tailed t-test using GraphPad Prism 4 (San Diego, CA). Data are presented as mean \pm s.e.m.; values of $p < 0.05$ were considered statistically significant.

RESULTS

Chapter 1

Ly6C^{hi} monocytes in the inflamed colon give rise to proinflammatory effector cells and migratory antigen-presenting cells.

Intestinal steady state CX₃CR1/GFP^{hi} macrophages are replenished from monocytes and exhibit an anti-inflammatory gene expression signature

Macrophages (MF) are the most abundant mononuclear phagocytes in the steady state lamina propria of the colon, (**Fig 1A**), characterized by surface expression of the integrins CD11c and CD11b, as well as the F4/80 antigen. Intestinal MF also express unique high levels of the chemokine receptor CX₃CR1, rendering them readily detectable by flow cytometry and histology in mice harboring a GFP reporter gene insertion in their CX₃CR1 gene (Jung et al., 2000). The colonic steady state mononuclear compartment includes also CD11c^{hi}CD103⁺CD11b⁻ and to a lesser extent the CD11c⁺CD103⁺CD11b⁺ DC (**Fig 1A**). Adoptive monocyte transfers into MF-depleted animals have established that these cells are derived from Ly6C^{hi} blood monocytes (Bogunovic et al., 2009; Varol et al., 2009). Upon arrival in the tissue, monocytes are presumably by the tissue context imprinted to acquire a discrete non-inflammatory gene expression profile compatible with tissue homeostasis and their extended half-life (Rivollier et al., 2012).

To molecularly define this education process we determined gene expression signatures of Ly6C^{hi} monocytes and their descendants isolated from the colon of diphtheria toxin (DTx)-treated CD11c-DTR mice after monocyte engraftment and reconstitution (Varol et al., 2009). Graft-derived cells acquired a gene expression profile highly similar to CX₃CR1/GFP^{hi} resident MF (**Fig 1B**) with a Pearson's correlation coefficient of 0.95 by correlation matrix analysis (**Fig 1C**). This included induction of IL-10 and Triggering receptor expressed on myeloid cells 2 (TREM-2), IRAK-M, and TNFAIP3 (A20), but also expression of TNF α , known to exert both pro-and anti-inflammatory activities (Kassiotis and Kollias, 2001), although expression of these molecules not always reached the levels observed in CX₃CR1/GFP^{hi} resident MF.

Experiments like the above have established that CX₃CR1/GFP^{hi} resident MF can derive from Ly6C^{hi} monocytes (Varol et al., 2009). The extended half-life of these cells (Jaensson et al., 2008; Schulz et al., 2009) however so far precluded the

direct demonstration that Ly6C^{hi} monocytes differentiate in steady state in situ into CX₃CR1/GFP^{hi} resident MF. To nevertheless study the fate of a monocyte graft in the intestinal tissue context we resorted to an endoscopy-guided injection of CX₃CR1^{gfp/+} monocytes into the colonic lamina propria of healthy wt C57BL/6 mice using a protocol we recently established for an orthotopic colon cancer model (Zigmond et al., 2011). As seen in **Fig 1D**, 12 hours after injection, Ly6C^{hi} monocytes could readily be detected as CX₃CR1/GFP^{int}Ly6C^{hi} cells in colonic cell suspensions and by 72 hours gave rise to MF that expressed high levels of CX₃CR1/GFP, lost Ly6C expression and acquired the F4/80 marker. Collectively, these data corroborate earlier findings (Rivollier et al., 2012; Varol et al., 2009) that Ly6C^{hi} monocytes are educated in the steady state colon to differentiate into CX₃CR1/GFP^{hi} MF displaying a non-inflammatory gene expression signature.

Figure 1

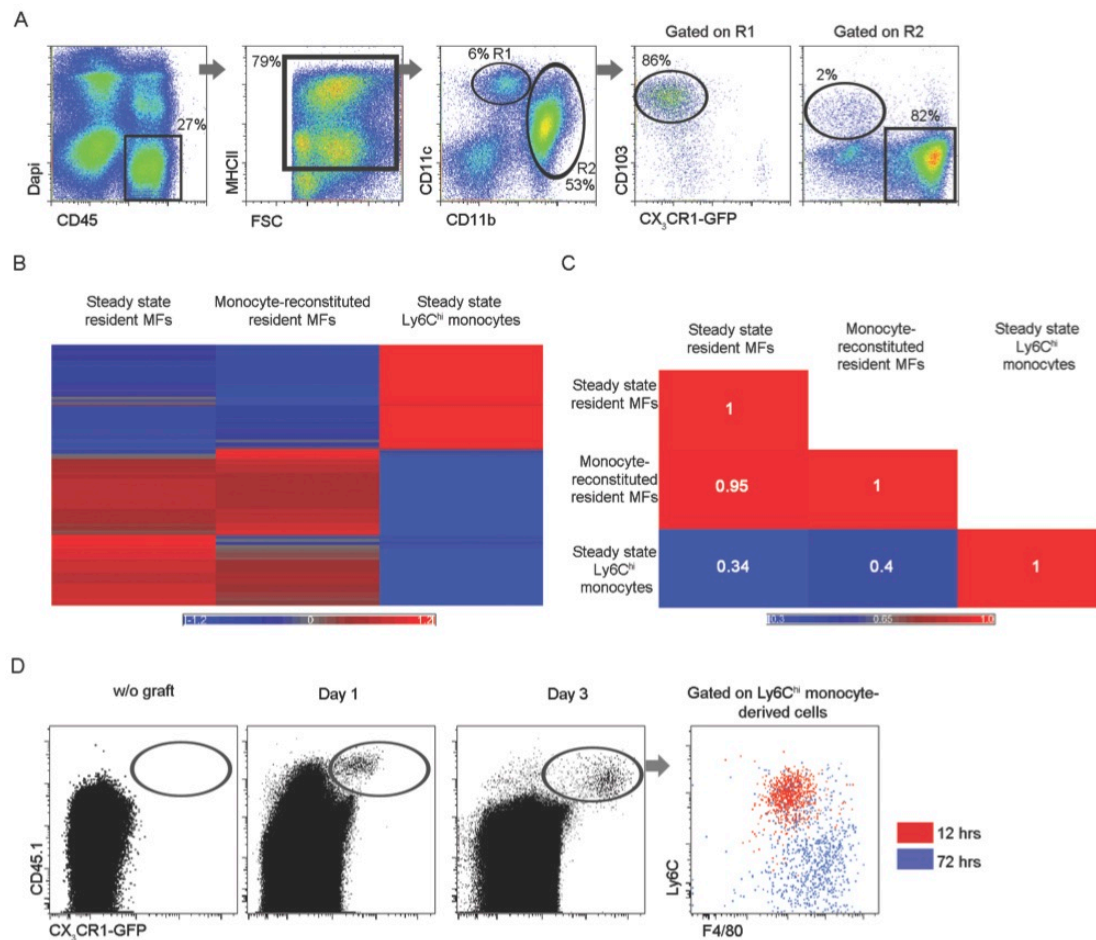


Figure 1. Steady state colonic lamina propria predominantly harbors Ly6C^{hi} monocyte-derived CX₃CR1/GFP^{hi} MFs

(A) Flow cytometry analysis of steady state colonic lamina propria of CX₃CR1^{+/gfp} mice indicating definitions and gating strategy. Note that the CX₃CR1/GFP^{hi} MFs constitute the most prominent mononuclear phagocyte subset in steady state.

(B) Based on the microarray data, a total of 4412 differentially expressed genes were chosen, with at least 2 fold change between any of the three investigated cell populations: Steady state CX₃CR1/GFP^{hi} MFs (pooled isolate of 10 mice), Ly6C^{hi} monocyte-graft-derived CX₃CR1/GFP^{hi} MFs (pooled isolate of 14 engrafted [CD11c-DTR>wt] BM chimeras, 14 days after monocyte transfer), and Ly6C^{hi} monocytes (isolated from 6 spleens). The log₂ intensities were standardized to have for each gene zero mean and unit standard deviation. Hierarchical clustering of the standardized values was performed using the Pearson dissimilarity measure. The expression profile is accompanied by a colored bar indicating the standardized log₂ intensities.

(C) The correlation matrix of pair-wise correlations (Pearson coefficient) describing the similarity between the different investigated cell populations is shown for the genes that are shown in Fig 1b. Correlations are color-coded according to the shown bar. Note the high similarity between CX₃CR1^{hi} resident MFs isolated from steady state colon and colon mononuclear phagocyte-depleted mice reconstituted with Ly6C^{hi} monocytes.

(D) Flow cytometry analysis of recipient colons (CD45.2) 1 and 3 days after endoscopy-assisted submucosal injection of 2x10⁵ Ly6C^{hi} monocytes (CX₃CR1^{gfp}, CD45.1). Note differentiation of Ly6C^{hi} monocytes into CX₃CR1/GFP^{hi}F4/80^{hi} resident MFs.

Intestinal inflammation induces the infiltration of CX₃CR1/GFP^{int} cells

To probe for alterations in the mononuclear phagocyte composition of the colonic lamina propria in response to acute inflammatory challenges, we subjected CX₃CR1^{gfp/+} mice to an oral dextran sodium sulfate (DSS) regimen. This established colitis model is characterized by ulceration and submucosal inflammation provoked by disruption of the epithelial barrier and resulting exposure to luminal microbiota (Okayasu et al., 1990). In accordance with earlier reports using other colitis models (Rivollier et al., 2012; Weber et al., 2011) or DSS-induced colitis (Platt et al., 2010; Waddell et al., 2011) flow cytometry analysis of the inflamed colonic lamina propria revealed the progressive emergence of CX₃CR1/GFP^{int} cells concomitant with a marked reduction in the frequency of CX₃CR1/GFP^{hi} resident MFs (**Fig 2A**). The accumulation of CX₃CR1/GFP^{int} cells reached its peak at day 7 following the initial DSS exposure, ten-fold outnumbering CX₃CR1/GFP^{hi} resident MFs, and was associated with neutrophil infiltration and significant destruction of the crypt architecture, as determined by histology (**Fig 2A-C**). Flow cytometric characterization of the CX₃CR1/GFP^{int} infiltrate identified them as CD11b^{hi} cells that expressed low levels of F4/80 and could be further divided into Ly6C^{hi} and Ly6C^{lo} subpopulations (**Fig 2D**). Of note, CX₃CR1/GFP^{int} cells are also detectable at low frequency in healthy colonic lamina propria (Platt et al., 2010; Schulz et al., 2009; Varol et al., 2009); however most of these cells were negative for the Ly6C marker (**Fig 2D**). Comparative analysis of the CX₃CR1/GFP^{int} infiltrate and the CX₃CR1/GFP^{hi} resident MFs revealed that the former were according to their side and forward scatter smaller and less granular (**Fig 3A**). All populations expressed the pattern recognition receptor CD14, as well as the co-stimulatory molecule CD86 although expression of the latter was lower on CX₃CR1/GFP^{int} subsets. Importantly, Ly6C^{hi} CX₃CR1/GFP^{int} cells were negative for CD11c and about half of the cells expressed intermediate levels of MHC class II, while CX₃CR1/GFP^{int}Ly6C^{lo} cells were uniformly positive for both CD11c and MHC II (**Fig 3B**).

Collectively, these results show that within the acutely inflamed colon CX₃CR1/GFP^{hi} resident MFs are progressively, but transiently, replaced by a heterogeneous CD11b^{hi}CX₃CR1/GFP^{int} cell population composed of a Ly6C^{hi}CD11c⁻MHCII^{+/+} and a Ly6C^{lo}CD11c⁺MHCII^{hi} cell subsets.

Figure 2

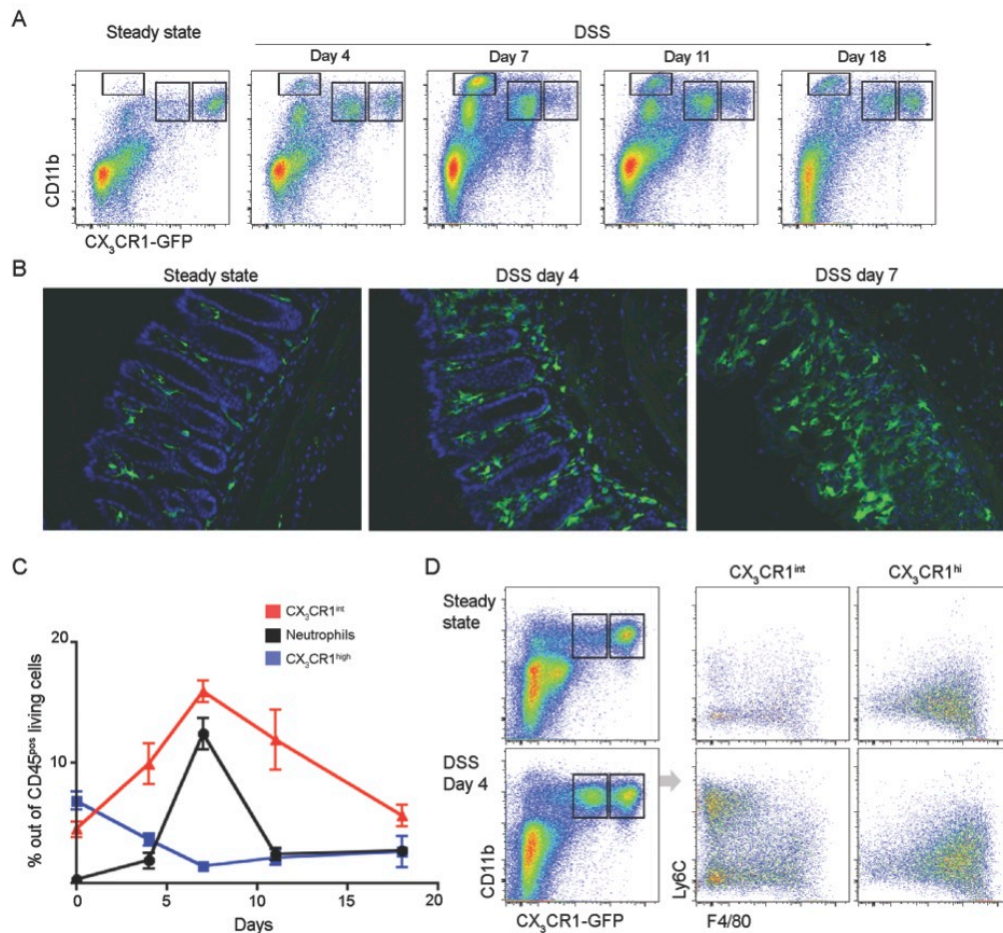


Figure 2. The colitic colon recruits CX₃CR1/GFP^{int} cells

(A) Representative flow cytometry plots gated on CD45⁺ living cells isolated from steady state colonic lamina propria of CX₃CR1^{+/gfp} mice and on days 4, 7, 11 and 18 after DSS challenge. Note progressive accumulation of CD11b^{hi}CX₃CR1/GFP^{int} cells and concomitant reduction of CX₃CR1/GFP^{hi} resident MFs.

(B) Representative fluorescent microscopy images of CX₃CR1^{gfp/+} colons at steady state and day 4 and 7 after DSS challenge (green- CX₃CR1-gfp, blue-Hoechst, original magnifications 10x).

(C) Dynamics of cellular infiltrates in colitic colon; CX₃CR1/GFP^{int} cells (red triangle), CX₃CR1/GFP^{hi} resident-MFs (blue square) and CD11b^{hi}Gr1^{hi} neutrophils (black circle), presented as percentages out of CD45⁺ living cells, mean (SEM) (n=4 for any time point).

(D) Flow cytometry analysis of steady state and DSS day 4 colitis showing selective expression of Ly6C and F4/80 markers on CX₃CR1/GFP^{int} and CX₃CR1/GFP^{hi} mononuclear phagocytes, respectively. Results are representative of three or more independent experiments.

Figure 3

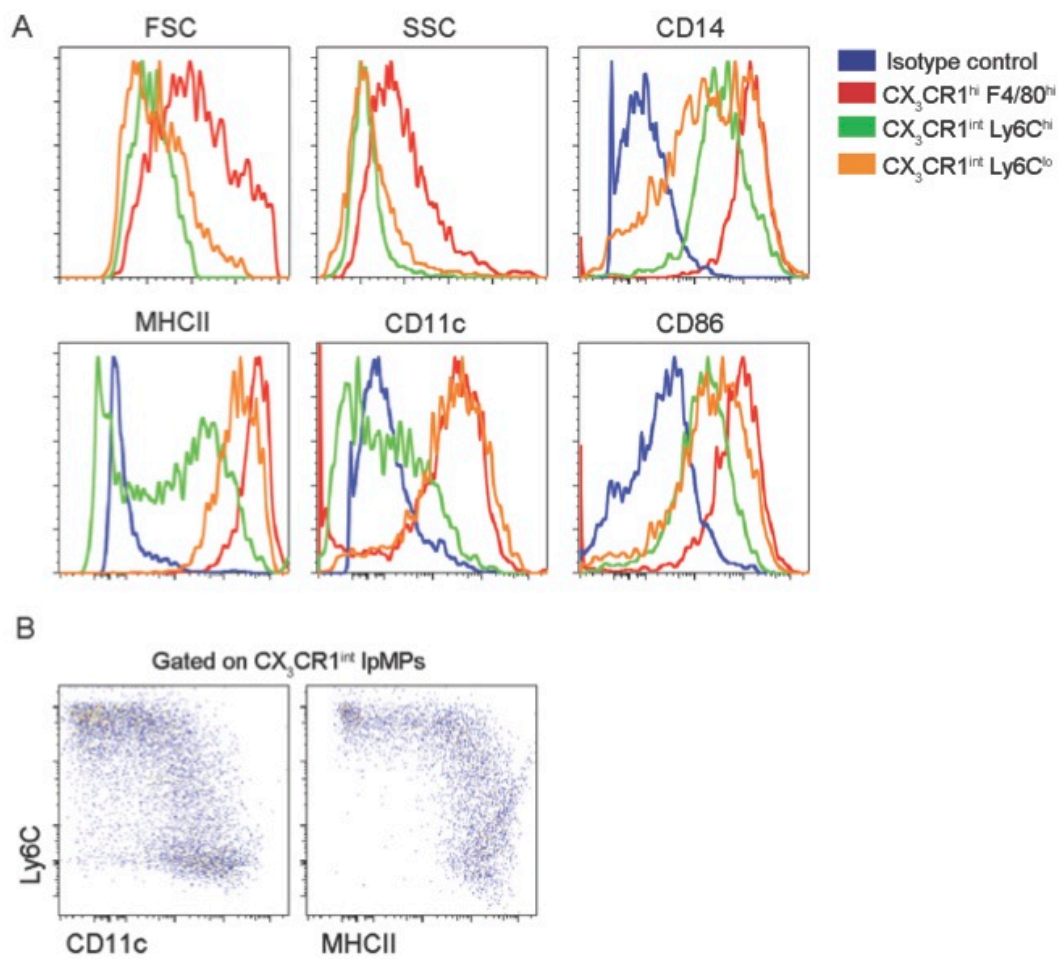


Figure 3.

(A) Flow cytometric analysis of CX₃CR1⁺/GFP LPCs, in mice subjected to DSS for 4 days. Focusing on Ly6C^{hi} monocyte derived cells: CX₃CR1/GFP^{int}Ly6C^{hi}, CX₃CR1/GFP^{int}Ly6C^{lo} and CX₃CR1^{hi}F4/80^{hi}. All three populations were analyzed for FSC, SSC and the expression of CD14, CD11c, MHC II and CD86.

(B) Flow cytometric analysis of CX₃CR1⁺/GFP LPCs, in mice subjected to DSS for 4 days. Focusing on CX₃CR1/GFP^{int} cells. Dot plots shows the different expression profile of CD11c and MHC II in CX₃CR1/GFP^{int}Ly6C^{hi} versus CX₃CR1/GFP^{int}Ly6C^{lo} cells.

Ly6C^{hi} and Ly6C^{lo} CX₃CR1/GFP^{int} cell subsets arise from Ly6C^{hi} monocytes under inflammatory conditions and are recruited to the gut in a CCR2-dependent manner

To probe for the origin of the CX₃CR1/GFP^{int} cell subsets we performed adoptive monocyte transfers into DSS-challenged animals. Rather than differentiating into CX₃CR1/GFP^{hi} F4/80^{hi} MFs (**Fig. 1D**), grafted Ly6C^{hi} monocytes gave by one day after transfer rise to CX₃CR1/GFP^{int} Ly6C^{hi} F4/80^{lo}CD11c⁻ cells. Moreover, by 72 hrs after transfer the graft had further differentiated into CX₃CR1/GFP^{int} Ly6C^{lo}F4/80^{lo} cells expressing higher levels of MHCII and CD11c (**Fig 4A**).

The chemokine receptor CCR2 is required for emigration of Ly6C^{hi} monocytes from the BM resulting in a paucity of Ly6C^{hi} monocytes in the circulation of CCR2^{-/-} mice (Serbina and Pamer, 2006). Interestingly, flow cytometry analysis of CCR2^{-/-}:CX₃CR1^{gfp/+} mice subjected to DSS-induced colitis revealed a failure of these animals to recruit both Ly6C^{hi} and accumulation of Ly6C^{lo} CX₃CR1/GFP^{int} infiltrating cells to their inflamed colon, further supporting the notion that both these subsets cells derive from Ly6C^{hi} monocytes (**Fig 4B**). Moreover, adoptive transfer of a mixed monocyte graft consisting of CD45.2 CCR2-deficient and CD45.1 CCR2-proficient CX₃CR1^{GFP/+} Ly6C^{hi} monocytes into wt recipients at day 4 after DSS challenge resulted in the exclusive recruitment of CD45.1⁺ wt cells to the inflamed colonic lamina propria (**Fig 4C**). This establishes that CCR2 is required for the recruitment of Ly6C^{hi} monocytes from the blood to the inflamed colon. Collectively, these data highlight the context-dependent fate of CCR2⁺ Ly6C^{hi} monocytes within the colonic lamina propria differentiating into CX₃CR1/GFP^{hi} resident MFs in steady state, but giving rise to Ly6C^{hi} and Ly6C^{lo} CX₃CR1/GFP^{int} cells under inflammatory settings.

Figure 4

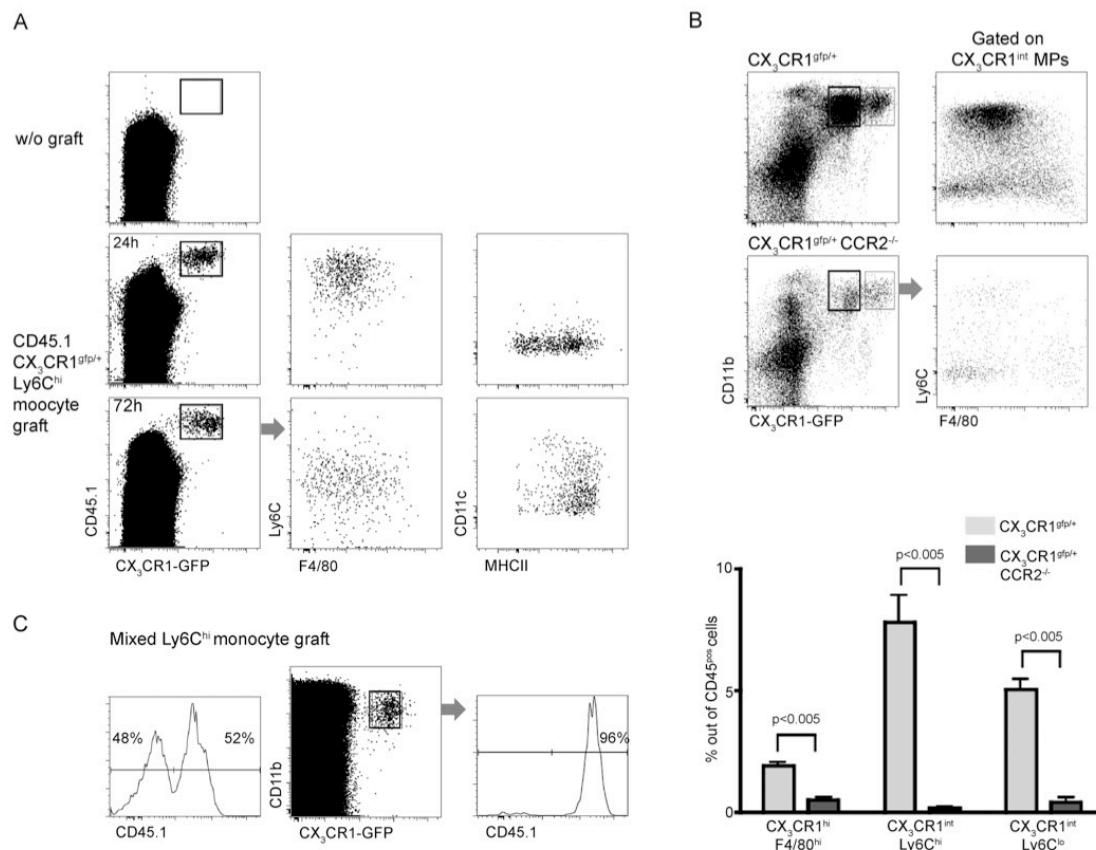


Figure 4. CX₃CR1/GFP^{int} cells arise from Ly6C^{hi} monocytes under inflammatory conditions in a CCR2-dependent manner

(A) Flow cytometry analysis of DSS-challenged wt recipient mice (CD45.2) of Ly6C^{hi} monocytes (3×10^6 ; CX₃CR1^{GFP/+}:CD45.1). Monocytes were engrafted on day 4 after onset of DSS treatment; analysis was performed 24 and 72 hrs post transplantation.

(B) Flow cytometry analysis of colon of CX₃CR1^{+ / GFP} and CX₃CR1^{+ / GFP}CCR2^{- / -} mice for CD45⁺ living cells at day 5 after DSS onset. Graphical summary of percentage of indicated cell subset out of CD45⁺ cells, mean (SEM) (n=3)

(C) Flow cytometry analysis of colon of CD45.2 wt recipient mice 72 hrs following intravenous adoptive transfer of Ly6C^{hi} monocyte graft composed of 1.5×10^6 CX₃CR1^{+ / GFP} (CD45.1) cells and 1.5×10^6 CX₃CR1^{+ / GFP}CCR2^{- / -} (CD45.2) cells at day 4 after onset of 2% DSS treatment. Results are representative of two independent experiments.

Molecular characterization of infiltrating CX₃CR1^{int} and resident CX₃CR1^{hi} F4/80^{hi} colonic mononuclear phagocytes

To study molecular aspects of intestinal monocyte-derived mononuclear phagocyte subsets under inflammatory conditions, we performed an mRNA microarray analysis on highly purified cells freshly isolated from the colonic lamina propria of DSS-challenged colitic CX₃CR1^{gfp/+} mice. CX₃CR1/GFP^{hi} resident MFs, CX₃CR1/GFP^{int}Ly6C^{hi} cells and CX₃CR1/GFP^{int}Ly6C^{lo} cells were sorted on day 4 after DSS challenge. For comparison, we isolated CX₃CR1/GFP^{hi} resident MFs from untreated, healthy CX₃CR1^{gfp/+} animals (**Fig 5**). Furthermore, we profiled Ly6C^{hi} monocytes sorted from the spleens on day 4 after DSS challenge, as the splenic monocyte reservoir has been proposed to be mobilized to inflammatory foci (Swirski et al., 2009) and might hence serve as direct source of the CX₃CR1/GFP^{int}Ly6C^{hi} cells. Microarray analysis for genes differentially expressed between the subsets revealed high similarity between CX₃CR1/GFP^{hi} MFs in steady state and DSS conditions (**Fig 6A, B**). The fact that this population remains largely unaffected by acute inflammation highlights the robustness of its gene expression signature. Selected gene expression analysis correlated with the markers used to sort the cells, i.e. CX₃CR1, F4/80 and Ly6C (**Fig 6B**). While CX₃CR1/GFP^{hi} resident MFs isolated from inflamed colons displayed the typical non-inflammatory expression pattern, CX₃CR1/GFP^{int}Ly6C^{hi} cells exhibited a pronounced pro-inflammatory signature with high expression of TREM-1, iNOS, IL-6 and IL-23. Interestingly though and in accordance with our previous report (Varol et al., 2009), the cytokine TNF α was found to be exclusively expressed by CX₃CR1/GFP^{hi}F4/80^{hi} resident MFs (**Fig 6B, C**). QRT-PCR analysis of mRNA extracted from CX₃CR1/GFP^{int} Ly6C^{hi} and Ly6C^{lo} cell subsets and resident MFs at day 4 of DSS challenge confirmed their differential cytokine expression (**Fig 6C**).

In agreement with the role of CCR2 in its establishment (**Fig 4B, C**), the CX₃CR1/GFP^{int}Ly6C^{hi} infiltrate uniquely expressed this chemokine receptor. The notion that CX₃CR1/GFP^{int} Ly6C^{lo} cells are CCR2^{neg}, yet significantly reduced in CCR2-deficient mice (**Fig 4B, C**), links these cells with circulating Ly6C^{hi} monocytes and Ly6C^{hi} effector monocytes. Interestingly, the CCR2 ligands CCL2, 7 and 8 were found expressed by resident MFs and moderately upregulated under inflammation potentially implying involvement of the latter in the recruitment of the monocytes (**Fig 6B**).

Resident and infiltrating cells also differed significantly in their expression of C-type lectin receptors (CLRs) known to contribute to innate immune responses through pathogen pattern recognition (Mukhopadhyay et al., 2009). Accordingly, the DC-specific ICAM-3 grabbing non-integrin (DC-SIGN) isoform A (CD209a) was highly expressed by the infiltrating cells, while macrophage mannose receptor 1 (MRC1) expression was elevated on resident MFs. The latter also expressed higher levels of the CD163 scavenger receptor (**Fig 6B**).

The CX₃CR1/GFP^{int}Ly6C^{lo} cells exhibited significantly lower expression of the pro-inflammatory mediators IL-6, IL-23, NOS2, VEGFa, IL-1a and TREM1 and differed considerably from the other monocyte-derived subsets by high expression of CCR7 (**Fig 6 B,C**).

Collectively, the molecular profiles further elaborate on the phenotypic and functional variance between monocyte-derived mononuclear phagocyte subsets in steady state and inflamed colon and suggest that CX₃CR1/GFP^{int}Ly6C^{hi} cells are pro-inflammatory effector monocytes.

Figure 5

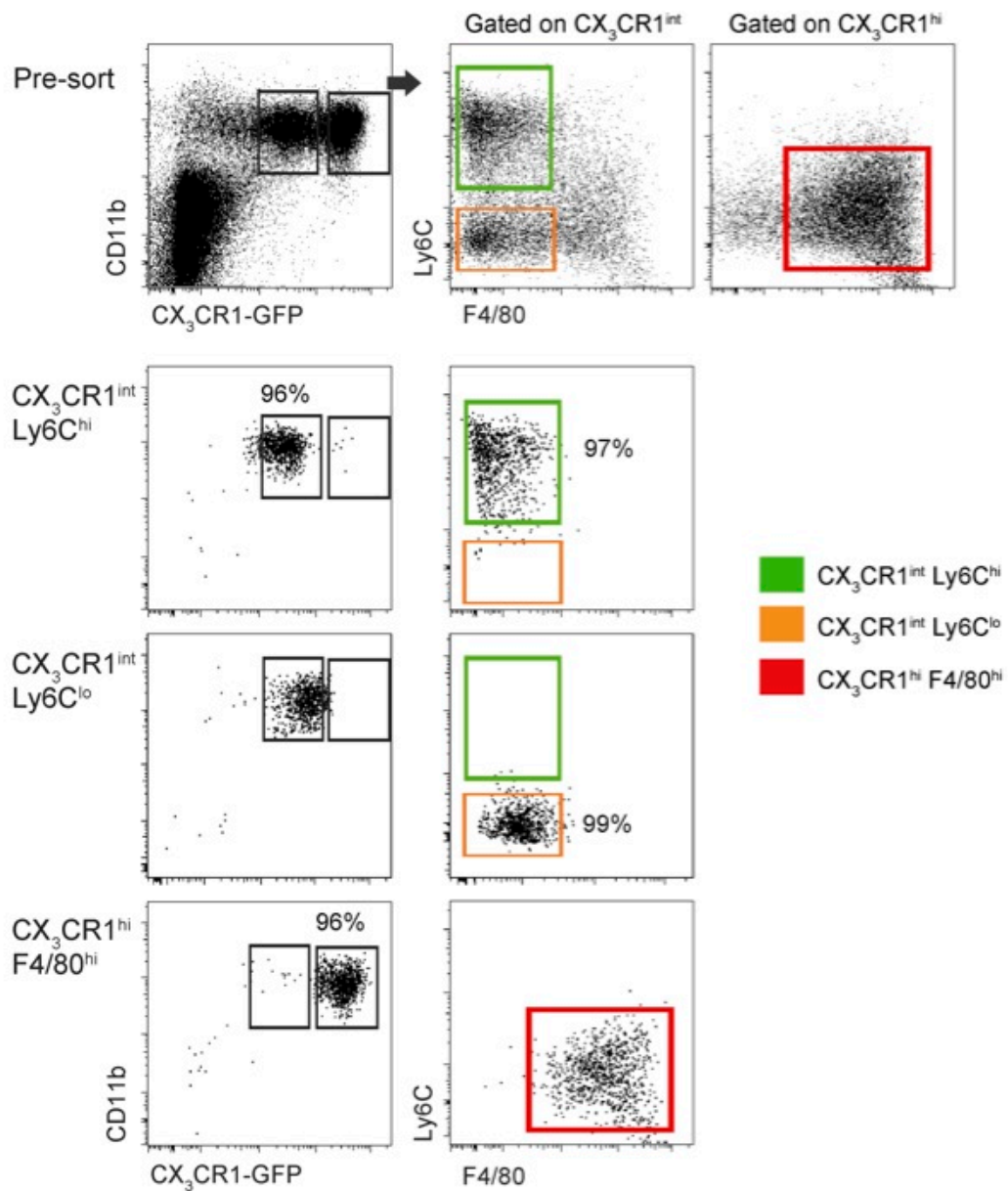


Figure 5. Flow cytometry sorting strategy of the three distinct Ly6C^{hi} monocyte-derived MP subsets from colonic lamina propria of CX₃CR1^{+gfp} DSS day 4 mice.

Representative flow cytometry images showing the strategy used here to identify and sort to high purity the CX₃CR1/GFP^{int}Ly6C^{hi} effector monocytes, CX₃CR1/GFP^{int}Ly6C^{lo} MPs and the CX₃CR1/GFP^{hi}F4/80^{hi} resident MFs. Results are representative of more than 5 independent experiments using pooled cells from 8-12 mice per experiment.

Figure 6

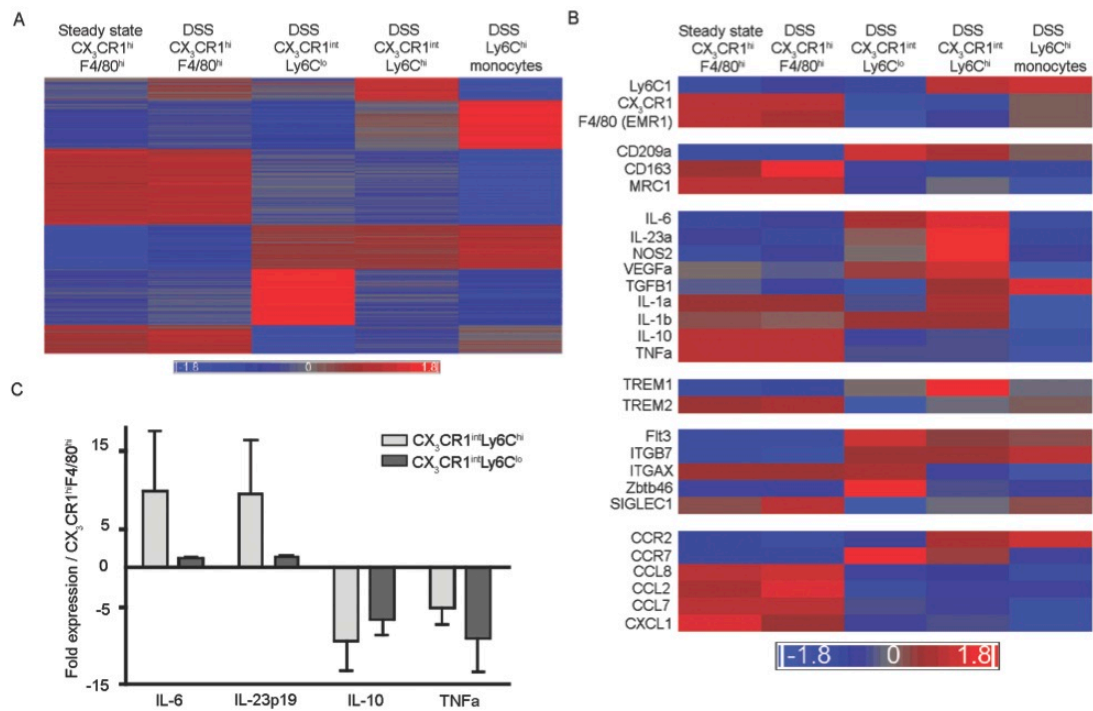


Figure 6. Molecular characterization of infiltrating CX₃CR1/GFP^{int} and resident CX₃CR1/GFP^{hi} F4/80^{hi} colonic mononuclear phagocytes

(A) Affymetrix microarray performed on mRNA of sorted CX₃CR1/GFP^{hi}F4/80^{hi} resident MFs [steady state (n=10), and DSS day 4 (n=12)], CX₃CR1/GFP^{int}Ly6C^{hi} cells and CX₃CR1/GFP^{int}Ly6C^{lo} [DSS day 4 (n=12)] and splenic Ly6C^{hi} monocytes [DSS day 4 (n=7)]. Genes which exhibited a fold change of at least 2 between any two of the investigated cell populations were chosen (5980 genes). The log₂ intensities were standardized to have for each gene zero mean and unit standard deviation. K-means partitioning clustering was performed using Pearson dissimilarity as a distance measure. The number of partition clusters was set to six. The expression profile is accompanied by a colored bar indicating the standardized log₂ intensities.

(B) The heat map demonstrates expression changes for selected genes (derived from Fig 4A). The expression profile is accompanied by a colored bar indicating the standardized log₂ intensities.

(C) Graphical summary of qRT-PCR analysis showing the mRNA level ratio of indicated cytokines between CX₃CR1^{int}Ly6C^{hi}, CX₃CR1^{int}Ly6C^{lo} mononuclear phagocytes and CX₃CR1^{hi}F4/80^{hi} resident MFs sorted from colonic lamina propria of DSS-challenged mice (day 4). Results represent mean (SEM) of two independent experiments using pooled cells from 8-12 mice per experiment.

Ablation of CX₃CR1/GFP^{int} Ly6C^{hi} effector monocytes ameliorates DSS-induced colitis

CX₃CR1/GFP^{int}Ly6C^{hi} effector monocytes, and their immediate precursors, the Ly6C^{hi} blood monocytes, express CCR2 and are hence amenable to conditional *in vivo* ablation by the depleting anti-CCR2 antibody MC-21 (Bruhl et al., 2007; Shechter et al., 2009). Notably, this protocol spares CCR2^{neg} resident CX₃CR1/GFP^{hi}F4/80^{hi} MFs (**Fig 7A, B**). To investigate the functional contribution of the CX₃CR1/GFP^{int}Ly6C^{hi} effector monocytes to the DSS-induced gut inflammation, we injected CX₃CR1^{gfp/+} animals with MC21 starting at day 2 after DSS exposure, once a day, for a period of 5 days, i.e. throughout the window of progressive colonic recruitment of Ly6C^{hi} monocytes (**Fig 2A-C**). Flow cytometry analysis of blood of the MC21-treated animals confirmed the depletion of Ly6C^{hi}, but not CCR2⁻ Ly6C^{lo} monocytes (**Fig 7A**). Analysis of the colonic lamina propria revealed the absence of CX₃CR1/GFP^{int}Ly6C^{hi} effector monocytes. Importantly, no alterations of resident MFs and neutrophil frequencies were observed, while also CCR2^{neg} CX₃CR1/GFP^{int}Ly6C^{lo} cells were significantly reduced supporting their origin from CCR2⁺ effector monocytes (**Fig 7A, B**). Strikingly, DSS challenged mice depleted of Ly6C^{hi} blood monocytes and the CX₃CR1/GFP^{int} infiltrate exhibited significantly milder features of colitis as evaluated and quantified by colonoscopy and body mass change at day 7 after DSS onset (**Fig 7C-E**). Moreover, ELISA on colon explant cultures showed a significant reduction of pro-inflammatory cytokines, such as IL-6 and IL-1 β , as well as IFN γ (**Fig 7F**). Collectively these data establish CX₃CR1/GFP^{int}Ly6C^{hi} effector monocytes in this acute experimental colitis model as pivotal drivers of the colonic inflammation.

Figure 7

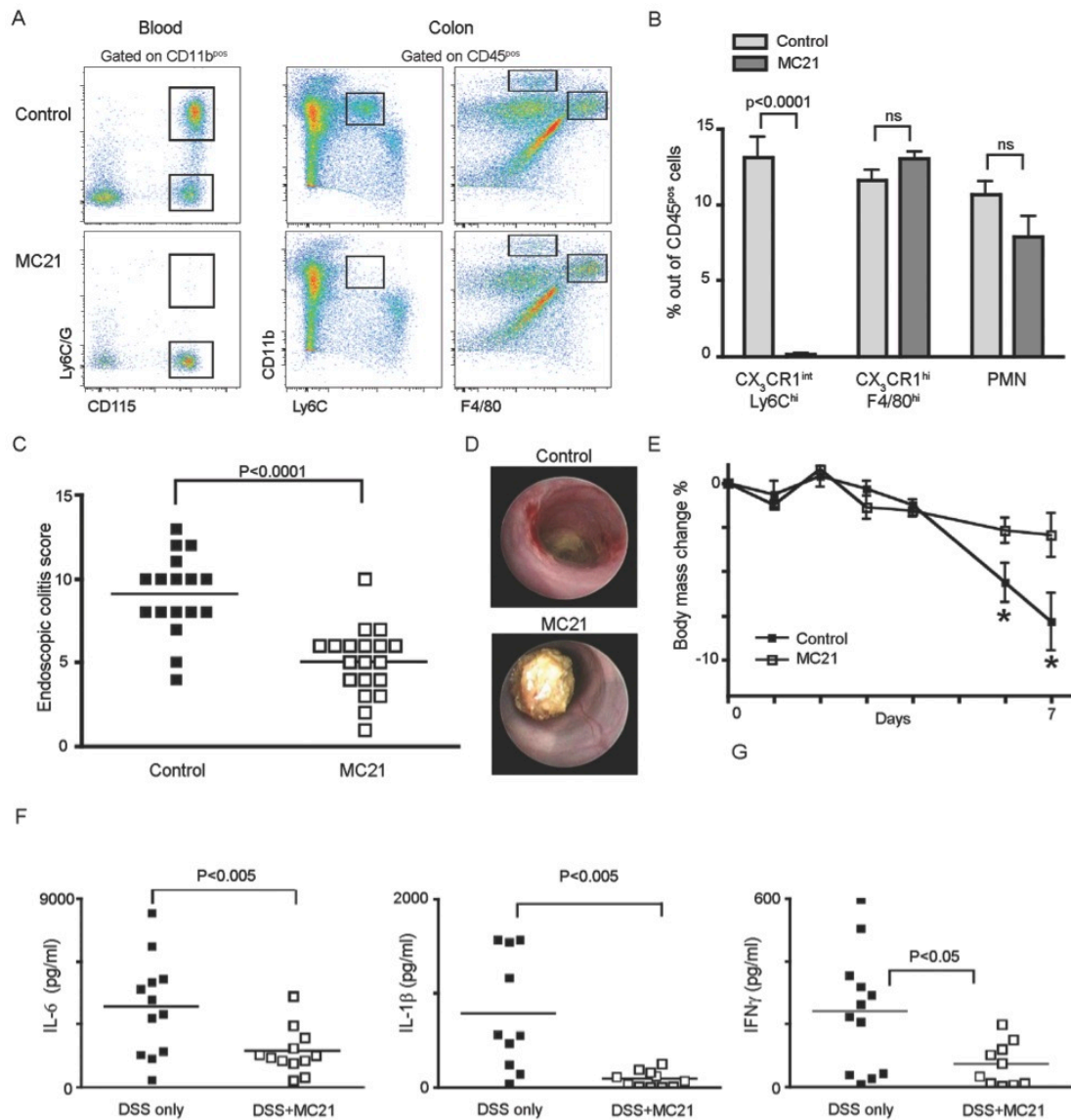


Figure 7. Ablation of CX₃CR1/GFP^{int}Ly6C^{hi} effector monocytes ameliorates DSS-induced colitis

(A) Flow cytometry analysis of blood (gated on CD11b⁺ cells) and colonic lamina propria (gated on CD45⁺ living cells) of mice subjected to DSS (day 7) and treated with MC21 antibody or saline for 5 days. Note efficient selective ablation of blood Ly6C^{hi} monocytes, as well as of colonic lamina propria CD11b⁺Ly6C^{hi} effector monocytes.

(B) Graphical summary of MC21 antibody treatment effect on colonic lamina propria MF subsets, as well as PMNs, mean (SEM) out of CD45⁺ living cells.

(C) Graphical summary of endoscopic colitis grades assessed on day 7 after DSS initiation for mice left untreated or receiving concomitant MC21 antibody treatment (n=19 and n=17, respectively).

(D) Representative colonoscopy images of indicated DSS-treated mice (day 7) with or without MC21 antibody treatment (stills taken from supplementary movie 1)

(E) Graphical summary of body mass changes following DSS challenge of mice left untreated or receiving concomitant MC21 antibody treatment, * indicates p<0.05 at a specific time point.

(F) Graphical summary of IL-6, IL-1 β and IFN γ levels determined by ELISA in colon explant culture supernatants extracts from colons of mice subjected to 7 day DSS treatment with or without MC21 antibody supplement. Results in this figure are representative of two or more independent experiments.

Pro-inflammatory activities of CX₃CR1/GFP^{int} Ly6C^{hi} effector monocytes can be triggered by TLR2 / NOD2 ligands

A comprehensive '*function and pathway*' analysis of our microarray data revealed the selective activation of Nucleotide-binding oligomerization domain-containing protein (NOD) like receptor signaling pathway in CX₃CR1/GFP^{int} Ly6C^{hi} effector monocytes vs. resident CX₃CR1/GFP^{hi} MFs and CX₃CR1/GFP^{int} Ly6C^{lo} cells. More specifically, the array data and subsequent qRT-PCR analysis showed high mRNA expression levels of NOD1/2, Caspase recruitment domain-containing protein 9 (CARD 9), as well as increased expression of Toll-like receptor 2 (TLR2), Inhibitor of nuclear factor kappa-B kinase subunit beta (IKK-β or IKBKB) and the NF-kappa-B complex proteins RelB, NFKB1 (p50) and NFKB2 (p52) in infiltrating compared to resident cells (**Fig 8A, B**). Importantly, TLR2 and NOD2 expression were also upregulated in effector monocytes, as compared to splenic Ly6C^{hi} monocytes (**Fig 8A**).

To probe whether the pro-inflammatory signature of the effector monocytes could have been a result of TLR and NOD-2 engagement, we isolated the cells from colitic mice and exposed them to the respective ligands. CX₃CR1/GFP^{int} Ly6C^{hi} effector monocytes treated with the synthetic TLR2 ligand Pam3CSK4 but also the TLR4 ligand LPS responded to the stimuli with substantial IL-6 secretion (**Fig 8C**), well exceeding the response of CX₃CR1/GFP^{int} Ly6C^{lo} cells and CX₃CR1/GFP^{hi} resident MFs, included in this assay. Addition of muramyl dipeptide (MDP), a peptidoglycan constituent of Gram positive and -negative bacteria and ligand for the intracellular sensor NOD2, resulted in synergistic augmentation of IL-6 production.

To test the role of TLR2, NOD2 in the development of acute gut inflammation, we generated BM chimeras with the respective mutant BM. After exposure of the animals to DSS [TLR2^{-/-} > wt] and [NOD2^{-/-} > wt] chimeras exhibited significantly milder features of colitis as assessed and quantified by colonoscopy at day 7 after onset of DSS application (**Fig 8D, E**). Moreover, in support of the notion an exacerbating role of microbial product-sensing innate immune cells in the DSS model, also [Myd88^{-/-} Trif^{-/-} > wt] mice showed a relative protection as compared to [wt > wt] controls (**Fig 8D, E**). Expression of IL-6 and IL23 (p19) was found only moderately reduced in TLR2^{-/-} and NOD2^{-/-} Ly6C^{hi} effector monocytes compared to wt cells, but most evident in Myd88^{-/-} Trif^{-/-} Ly6C^{hi} effector monocytes (**Fig 8F**). Thus, TLRs other than TLR2 might also be critical for induction of pro-inflammatory cytokines in CX₃CR1/GFP^{int} Ly6C^{hi} effector monocytes.

Collectively, these results suggest that the pro-inflammatory signature of CX₃CR1/GFP^{int}Ly6C^{hi} effector monocytes results from their exposure to bacterial products in the lamina propria and the activation of the TLR and NOD2 pathways in these cells.

Monocyte-derived CX₃CR1/GFP^{int}Ly6C^{lo} cells are migratory, acquire and process luminal antigens and can stimulate T cells

The prominent hallmarks of classical DC are their ability to migrate to the tissue draining LNs and stimulate naïve T cells. In the intestinal lamina propria, CCR7 dependent migration to the mLNs has been shown to be specific feature of CD103⁺ lamina propria DC (Jang et al., 2006; Bogunovic et al., 2009; Coombes et al., 2007; Jaensson et al., 2008; Johansson-Lindbom et al., 2005; Schulz et al., 2009), while CCR7-negative CX₃CR1/GFP^{hi}F4/80^{hi} resident MF are considered non-migratory and hence absent from lymph and mesenteric LNs (Schulz et al., 2009). Our adoptive transfer established that in inflamed colon Ly6C^{hi} monocytes give sequential rise to CX₃CR1/GFP^{int}Ly6C^{hi} and CX₃CR1/GFP^{int}Ly6C^{lo} cells (**Fig 4A**). Interestingly, our microarray analysis revealed significant CCR7 mRNA expression in Ly6C^{hi} effector monocytes as compared to CX₃CR1/GFP^{hi}F4/80^{hi} resident MFs and Ly6C^{hi} splenic monocytes. Moreover, CCR7 transcription was further up-regulated in CX₃CR1/GFP^{int}Ly6C^{lo} cells (**Fig 6B**), as also confirmed by qRT-PCR analysis (**Fig 9A**). CX₃CR1/GFP^{int}Ly6C^{lo} cells did not respond to the Pam3/MDP challenge with IL-6 production and thus seem to have lost the pro-inflammatory activity of effector monocytes (**Fig 8C**). In order to examine whether CCR7 expression on CX₃CR1/GFP^{int} monocyte-derived cells endows these cells with a capability to migrate *in vivo*, we resorted to two photon microscopy imaging. To visualize afferent lymphatic vessels draining the proximal colon towards the mesenteric LNs and distinguish them from blood vessels, we i.v. injected mice with Evans Blue followed by injection of Dextran-FITC 30 minutes later. This resulted in lymphatic vessels labeled with the drained Evans Blue fluorescence (red), while blood vessels lit up in both red and green (**Fig 9B**). In agreement with earlier reports on the small intestine lymphatics (Schulz et al., 2009), scanning of the colonic lymphatic vasculature of CX₃CR1^{gfp/+} mice in steady state demonstrated only rare CX₃CR1/GFP⁺ cells inside the vessels (**Fig 9B**). In contrast, analysis of lymphatics draining the colon of DSS-challenged mice revealed numerous CX₃CR1/GFP⁺ cells in the vessel lumen (**Fig**

9B), supporting the notion that CCR7⁺ CX₃CR1/GFP^{int} monocyte-derived cells are migratory.

In light of our transfer results (**Fig 4A**), these data suggest that the monocyte graft gives sequential rise Ly6C^{hi} effector monocytes and migratory Ly6C^{lo} cells that upregulate MHC II expression and hence seem to acquire APC potential. To directly address this point we next tested the ability of the various monocyte-derived mononuclear phagocyte subsets to ingest and process orally applied antigen for naïve T cell stimulation. DSS-challenged colitic CX₃CR1^{gfp/+} mice were gavaged with ovalbumin (OVA) protein and 12 hrs later sacrificed to isolate colonic CX₃CR1/GFP^{int}Ly6C^{hi} effector monocytes, CX₃CR1/GFP^{int}Ly6C^{lo} cells and CX₃CR1/GFP^{hi} resident MF for co-culture with CFSE labeled OVA-specific CD4⁺ T cells (OT II cells). As seen in **Fig 9C**, CX₃CR1/GFP^{int}Ly6C^{lo} cells induced a significant proliferative expansion of the CD4⁺ T cells as indicated by the dilution of the CFSE dye (and TCR down-modulation). In contrast, the CX₃CR1/GFP^{int}Ly6C^{hi} cells exhibited only moderate antigen stimulatory capability, and, in accordance with previous studies (Schulz et al., 2009), CX₃CR1/GFP^{hi} F4/80^{hi} resident MF failed to prime the naïve CD4⁺ T cells altogether.

Besides their high MHC II and CCR7 expression, the gene expression analysis of CX₃CR1/GFP^{int}Ly6C^{lo} cells also revealed other DC signatures, such as expression of CD135, the receptor for the cytokine Fms-related tyrosine kinase 3 ligand (Flt3L) and expression of transcription factor Zbtb46 (BTBD4), a member of the BTB-ZF family, recently proposed to be specifically expressed in cDC among immune cells (Meredith et al., 2012; Satpathy et al., 2012). To further address the Zbtb46 expression within the CX₃CR1/GFP^{int}Ly6C^{lo} cell compartment, we reconstituted irradiated wt recipients with BM obtained from *Zbtb46*^{gfp/+} mice (Satpathy et al., 2012) and subjected the [*zbtb46*^{gfp/+} > wt] mice to a DSS challenge. DSS-treated [*zbtb46*^{gfp/+} > wt] mice displayed a prominent accumulation of Ly6C^{lo} cells - a fraction of which expressed the GFP label thus confirming Zbtb46 expression. Moreover, treatment of the mice with the CCR2-antibody, significantly reduced both Zbtb46/GFP⁺ and Zbtb46/GFP⁻ Ly6C^{lo} cells, confirming that both cell types were recently derived from CCR2-expressing cells.

Collectively, these results suggest that monocytes that enter the inflamed colon differentiate with time into migratory antigen presenting cells exhibiting phenotypic and functional characteristics of monocyte-derived DC.

Figure 8

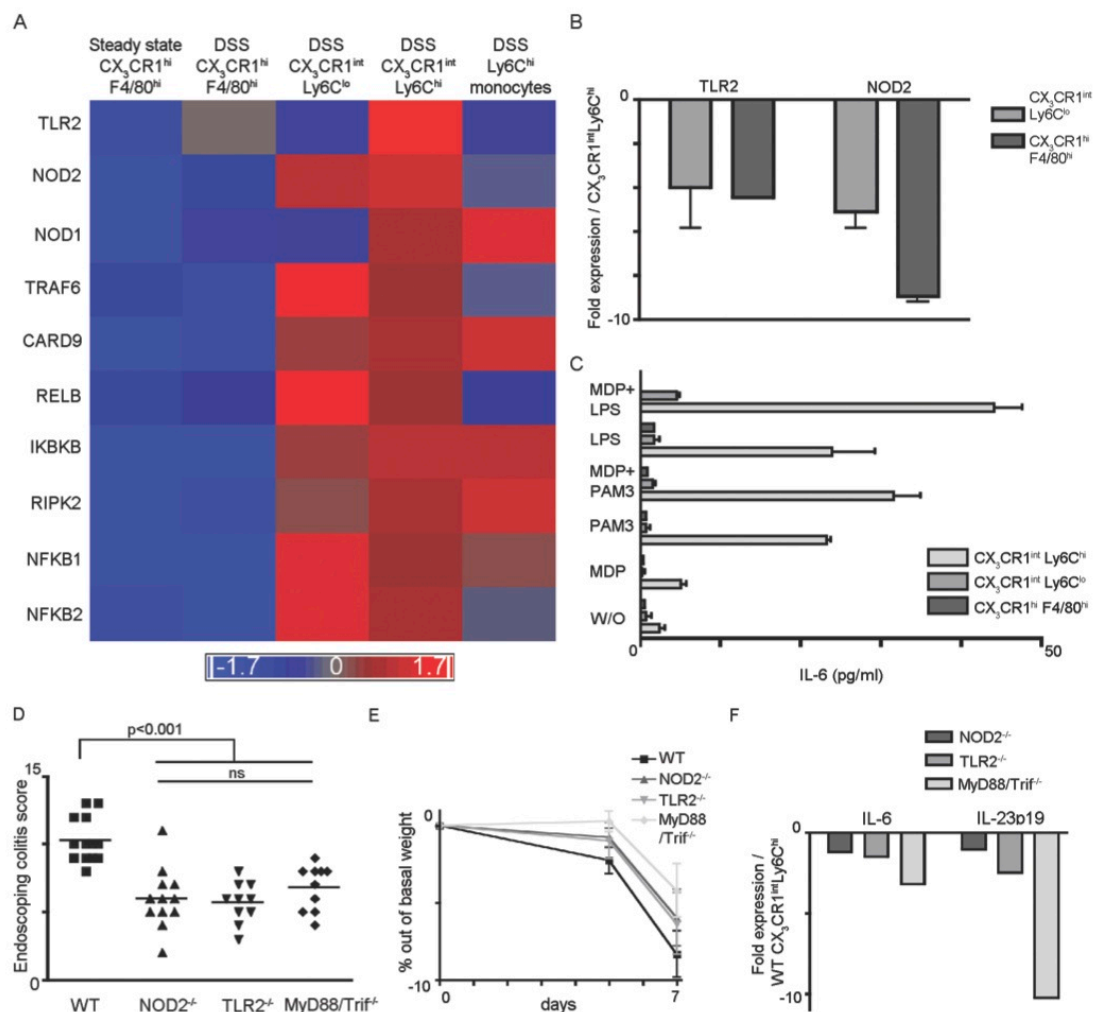


Figure 8. TLR2 / NOD2 ligands trigger pro-inflammatory activity of CX₃CR1/GFP^{int}Ly6C^{hi} effector monocytes

(A) Heat map demonstrating expression changes for genes involved in TLR2 / NOD signaling (derived from Fig 4A). Expression profile is accompanied by a colored bar indicating the standardized log₂ intensities. (B) Graphical summary of qRT-PCR analysis showing fold mRNA expression of TLR2 and NOD2 in CX₃CR1/GFP^{hi}F4/80^{hi} resident MFs and CX₃CR1/GFP^{int}Ly6C^{lo} cells over CX₃CR1/GFP^{int}Ly6C^{hi} effector monocytes. Graph depicts means (SEM) of two independent experiments, each of which comprised pooled RNA from 8-12 mice. (C) ELISA results of IL-6 production by CX₃CR1/GFP^{int}Ly6C^{hi} effector monocytes, CX₃CR1/GFP^{int}Ly6C^{lo} cells and CX₃CR1/GFP^{hi}F4/80^{hi} resident MFs sorted from the colonic lamina propria at DSS day 7 and cultured for 16 hr with MDP (Enzo Life Science) (10 mg/ml), Pam3CSK4 (InvivoGen) (10 μg/ml), LPS (Sigma) (100 ng/ml) or combinations of the above. Results are representative of two independent experiments. (D) Graphical summary of endoscopic colitis grades assessed on day 7 after DSS initiation for [TLR2^{-/-} > wt], [NOD2^{-/-} > wt] and [Myd88^{-/-} Trif^{-/-} > wt] BM chimeras, as well as [wt > wt] controls (n=19 and n=17, respectively). (E) Graphical summary of body mass changes of DSS-treated [TLR2^{-/-} > wt], [NOD2^{-/-} > wt] and [Myd88^{-/-} Trif^{-/-} > wt] BM chimeras, as well as [wt > wt] controls (n=19 and n=17, respectively). Note that the observed differences in body mass change did not reach significance between the groups, though by their tendency support the notion of ameliorated colitis [TLR2^{-/-} > wt], [NOD2^{-/-} > wt] and [Myd88^{-/-} Trif^{-/-} > wt] BM chimeras. (F) Graphical summary of qRT-PCR analysis showing fold mRNA expression of IL6 and IL23 (p19) of CX₃CR1/GFP^{int}Ly6C^{lo} cells isolated from DSS-challenged [TLR2^{-/-} > wt], [NOD2^{-/-} > wt] and [Myd88^{-/-} Trif^{-/-} > wt] BM chimeras, as well as [wt > wt] controls.

Figure 9

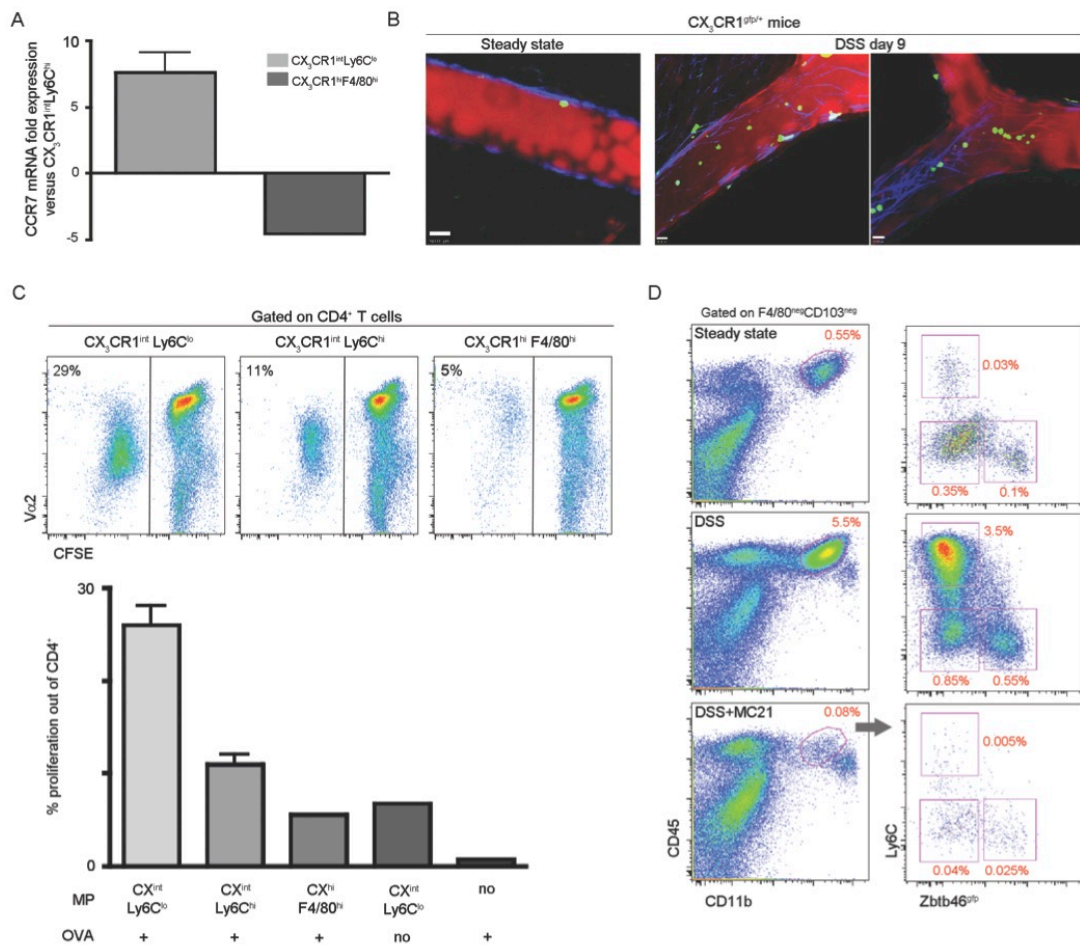


Figure 9. CX₃CR1/GFP^{int}Ly6C^{lo} cells are migratory, acquire luminal antigens and can stimulate naive T cells

(A) Graphical summary of qRT-PCR analysis of CCR7 expression by CX₃CR1/GFP^{int}Ly6C^{lo} and CX₃CR1/GFP^{hi}F4/80^{hi} resident MFs versus CX₃CR1/GFP^{int}Ly6C^{hi} cells isolated from colitic colon. Results are mean (SEM) of two independent experiments using pooled cells from 8-12 mice per experiment.

Note that both CX₃CR1/GFP^{int}Ly6C^{hi} and Ly6C^{lo} cells express CCR7, albeit at distinct levels.

(B) Representative pictures obtained by two photon microscopy imaging of lymphatic vessels draining the colon of CX₃CR1^{GFP/+} mice in steady state and at DSS day 9. Note accumulation of migratory CX₃CR1-GFP⁺ cells in the lymphatic vessels of colitic tissue.

(C) Flow cytometry analysis of OVA-specific CFSE-labelled CD4⁺ T cells (OT II) 3.5 days following their co-culture with CX₃CR1/GFP^{int}Ly6C^{lo} cells, CX₃CR1/GFP^{int}Ly6C^{hi} effector monocytes or CX₃CR1^{hi}F4/80^{hi} resident MFs (1:2 ratio) isolated from DSS day 7 colon of CX₃CR1^{GFP/+} mice gavaged with 100 mg OVA 1 day earlier. Graph summarizes percentages of proliferated / CFSE^{lo} CD4⁺ T cells out of total CD4⁺ T cells. Results represent mean (SEM) of three independent experiments using pooled cells from three mice per experiment for CX₃CR1/GFP^{int}Ly6C^{lo} and CX₃CR1/GFP^{int}Ly6C^{hi} cells, and a pool of seven mice for CX₃CR1/GFP^{hi}F4/80^{hi} cells.

(D) Flow cytometry analysis of colonic lamina propria of [zbtb46^{GFP} > wt] BM chimeras subjected to DSS (day 7) treated with MC21 antibody or saline for 5 days. Note presence of zbtb46/GFP⁺ and zbtb46/GFP⁺ CX₃CR1/GFP^{int}Ly6C^{lo} cells.

Chapter 2

Macrophage restricted IL-10 receptor -, but not IL-10 deficiency causes severe spontaneous colitis

Resident macrophages accumulate and gain pro-inflammatory and migratory traits in an IL-10 deficient environment

IL-10 deficient animals develop severe spontaneous colitis (Kuhn et al., 1993, Maloy et al., 2005). The latter is driven by the commensal gut microbiota (Hoshi et al., 2012, Chaudhry et al., 2011, Rakoff-Nahoum & Medzhitov, 2006) and hence displays variable kinetics and severity, depending on the facility the animals are housed. In order to evaluate the role of CX₃CR1⁺ lamina propria macrophages in this chronic IBD model, we backcrossed *IL-10*^{-/-} mice to *Cx3cr1*^{gfp} mice. Introduction of the reporter gene facilitates the identification of CX₃CR1^{hi} macrophages by flow cytometry and histology. In our animal facility *IL-10*^{-/-} *Cx3cr1*^{gfp/+} mice develop spontaneous intestinal inflammation mainly restricted to the large bowel. Flow cytometric and immunohistochemical analysis of colons of *IL-10*^{-/-} *Cx3cr1*^{gfp/+} mice revealed an accumulation of CX₃CR1^{hi} macrophages in the lamina propria (**Fig 10A, B**). Notably, the lamina propria of *IL-10*^{-/-} *Cx3cr1*^{gfp/+} mice also displayed a prominent infiltrate of CX₃CR1^{int} cells recently reported to be associated with acute colitis (Zigmond et al., 2012, Bain et al., 2012). The majority of the macrophages in the lamina propria exhibited however high expression levels of CX₃CR1, akin to resident macrophages (**Fig 10A**). To study the molecular aspects of these cells under chronic inflammatory condition, we performed an mRNA microarray analysis on cells purified from the colonic lamina propria of *IL-10*^{-/-} *Cx3cr1*^{gfp/+} mice. For comparison, we isolated lamina propria-resident CX₃CR1/GFP^{hi} macrophages from healthy *Cx3cr1*^{gfp/+} animals. Microarray analysis for genes differentially expressed between the two conditions revealed a marked pro-inflammatory signature of macrophages isolated from *IL-10*^{-/-} mice with high expression of Trem1, Nos2, IL-23a, Ccl5 and Serum amyloid A3 (Saa3). Interestingly, *IL-10*^{-/-}, but not WT macrophages also expressed the C-type lectin Clec9A, a steady state marker of CD8⁺ DC (Poulin et al., 2012), as well as CCR7, a chemokine receptor crucial for DC migration towards lymph nodes (Jang et al., 2006). *IL-10*^{-/-} CX₃CR1^{gfp/+} macrophages also displayed reduced expression of the metalloproteinase subunit meprin A, reported to confer

Ulcerative Colitis susceptibility (Banerjee et al., 2009) and the DC- specific ICAM-3 grabbing nonintegrin (DC-SIGN) isoform A (CD209a) (**Fig 10C**). qPCR analysis confirmed the differential expression of these genes and the lack of IL10 mRNA in macrophages isolated from *IL10^{-/-}* mice (**Fig 10D**). In steady state conditions CX₃CR1^{hi} macrophages are non-migratory (Schulz et al., 2009, Zigmond et al., 2012), as indicated by their lack of CCR7 expression. Accordingly, CX₃CR1^{hi} cells are absent from the draining mesenteric lymph nodes (MLN), a feature that also extends to acute inflammation (Schulz et al., 2009, Zigmond et al., 2012). Interestingly though, and in accordance with the observed CCR7 expression in our array analysis, MLN of *IL-10^{-/-} Cx3cr1^{sgfp/+}* mice harbored a sizable population of CX₃CR1^{hi} macrophages (**Fig 10E**). Moreover, the CX₃CR1^{hi} macrophages found in the inflamed lymph nodes expressed intermediate levels of the integrin CD11c and high levels of MHC II and the Fc receptor CD64 similarly to lamina propria-resident colonic macrophages, as well as the chemokine receptor CCR7 (**Fig 10F**). These data corroborate a recent report that these cells can drain from the tissue to the LN under conditions of dysbiosis (Diehl et al., 2013).

Figure 10

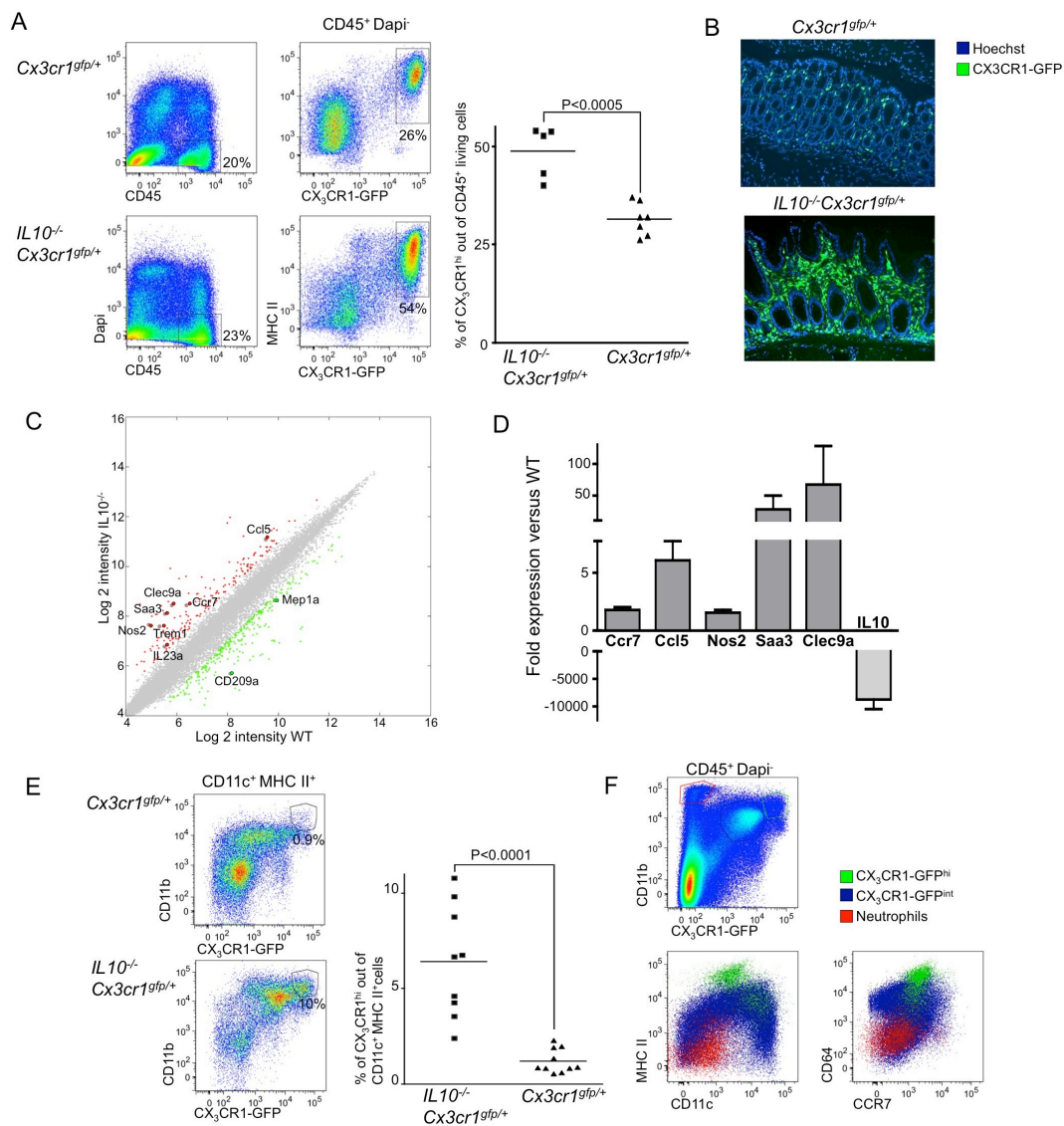


Figure 10. Resident macrophages accumulate and gain pro-inflammatory and migratory traits in an IL-10 deficient environment Flow cytometry analysis (A) and histology (B) of colons of 6 months old *IL10^{-/-}Cx3cr1^{gfp/+}* and *Cx3cr1^{gfp/+}* mice. Percentages of macrophages are out of CD45⁺ living cells. Data are pooled from two independent experiments (n=3-4). Statistical comparisons were performed using the Student's t-test. (C) Scatter plot presenting the differentially expressed genes in *IL10^{-/-}* versus WT resident colonic macrophages. Genes down-regulated or up-regulated above 2 fold are colored in green and red, respectively (based on microarray data). (D) Graphical summary of qPCR analysis showing the mRNA level ratio of indicated molecules between *IL10^{-/-}* and WT resident macrophages sorted from the colonic lamina propria. Data represent mean \pm s.e.m of two independent experiments using sorted cells from a pool of 6 mice per experiment. (E) Flow cytometry analysis of mesenteric lymph nodes of 6 months old *IL10^{-/-}Cx3cr1^{gfp/+}* and *Cx3cr1^{gfp/+}* mice and graphical summary of the prevalence of CX₃CR1/GFP^{hi} macrophages out of CD11c⁺ MHC II⁺ cells. Data are pooled from three independent experiments (n=3-4). Statistical comparisons were performed using the Student's t-test. (F) Flow cytometry analysis of mesenteric lymph nodes of 6 months old *IL10^{-/-}CX₃CR1^{gfp/+}* mice. CD45⁺ Dapi cells were gated for CD11b^{hi}CX₃CR1^{neg} neutrophils (red), CX₃CR1^{hi} cells (green) and CX₃CR1^{int} cells (blue). Data are representative of two independent experiments (n=3).

Cultured macrophages are subject to an IL10-based autocrine regulatory loop curbing their activation and pro-inflammatory activity

CX₃CR1^{hi} macrophages have been established as major producers of intestinal IL10 (Murai et al., 2009, Hadis et al 2011, Rivollier et al., 2012, Zigmond et al., 2012) and these cells can at the same time sense IL10 by virtue of their expression of IL10R (Pils et al., 2010). Of note, qPCR analysis demonstrated unique high expression levels of IL10 and IL10Ra mRNA levels by colonic lamina propria macrophage among immune cells sorted from the colonic lamina propria (**Fig 11A**). To investigate the physiological importance of macrophage-derived IL10, the consequence of IL10 exposure of macrophages, as well as the possible existence of an earlier reported IL10-based autocrine regulatory loop (Pils et al., 2010, Siewe et al., 2006) in the gut, we generated mice that harbor either macrophage-restricted IL10 or IL10Ra mutations. Specifically, we crossed *Cx3cr1^{cre}* animals to animals harboring conditional mutant *IL10* or *IL10Ra* loci.

Flow cytometry analysis of the colonic lamina propria of *Cx3cr1^{cre}Rosa26-RFP^{fl/fl}* reporter mice revealed that almost all intestinal macrophages are affected by this transgenic system, while only a third of the CD11c⁺ CD11b⁻ DC, which represent the main DC population in the colon displayed reporter gene activation (**Fig 11B**).

Interestingly, qPCR analysis of whole colonic tissue of *Cx3cr1^{cre}IL10^{fl/fl}* mice and their *IL10^{fl/fl}* littermates revealed a significant reduction in IL10 mRNA levels in mice with the macrophage-restricted IL10 deficiency, further supporting the notion of macrophages as significant IL10 source in the colon (**Fig 11C**).

To probe for the existence of an IL10-based autocrine regulatory loop, we established monocyte-derived macrophage cultures by exposing CD115⁺ bone marrow (BM) fractions of *Cx3cr1^{gfp/+}*, *Cx3cr1^{cre}IL10^{fl/fl}* and *Cx3cr1^{cre}IL10Ra^{fl/fl}* mice to M-CSF/ Csf-1. After 6 days of culture this protocol yielded a homogeneous population of F4/80⁺MHC II⁺ macrophages that displayed uniform high expression of the CX₃CR1 chemokine receptor (**Fig 11D**). Following stimulation with LPS, *WT* and *Cx3cr1^{cre}IL10Ra^{fl/fl}* macrophages, but not *Cx3cr1^{cre}IL10^{fl/fl}* macrophages, secreted IL10 (**Fig 11E**), establishing efficient rearrangement of the ‘floxed’ IL10 loci in the latter cells. Macrophages stimulated with LPS responded with an inflammatory phenotype, secretion of TNFα and IL6 (**Fig 11F**), and an upregulation of CD40 and TREM-1 surface markers (**Fig 11G**). The levels of pro-inflammatory cytokine secretion by both IL10- and IL10R-deficient macrophages were significantly higher

than that of WT cells. Addition of recombinant IL10 simultaneously with LPS reduced IL6 and TNF α production of *Cx3cr1^{cre}IL10^{fl/fl}* macrophages to WT levels, while *CX3CRI^{cre}IL10Ra^{fl/fl}* macrophages remained unaffected (Fig. 11F). Collectively these data corroborate the previously reported (Pils et al., 2010, Siewe et al., 2006) existence of an autocrine regulatory loop and that in a culture system macrophage-derived IL10 can act back on its source to suppress the production of pro-inflammatory cytokines and hyper-activation.

Figure 11

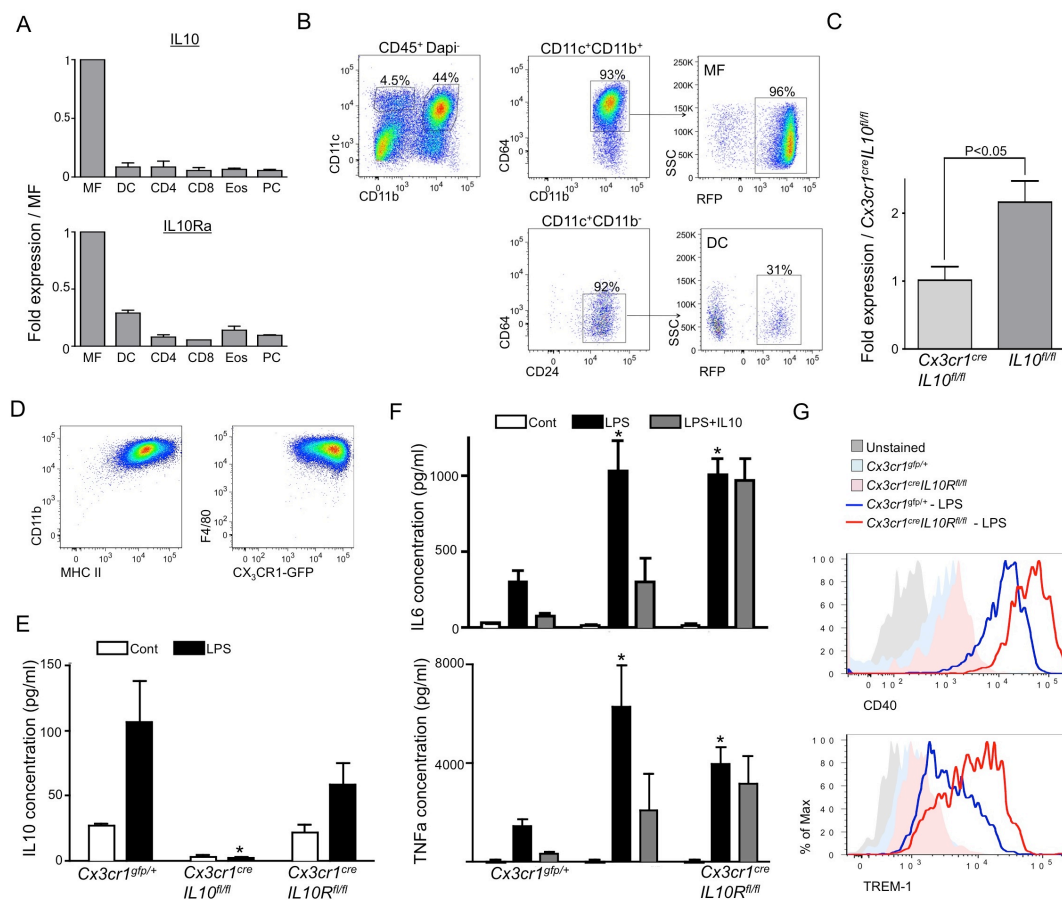


Figure 11. Interleukin 10-based autocrine regulatory loop

(A) qPCR analysis for IL10 (upper) and IL10Ra (lower) performed on RNA extracted from cells sorted from the colonic lamina propria of *Cx3cr1^{fl/fl}* mice. MF, macrophages; DC, dendritic cells; CD4, CD4⁺ T cells; CD8, CD8⁺ T cells; Eos, Eosinophils; PC, Plasma cells. Data are pooled from two independent experiments (n=10). (B) Flow cytometry analysis of mononuclear phagocytes in the colonic lamina propria of *Cx3cr1^{cre}Rosa26-RFP^{fl/fl}* mice. Data are representative of three independent experiments. (C) qPCR for IL10 performed on RNA extracted from the colons of *Cx3cr1^{cre}IL10^{fl/fl}* and *IL10^{fl/fl}* mice. Data are pooled from two independent experiments (n=3). (D) Flow cytometry analysis of macrophages derived from BM of *Cx3cr1^{fl/fl}* mice. Data are representative of three independent experiments. (E) BM-derived macrophages from *Cx3cr1^{fl/fl}*, *Cx3cr1^{cre}IL10^{fl/fl}* and *Cx3cr1^{cre}IL10R^{fl/fl}* mice were stimulated with LPS. Supernatants were analyzed by ELISA for IL10. Data are pooled from two independent experiments.

(F) ELISA for IL6 and TNF α performed on culture supernatants of BM-derived macrophages from *Cx3cr1^{gfp/+}*, *Cx3cr1^{cre}IL10^{fl/fl}* and *Cx3cr1^{cre}IL10R^{fl/fl}* mice treated with LPS or LPS and IL10. Data are pooled from three independent experiments. Results for E-F are shown as mean \pm s.e.m. Statistical comparisons were performed using one-way ANOVA followed by Bonferroni (*P < 0.05). (G) BM-derived macrophages from *Cx3cr1^{gfp/+}* and *Cx3cr1^{cre}IL10R^{fl/fl}* were analyzed by flow cytometry for specific surface markers. Data are representative of two independent experiments.

Macrophage-restricted IL10 deficiency does not result in spontaneous enterocolitis or impairment of T regulatory cell compartment

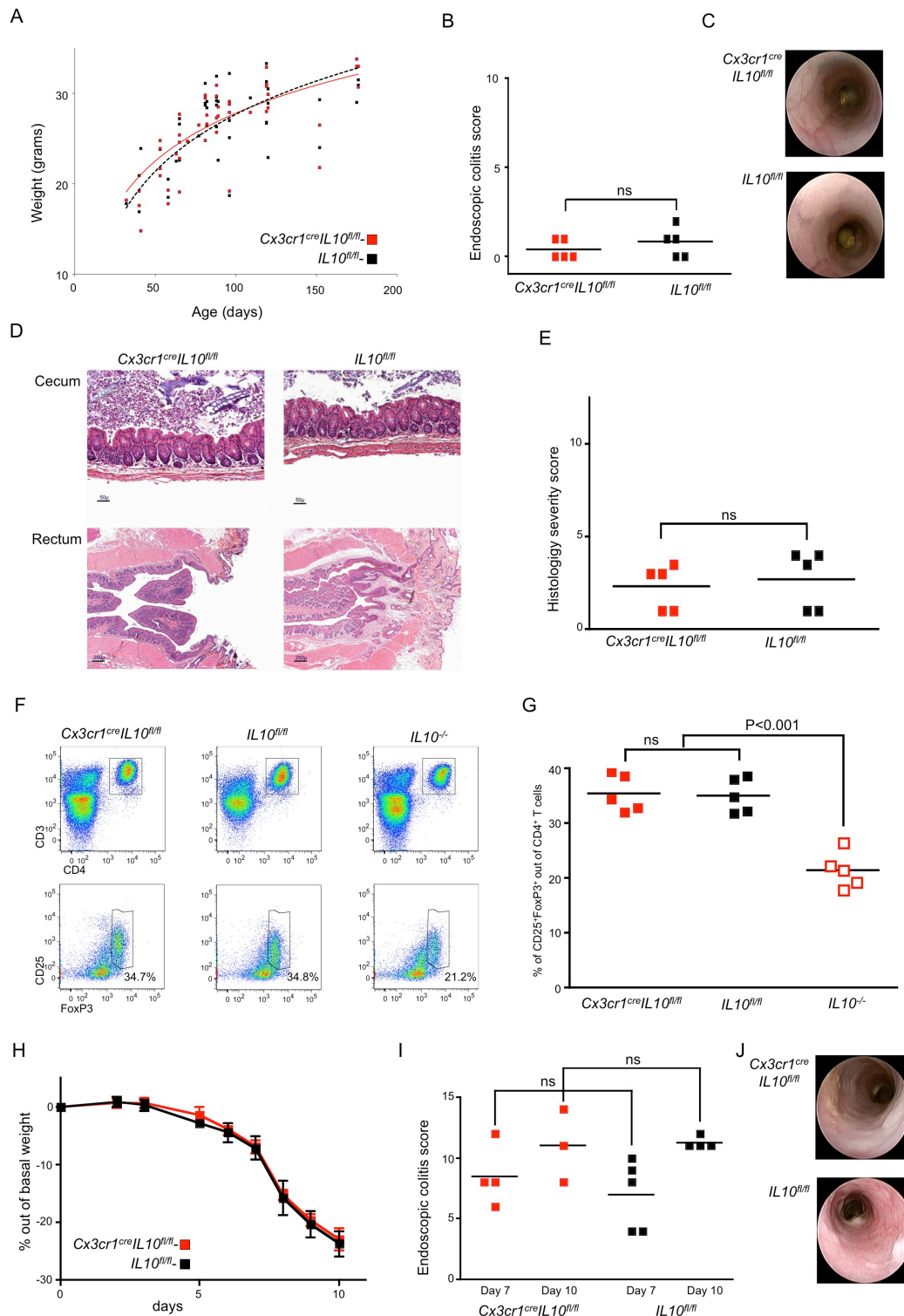
To probe the importance of macrophage-derived IL10 and the above described IL10-based autoregulatory loop in the control of physiological macrophage hyper-activation, we monitored *Cx3cr1^{cre}IL10^{fl/fl}* mice and their littermates weekly for body mass gain and general well being. Curiously, mice harboring IL10-deficient resident CX₃CR1^{hi} macrophages developed normally and did not display any signs of colitis defined by endoscopic or histological examination up to the age of six months (**Fig 12A-E**). Notably, macrophage-derived IL10 has been proposed to be critical for the maintenance of gut homeostasis through its impact on T_{reg} cells (Murai et al., 2009, Hadis et al., 2011, Liu et al., 2011). Comparison of the intestinal T_{reg} pool of *Cx3cr1^{cre}IL10^{fl/fl}* mice to that of their *IL10^{fl/fl}* littermates revealed however no difference in the prevalence of these cells (**Fig 12F, G**). This was in contrast to colitic *IL10^{-/-}* mice that displayed lower percentages of T_{reg} cells (out of total CD4⁺ T cells), likely due to inflammation-associated CD4⁺ non-T_{reg} infiltrates (**Fig 12F, G**). Although unchallenged *Cx3cr1^{cre}IL10^{fl/fl}* mice did not develop spontaneous gut pathology, they might be more susceptible to the development of intestinal inflammation. To test this issue, *Cx3cr1^{cre}IL10^{fl/fl}* mice and their *IL10^{fl/fl}* littermates were subjected to the acute dextran sodium sulphate (DSS) colitis model. Surprisingly, presence or absence of IL10 production by CX₃CR1^{hi} macrophages made no difference and colitis severity was similar in both groups of animals as evaluate by body mass change and colonoscopy (**Fig 12H-J**). Collectively, these data establish that CX₃CR1^{hi} macrophage-derived IL10 is dispensable for the maintenance of gut homeostasis, potentially due to the redundancy of IL10 sources.

Figure 12. Mice harboring macrophage-restricted IL10 mutations display neither developmental abnormalities nor intestinal pathology

(A) Graphical summary of body mass follow up of male *Cx3cr1^{cre}IL10^{fl/fl}* and *IL10^{fl/fl}* mice. ns, non significant. (B) Graphical summary of endoscopic colitis grades for 6-months-old *Cx3cr1^{cre}IL10^{fl/fl}* and their *IL10^{fl/fl}* littermates. (C) Representative colonoscopy images of indicated mice. (D) Representative histological images of cecum and rectum of 6-months-old *Cx3cr1^{cre}IL10^{fl/fl}* and *IL10^{fl/fl}* mice. (E) Graphical summary of histological severity score of indicated mice. (F) Flow cytometry analysis of CD4⁺ CD25⁺ FoxP3⁺ regulatory T cells in the lamina propria of *Cx3cr1^{cre}IL10^{fl/fl}*, *IL10^{fl/fl}* and *IL10^{-/-}* mice. (G) Graphical summary of regulatory T cell prevalence in

the lamina propria of indicated mice. (H) Graphical summary of body mass changes following DSS challenge of *Cx3cr1^{cre}IL10^{fl/fl}* and *IL10^{fl/fl}* mice. (I) Graphical summary of endoscopic colitis grades in day 7 and 10 following DSS initiation in indicated mice. (J) Representative colonoscopy images of indicated mice in day 10 following DSS initiation. Data are representative of at least two independent experiments (n=5), results are shown as mean \pm s.e.m. Statistical comparisons were performed using Student's t-test (B, E, I), or one-way ANOVA followed by Bonferroni (G).

Figure 12



Macrophage-restricted IL10 receptor deficiency results in severe enterocolitis

In order to evaluate the physiological significance of IL10 receptor expression by resident macrophages, *Cx3cr1^{cre}IL10Ra^{fl/fl}* mice and their *IL10Ra^{fl/fl}* littermates were evaluated weekly for body mass gain and general well being. *Cx3cr1^{cre}IL10Ra^{fl/fl}* males exhibited growth retardation compared to their *IL10Ra^{fl/fl}* littermates, with reduced body mass as early as 6 weeks of age and about 20 percent reduction in average weight at the age of 6 months (**Fig 13A**). Rectal prolapse developed progressively and was by six months of age detected in all male *Cx3cr1^{cre}IL10Ra^{fl/fl}* mice but none of their *IL10Ra^{fl/fl}* littermates (**Fig 13B**). Importantly, although *IL10Ra^{fl/fl}* animals were co-housed up to an age of 12 months with their sick *Cx3cr1^{cre}IL10Ra^{fl/fl}* littermates, they did not display any sign of pathology, excluding the appearance of a dominant colitogenic microbiota in this experimental system. Colonoscopy assessment revealed features compatible with chronic colitis including mild to moderate diarrhea, thickening of the colonic wall, ulcers with fibrin deposits, and irregularity of the structural pattern of the blood vessels (**Fig 13C, D**). Histological assessment revealed chronic inflammation characteristics only in *Cx3cr1^{cre}IL10Ra^{fl/fl}* mice with normal appearance of their *IL10Ra^{fl/fl}* littermates (**Fig 13E, F**). Histopathological alterations in *Cx3cr1^{cre}IL10Ra^{fl/fl}* included multifocal infiltrates composed of mononuclear cells, neutrophils and lymphocytes in the lamina propria, sub-mucosa and rarely transmural, accompanied by epithelial hyperplasia, erosions and occasionally ulcers (**Fig 13E, F**). These changes were most prominent in the cecum and the distal colon, while in the terminal ileum only mild inflammatory infiltrates were observed in few mice. Multiplex cytokine analysis of sera and supernatants of colon explant cultures disclosed a significant increase in IL6, IL17 and IL10 in *Cx3cr1^{cre}IL10Ra^{fl/fl}* mice (**Fig 13G**). Fluorescent histological staining for T cells (CD3) and neutrophils (Ly6G) revealed prominent accumulation of these cells in the lamina propria of *Cx3cr1^{cre}IL10Ra^{fl/fl}* mice (**Fig 13H**). Collectively these results establish that CX₃CR1^{hi} macrophages have to sense IL10 to maintain gut homeostasis. Together with the above data obtained from CX₃CR1^{hi} macrophages isolated from IL10^{-/-} mice, these findings highlight (1) the central role CX₃CR1^{hi} macrophages as drivers of intestinal pathology and (2) IL10 as a critical conditioning factor of the monocyte-derived cells.

Figure 13

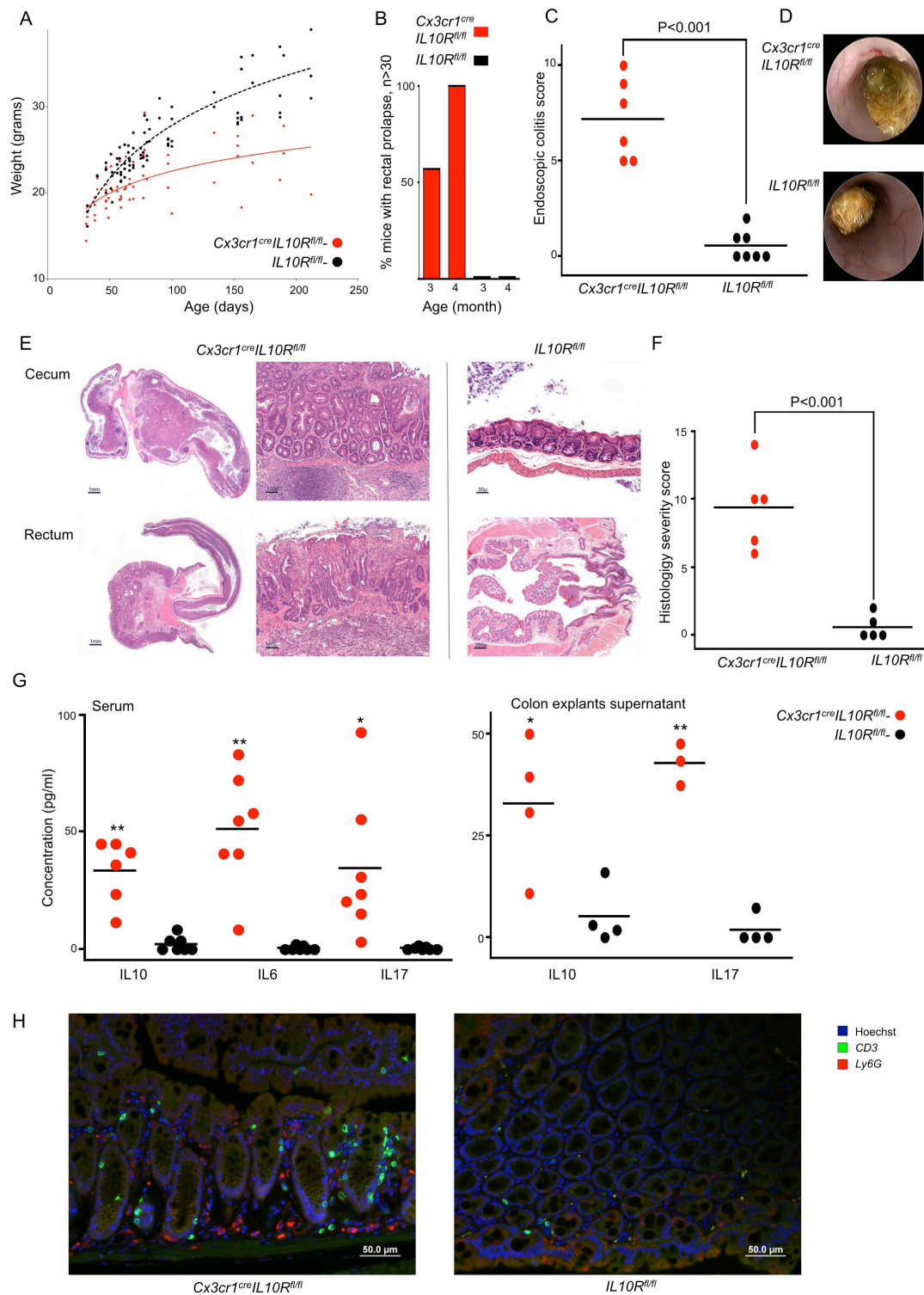


Figure 13. Mice harboring a macrophage-restricted IL10R mutation display spontaneous colitis and growth retardation (A) Graphical summary of body mass follow up of male *Cx3cr1^{cre}IL10R^{fl/fl}* and *IL10R^{fl/fl}* mice. (B) Graphical summary of rectal prolapse incidence of indicated male mice. (C) Graphical summary of endoscopic colitis grades for 6-months-old male *Cx3cr1^{cre}IL10R^{fl/fl}* mice and their *IL10R^{fl/fl}* littermates. Data are representative of two independent experiments (n=6-7). (D) Representative colonoscopy images of indicated mice. (E) Representative histological images of cecum and rectum of 6-months-old *Cx3cr1^{cre}IL10R^{fl/fl}* and *IL10R^{fl/fl}* mice. (F) Graphical summary of histological severity score of indicated mice (n=5). (G) Graphical summary of IL10, IL6 and IL17 levels determined by Multiplex assay in colon explants culture supernatants (n=4) and sera (n=7) of 6-months-old *Cx3cr1^{cre}IL10R^{fl/fl}* and *IL10R^{fl/fl}* mice. (H) Immuno-fluorescence analysis for CD3 (T cells) and Ly6G (Neutrophils) done on sections from the distal colon of the indicated mice. Statistical comparisons were performed using the Student's t-test (A, C, F, G), (*P < 0.05, **P < 0.005).

IL10 receptor deficient lamina propria macrophages exhibit a pro-inflammatory gene expression signature characteristic of intestinal inflammation

To study molecular aspects of the pathology driven by intestinal IL10R-deficient macrophages we performed mRNA microarray analysis on highly purified resident CX₃CR1^{hi} macrophages freshly isolated from the colonic lamina propria of 6 weeks-old *Cx3cr1^{cre}IL10R^{fl/fl}* mice. For comparison, we isolated resident macrophages from *CX₃CR1^{gfp/+}* animals. Hierarchical clustering of the samples demonstrated high resemblance of the duplicate data sets obtained from mutant and WT macrophages (**Fig 14A**). Microarray analysis revealed 156 up-regulated and 176 down-regulated genes that significantly changed at least two fold in IL10R-deficient versus WT macrophages (**Fig 14B**). The list of genes up-regulated in *IL10R^{-/-}* macrophages revealed a marked pro-inflammatory signature with similarity to the profile obtained from colonic macrophages isolated from *IL10^{-/-}* mice (**Fig 10C**). This included elevated expression of Trem-1, Nos2, IL-23a, Ccl5, Clec9A, Ccr7 and Saa3. qPCR analysis confirmed the differential expression of these genes and the lack of IL10Ra mRNA in macrophages isolated from *Cx3cr1^{cre}IL10R^{fl/fl}* mice (**Fig 14C**). Since the IL10R-deficient intestinal macrophages initiate the inflammatory process in the CX₃CR1^{cre}IL10Ra^{fl/fl} model, their gene signature might offer new insights into the pathogenesis and potential targets of future therapeutic IBD intervention. Accordingly, the comparison of the genes up-regulated in colonic CX₃CR1^{cre}IL10Ra^{fl/fl} macrophages with Inflammatory Bowel Disease (IBD) / Ulcerative colitis (UC) susceptible genes retrieved from GWAS (Jostins et al., 2012) revealed significant overlap highlighting the potential value of this novel colitis model for IBD studies (**Fig 14D**). Interestingly, this included a signature of altered lipid

metabolism with a shift in eicosanoid synthesis from leukotriene to prostaglandin, suggesting a potential rise of prostaglandin E₂ (PGE₂). Local levels of this highly bioactive fatty acid-derived lipid compound, which has been implicated in the IBD pathophysiology and correlates with UC disease severity (Lauritsen et al., 2006), are determined by the balance of PGE₂ synthesis by Cyclo-oxygenases (COX1 and 2) and PGE₂ degradation by 15-hydroxyprostaglandin dehydrogenase (Hpgd) (**Fig 14E**). *Cx3cr1^{cre}IL10R^{fl/fl}* macrophages displayed significantly reduced levels of Hpgd, a finding confirmed by qPCR (**Fig 14F**). Furthermore, *Cx3cr1^{cre}IL10R^{fl/fl}* macrophages exhibited a significant reduction of arachidonate 5-lipoxygenase (*Alox5*) and leukotriene C4 synthase (*Ltc4s*) expression, i.e. two enzymes required for leukotriene synthesis (**Fig 14E**). Moreover, culture supernatants of colon explants isolated from *Cx3cr1^{cre}IL10R^{fl/fl}* mice displayed significantly elevated PGE₂ levels, as compared to littermate controls (**Fig 14G**). Finally, and supporting the notion of an increased PGE₂ concentration due to reduced degradation in immediate vicinity of the mutant macrophages, we detected a number of genes reported to be induced by PGE₂ in the gene expression signature of the CX₃CR1^{cre}IL10R^{fl/fl} macrophages, most notably *Il23a* and *Ccr7* (Sheibanie et al., 2007, Muthuswamy et al., 2010). Collectively, the molecular profiling defined the impact of the inability of the CX₃CR1^{hi} macrophages to sense IL10 and the impaired conditioning of their immediate monocytic precursors. Comparison of the gene expression signature of IL10R-deficient macrophages and gene expression profiles obtained from IBD patient might provide leads for novel therapeutic approaches.

Figure 14. Gene expression profiling of IL10 receptor deficient lamina propria macrophages

- (A) Hierarchical clustering of the samples of the microarray data obtained from sorted colonic lamina propria macrophages of *Cx3cr1^{cre}IL10R^{fl/fl}* and *Cx3cr1^{gfp/+}* mice. Each sorting was done from a pool of 4-6 mice. The clustering was performed on the log 2 intensities, using Pearson dissimilarity as a distance measure.
- (B) Volcano plot based on the microarray data comparing gene expression levels in IL10R deficient and WT colonic macrophages.
- (C) Graphical summary of qPCR analysis showing the mRNA level ratio of indicated genes between colonic lamina propria macrophages sorted from *Cx3cr1^{cre}IL10R^{fl/fl}* and *Cx3cr1^{gfp/+}* mice. Results represent mean ± s.e.m of 2 independent experiments.
- (D) List of 156 significantly up-regulated and 176 significantly down-regulated genes in CX₃CR1^{cre}IL10R^{fl/fl} colonic resident macrophages segregated into biological / functional categories. Genes which were up regulated in GWAS of Inflammatory Bowel Disease (IBD) and Ulcerative colitis (UC) ⁴⁵ as well are marked in red and green, respectively. The p-values for the overlap between the up-regulated genes and IBD / UC GWAS genes are 0.005 and 0.045 respectively (calculated using the hypergeometric distribution).

Chapter 3

Utilization of Murine Colonoscopy for Orthotopic Implantation of Colorectal Cancer

Establishment of orthotopic mouse model of CRC utilizing the murine colonoscopy system

Small animal endoscopy is considered today as the gold standard tool for the surveillance of colonic inflammatory disorders and CRC. In order to adapt this system for the purpose of orthotopic implantation of CRC tumor cells into the colonic sub-mucosa we have specially designed a hypodermic needle that can pass through the endoscopic sheath working channel of the Karl Storz Coloview mini-endoscopic system. The hypodermic needles were custom made according to our specification by Cadence Inc. U.S.A., and are made from 8 inch long flexible stainless flexible steel, with 30 gauge outer diameters, and a short bevel at a 45 degree angle. This hypodermic needle confers several design advantages; the flexible steel together with needle's dimensions alleviate the injection maneuver and allow the smooth pass through the working channel and the Luer lock, which is screwed on it to avoid air leakage. Moreover, the blunt bevel allows injection into the sub-mucosa with reduced risk for perforation or spilling of the injected material to the lumen. We first examined the tissue distribution of injected reagents and assessed the appropriate injection volume by injecting India ink marking dye into the colonic sub-mucosa layer. An injection volume of 50 μ l gave the best combination of minimal leakage and focal scattering of the ink beneath the epithelial layer (**Fig. 15A**). Flushing of the colonic lumen by applying saline through the examination sheath of the endoscope confirmed the localization of the injected ink beneath the epithelial layer. Histological analysis confirmed that the India ink is retained within the colonic lamina propria even 5 days following its orthotopic injection. Importantly, histological analysis of mice injected with sterile Dulbecco's Phosphate Buffered Saline without calcium and without magnesium (PBS^{-/-}) revealed a normal healthy colonic architecture at the injection site confirming that this method is minimally invasive.

The MC-38 murine colon tumor is a grade III adenocarcinoma, which was chemically induced in a female C57BL/6 mouse and used since then as a transplantable mouse tumor model. To test the feasibility of the orthotopic tumor implantation method, we injected 1x10⁵ MC38 CRC tumor cells into the colonic sub-mucosa of syngeneic

C57BL/6 mice. Repetitive colonoscopy of recipient mice revealed the progressive rapid development of the tumor breaking into the gut lumen specifically at the injection site. Endoscopic grading according to tumor size relatively to the circumference of the colon revealed progressive tumor growth from grade 1 at day 5 to grade 4 by day 12 and reaching grade 5, occupying almost the entire colonic circumference by only day 19 (**Fig. 15B**). Hematoxyline and eosin (H&E) staining of histology sections revealed a typical CRC architecture of the tumors with normal adjacent mucosa and the projection of the tumor through the epithelial layer into the lumen (**Fig 15C,D**). Histological analysis of colonic tissue isolated from mice subjected to orthotopic implantation of 1×10^5 MC38 CRC cells expressing GFP confirmed the establishment of a small tumor within the lamina propria and the penetration of tumor derived GFP⁺ cells through the epithelial layer already by day 5 (**Fig. 15E,F**).

In order to evaluate the growth kinetics of the CRC tumors using this method we injected C57BL/6 mice with distinct amounts of MC38 cells (10^3 , 10^4 and 10^5 cells) and followed the colonic circumference and developmental grade of established tumors over time by colonoscopy (**Fig 16A**). The results graphically summarized in **figure 16B** show that the tumor growth kinetics was in direct correlation to the amount of injected cells reaching colon circumference of 21% (+/- 4.22), 54.1% (+/- 7.0), and 80% (+/- 7.2) 3 weeks following the injection of 10^3 , 10^4 , and 10^5 MC38 cells, respectively. Statistical analysis comparing each time point (1,2 and 3 weeks) for the different groups (10^3 , 10^4 and 10^5 cells) confirmed significant differences (at least $p < 0.05$) in all the time points for percentage of colonic circumference as well as for tumor grade. Exceptional was the comparison of tumor grade between the 10^4 & 10^5 groups at week 3 as most of the tumors in these groups were already grade 5 that includes all tumors above 50% of colonic circumference.

Collectively, we established here a new method for the efficient orthotopic implantation of CRC tumors using murine endoscopy in a rapid and minimal invasive manner, with a limited amount of cells required for injection, and with an absolute control on tumor's incidence, location and growth kinetics.

Figure 15

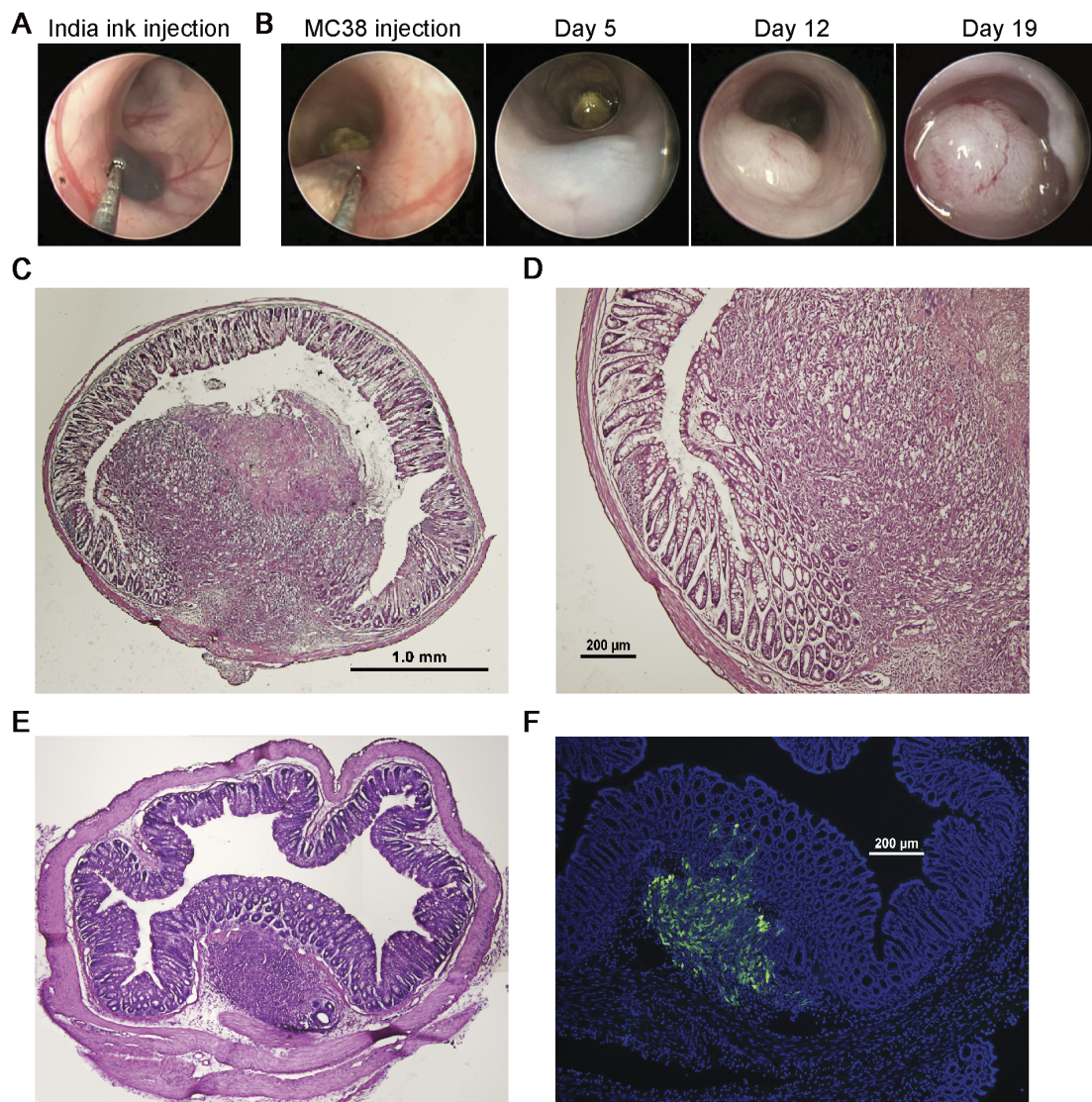


Figure 15. Orthotopic induction of CRC using the mouse colonoscopy system.

(A) Colonoscopy image presenting colonic sub-mucosal injection of India-ink dye in C57BL/6 mouse for the assessment of the appropriate injection volume and its distribution at the colonic lamina propria.

(B) Representative colonoscopy images indicating the progressive development of CRC tumor within the same C57BL/6 mouse following orthotopic implantation of 1×10^5 MC38 CRC cells from day 5, through day 12 to day 19.

(C-D) Representative image of histology specimen stained with hematoxyline and eosin (H&E) and isolated from colonic injection site at day 14 following injection of 1×10^5 MC38 CRC cells. Magnifications: C- [x40], D - [x100]. Note the boundary area between the tumor and the adjacent normal mucosa and the projection of the tumor through the epithelial layer into the lumen.

(E) Representative image showing H&E staining of histology specimen of murine-CRC tumor generated 5 days following orthotopic implantation of MC38 CRC tumor cells into C57BL/6 mice (Magnification x40). (F) Fluorescent microscopic image showing GFP labeled tumor cells and their dissemination through the epithelial layer toward the lumen (Magnification x100). Data are representative of three independent experiments.

Figure 16

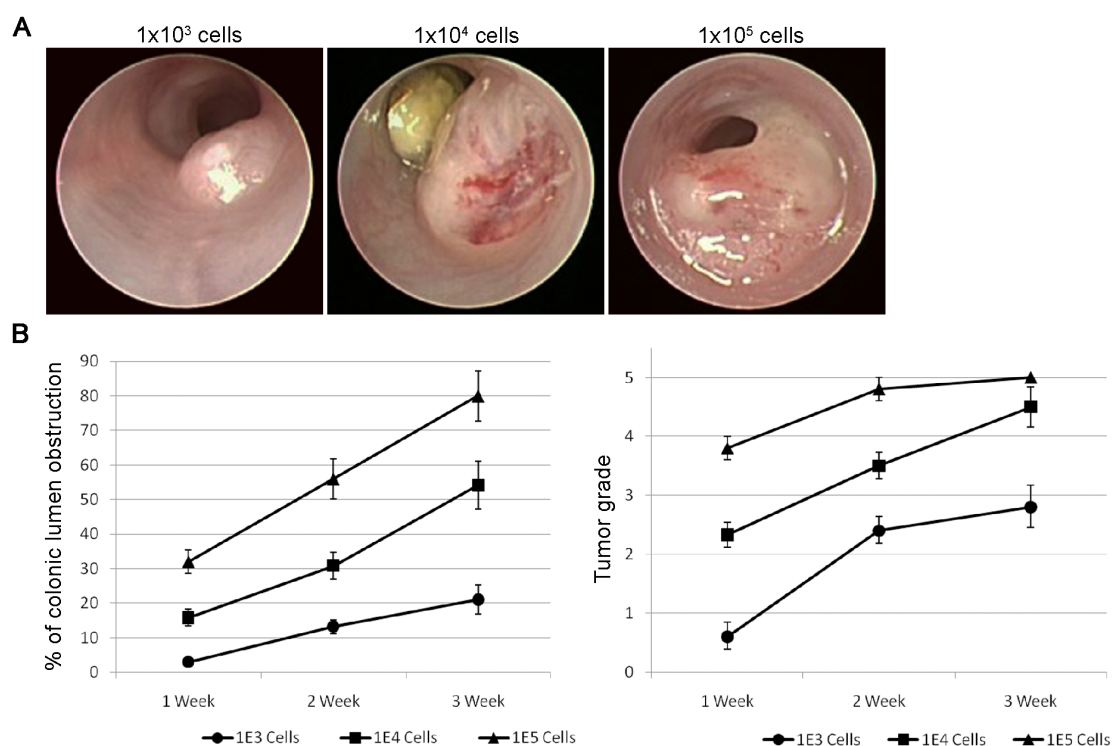


Figure 16. Absolute control on growth kinetics of orthotopically induced tumors (A) Representative colonoscopy images demonstrating the correlation between amount of injected MC38 tumor cells and the size of the established CRC tumor 3 weeks following orthotopic tumor cell implantation. (B) Graphs summarizing the growth kinetics, circumference percentage and developmental grade of colonic tumor in correlation to the amount of injected MC38 CRC cells. Note the rapid establishment of grade 5 tumors already 2 weeks following implantation of only 1×10^5 MC38-CRC cells. Each group consisted of 5 mice.

Orthotopic implantation of genetically manipulated CRC-tumor cells

One of the benefits of cancer implantation over spontaneous developing tumor models is the ability to genetically modify the established tumor. As a proof of principle, we injected BALB/c mice with 1×10^5 CT26 murine CRC cells, which had previously been genetically manipulated to express luciferase. Whole body bioluminescence optical imaging (Biospace Photon imager) revealed the existence of a CRC tumor specifically around the injection site that could be further semi-quantified according to its emitted luminescence (**Fig 17A**). Notably, this approach may be useful for the assessment of tumor burdens without the need to sacrifice the mice. An additional genuine advantage of the endoscopic implantation model is the capability to implant several adjacent yet distinct tumors in the same mouse, which were genetically modified to over-express or silence genes of interest, enabling their direct comparison in an identical host milieu. Using a lentiviral reporter system, we transduced two

distinct fluorescent reporter genes into the MC38 cell line to establish the MC38-GFP and MC38-RFP lines (**Fig. 17B upper left panel**). Injection of the MC38-GFP cells and adjacent to them the MC38-RFP cells resulted in the co-formation of two genetically identical tumors that vary only by their location and expression of the inserted reporter genes (**Fig. 17B lower left panel and right panel**).

Figure 17

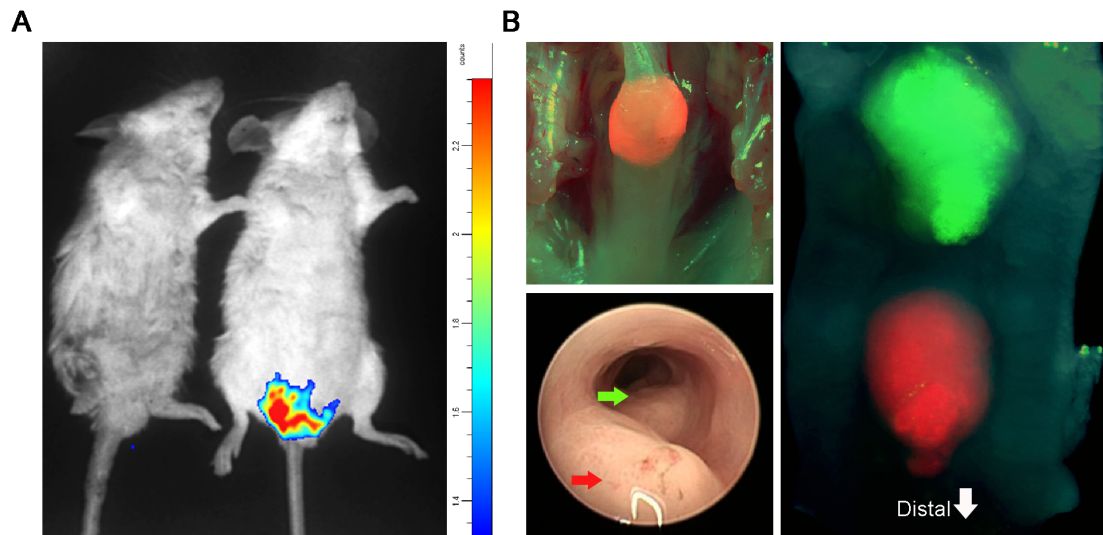


Figure 17. Orthotopic induction of distinct genetically manipulated CRC tumors

(A) Color-coded representative image of whole body bioluminescence optical imaging of BALB/c mice 2 weeks following sub-mucosal injection of PBS-/- (left mouse) or 1×10^5 CT26 CRC tumor cells expressing luciferase and 10 minutes following i.p injection of D-Luciferin. Note the luminescence emission specifically from the area of injected CRC tumor cells (right mouse).

(B) Upper left panel – fluorescent stereo-microscopic image overlaid on a photo graphic image of recipient C57BL/6 mouse colon 3 weeks following its orthotopic injection with MC38 CRC cells that were genetically manipulated by lentiviral reporter system to express RFP, magnification x10. Down left panel – colonoscopy image of C57BL/6 mouse colon following orthotopic implantation of two adjacent MC38 CRC tumor cells; MC38-RFP (red arrow) and MC38-GFP (green arrow). Right panel - fluorescent stereo-microscopic image overlaid on a photo graphic image of recipient C57BL/6 mouse opened colon 2 weeks following side-by-side orthotopic injection of MC38-RFP (distal) and MC38-GFP (proximal) CRC tumor cells, magnification x10. Note the induction of two adjacent CRC tumors that differ only by the expression of the transduced reporter gene. Data are representative of three independent experiments.

DISCUSSION

This PhD thesis is comprised of three parts that collectively revolve around the study of intestinal inflammation and pathogenesis. In the first study we explored differential fates of blood monocytes in the healthy and inflamed colon of mice. We showed that Ly6C^{hi} monocytes differentiated in healthy tissue into resident CX₃CR1^{hi} macrophages, acquiring a characteristic non-inflammatory gene expression profile. In contrast to their homeostatic differentiation fate, upon CCR2-dependent recruitment into acutely inflamed colonic tissue, Ly6C^{hi} monocytes activated TLR-NOD2 recognition pathways to become responsive to bacterial products and give rise to IL-6- and IL-23-secreting proinflammatory effector cells that critically promoted colitis. With time, however, monocytes differentiated further into CX₃CR1^{int}Ly6C^{lo}CD11c^{pos}MHCII^{hi} cells, increased CCR7 expression, and acquired the ability to migrate to draining LNs as well as the potential to stimulate naive T cells toward luminal gut antigens.

Ly6C^{hi} monocytes are mononuclear myeloid cells that, as a short-lived transient intermediate, allow BM-resident precursors to seed peripheral tissues with their progeny. Generally, Ly6C^{hi} monocytes are poised to migrate to sites of injury to both promote inflammation and assist the restoration of homeostasis. Ly6C^{hi} monocytes thereby provide a transient functionally versatile complement to tissue-resident macrophage compartments that are established before birth and subsequently maintain themselves through longevity and limited self-renewal potential (Schulz et al., 2012; Yona et al., 2013). Highlighting the uniqueness of the gut, intestinal CX₃CR1^{hi} macrophages emerge as an exception to this rule. Thus CX₃CR1^{hi} macrophages display a rather short steady-state half-life of about 3 weeks (Jaensson et al., 2008) and seem to rely on the continuous replenishment by blood monocytes (Bogunovic et al., 2009; Varol et al., 2009) even under homeostatic conditions. This feature is probably due to the unique exposure of the intestine and its epithelium to the commensal flora, causing tonic sustained low-grade inflammation.

Intestinal CX₃CR1^{hi} steady-state macrophages display a characteristic non-inflammatory gene expression profile, including their expression of IL-10, TREM-2, CD163, Stab1, MRC1, LYVE-1, TNFAIP2 (A20), and RETNLA (FIZZ-1). We show that this expression profile is robust in that it remains largely unaffected by DSS-induced acute colitis. We furthermore established that adoptively transferred Ly6C^{hi}

monocytes acquire the non-inflammatory signature when replacing endogenous CX₃CR1^{hi} macrophages in the healthy tissue, potentially being educated under the aegis of the epithelium (Artis, 2008). The exact contribution of non-migratory CX₃CR1^{hi} macrophages to the maintenance of gut homeostasis remains to be elucidated and might be related to their ability to penetrate the gut epithelium and sense luminal content (Niess et al., 2005; Rescigno et al., 2001). The failure of CX₃CR1-deficient mice to establish oral tolerance suggests that these cells are important for the maintenance or selective expansion of T regulatory cells (Hadis et al., 2011).

Monocytes entering inflamed intestinal tissue acquire fates distinct from the steady state. After transfer into mice bearing DSS-induced lesions in the colonic epithel, Ly6C^{hi} monocytes gave rise to two functionally discrete CX₃CR1-GFP^{int} cell populations. Shortly after transfer, graft-derived cells were retrieved from the inflamed tissue as Ly6C^{hi}CD11c^{neg}MHCII^{pos/neg} cells. Notably, the colon of DSS-challenged mice was reported to harbor two macrophage populations that can be discriminated according to CX₃CR1 expression, TLR profiles, and TNF- α production (Platt et al., 2010). Our findings are also in line with a report of CX₃CR1-GFP^{int} and CX₃CR1-GFP^{hi} cells displaying pro-inflammatory and non-inflammatory gene expression signatures that accumulate in the inflamed colon (Weber et al., 2011). Moreover, with the same adoptive transfer model of colitis (Powrie et al., 1993) but focusing on the small intestine, a CX₃CR1^{int}CD103^{neg} cell population derived from Ly6C^{hi} monocytes that expressed pro-inflammatory cytokines was identified (Rivollier et al., 2012). We show that Ly6C^{hi} effector monocytes significantly upregulated components of the TLR2 and NOD2 signaling cascade, as compared to blood monocytes. Furthermore, when isolated and exposed to TLR4, TLR2, and NOD2 agonists, CX₃CR1-GFP^{int}Ly6C^{hi} effector monocytes but not resident macrophages responded with the secretion of IL-6. Uncontrolled reactivity to bacterial products could hence explain the finding that ex vivo isolated Ly6C^{hi} effector monocytes display a pronounced pro-inflammatory signature as compared to resident macrophages and circulating monocytes.

Three days after transfer of Ly6C^{hi} monocytes into DSS-challenged colitic mice, grafted cells were retrieved from the inflamed host tissue as CX₃CR1-GFP^{int}Ly6C^{lo} cells, a population also readily identifiable in inflamed Cx3cr1^{gfp/+} colon. In addition to now discernible expression of MHCII and CD11c, monocyte-derived Ly6C^{lo} cells

differed from the acute Ly6C^{hi} effector monocytes in that they down-modulated expression of pro-inflammatory effectors and pathogen sensors. In contrast, these cells gained with increased CCR7 expression the ability to migrate toward draining lymphatic vessels. Furthermore, when isolated from OVA-gavaged colitic mice, Ly6C^{lo} cells, but neither Ly6C^{hi} effector monocytes nor CX₃CR1^{hi} resident macrophages, were able to efficiently stimulate naive OVA-specific CD4⁺ T cells. Interestingly, microarray analysis revealed that Ly6C^{lo} cells also prominently express CD135, the receptor for the cytokine Fms-related tyrosine kinase 3 ligand (Flt3L), known to be critical for cDC development and homeostasis (Bogunovic et al., 2009; Saunders et al., 1996; Schulz et al., 2009). As revealed by the gene expression profiling and flow cytometer-based single-cell analysis of the inflamed colon of Zbtb46^{gfp/+} mice, the Ly6C^{lo} cell population also displays prominent—though not homogeneous—expression of the transcription factor Zbtb46, proposed to be a cDC hallmark (Meredith et al., 2012; Satpathy et al., 2012). Notably, this finding is compatible with the demonstration that GM-CSF-treated monocytes display Zbtb46 expression (Satpathy et al., 2012). Of note, the analysis of Zbtb46^{gfp/+} mice revealed a considerable heterogeneity of the CX₃CR1^{int}Ly6C^{lo} cell population with respect to Zbtb46 expression. Generation of both Zbtb46^{pos} and Zbtb46^{neg} - CX₃CR1^{int}Ly6C^{lo} cells involves a CCR2^{pos} precursor, as shown by the fact that MC21 treatment resulted in their ablation. Moreover, both cells are potentially migratory as shown by the fact that they express CCR7. Future studies should hence focus on potential distinct activities of these cells with respect to T cell polarization or imprinting. Specifically, it will be interesting to analyze how Zbtb46^{pos} and Zbtb46^{neg} - CX₃CR1^{int}Ly6C^{lo} correspond to the CD11b^{pos}CX₃CR1^{int}CD103^{neg} DCs recently identified in the thoracic duct of mice after mesenteric lymphadenectomy and shown to induce IL-17 and IFN- γ expression by T cells (Cerovic et al., 2012). Also, a potential link of these lamina propria-resident cells with pro-inflammatory monocyte-derived E-cadherin^{pos} cells found in the MsnLN of colitic mice should be further explored (Siddiqui et al., 2010). Monocyte-derived DCs emerge as important cellular players in the initiation or resolution of local adaptive immune reactions (Cheong et al., 2010; Lin et al., 2008; Serbina and Pamer, 2006). However, the exact contribution of these inflammation-associated cells, in particular with respect to resident cDCs, remains to be defined. Finally, the fact that Zbtb46^{pos}CX₃CR1^{int}Ly6C^{lo} accumulates in the acutely inflamed lamina propria in a CCR2 dependent manner, and the in-vitro

data supporting differentiation of Ly6C^{hi} monocyte into Zbtb46^{pos} cells in response to GM-CSF suggest that these cells are of monocytic origin. However, it is possible that under acute inflammation another CCR2^{pos} precursor (eg. CDP or yet to be identified cell) might exit the bone marrow or spleen to seed the inflamed gut and give rise to these cells. Further studies should clarify this issue.

Human lamina propria macrophages isolated from healthy intestine were shown to exhibit profound inflammatory anergy as reflected by their inability to produce pro-inflammatory cytokines in response to a vast array of stimuli and explained by their lack of expression of innate response receptors, including the LPS co-receptor CD14 (Smythies et al., 2005). Interestingly, it was shown that autologous radio-labeled monocytes can, after transfer into IBD patients, give rise to a CD14⁺ macrophage population (Grimm et al., 1995). More recent extensive flow cytometry analysis has provided a more detailed characterization of this population as TREM-1⁺, CX3CR1⁺, DC-SIGN⁺, and TLR-2⁺ cells and further demonstrated their ability to secrete pro-inflammatory cytokines like IL-23 and IL-6 in both CD and UC patients (Kamada et al., 2008; Schenk et al., 2007). The high resemblance in surface marker profile and gene expression signature between these pro-inflammatory lamina propria cells and the CX₃CR1^{int}Ly6C^{hi} effector monocytes described here suggests that these cells might be identical. Studies like the present can, through providing a high-resolution characterization of monocyte-derived cells with respect to their origin, trafficking requirements, pathways of differentiation, and comprehensive gene expression signatures, improve our understanding of the pathogenesis of human IBD and might pave the road for novel therapeutic interventions.

Collectively, we have established in this study three distinct fates of Ly6C^{hi} monocytes in the healthy and inflamed intestinal mucosa, resulting in monocyte descendants with discrete functions as resident non-inflammatory sentinels, pro-inflammatory cells, and migratory T cell-stimulating antigen-presenting cells. Monocyte and their progeny thus critically contribute to the maintenance of gut homeostasis and its breakdown. Combined with emerging evidence from other laboratories, this study further highlights the plasticity of murine Ly6C^{hi} monocytes and their equivalent in the human, the CD14⁺CD16^{+/-} monocytes (Cros et al., 2010). In-depth understanding of the molecular cues that guide monocyte fates in their respective in vivo context should provide attractive targets for the management of inflammatory bowel disorders.

After exploring monocytes fate in a model of acute inflammation we decided to move forward and work in chronic models of intestinal inflammation, which more resembles the chronic condition of human IBD. IBD are considered polygenic diseases that develop in genetically susceptible individuals under certain environmental conditions (Cho 2008). GWAS revealed strong association of the allelic variants of the *IL10* and *IL10R* genes with IBD, and in particular UC. This suggested impaired IL10 signaling as a key afflicted pathway in the development of intestinal inflammation in humans (Franke et al., 2008, Engelhardt et al., 2013). This notion was corroborated by the report that severe early-onset colitis in children can be a monogenic disease caused by mutations in IL-10 or its receptor (Glocker et al., 2009). However, the cell type that requires silencing by IL10 to maintain gut homeostasis has remained elusive. Our finding that mice harboring IL10R-deficient colonic lamina propria macrophages develop spontaneous colitis that is in its severity comparable to *IL10*^{-/-} mice highlights CX₃CR1^{hi} macrophages as critical initiators of the inflammatory process. Of note, the transgenic CX₃CR1^{cre} system also partially affects intestinal DC. Impaired IL10R signaling in these cells could therefore contribute to the development of gut inflammation in our model and should be evaluated in the future when experimental models that allow the specific targeting of intestinal DC will be available.

Homeostatic resident CX₃CR1^{hi} macrophages are derived from Ly6C⁺ monocytes (Varol et al., 2009, Bogunovic et al., 2009), and in the healthy colon locally conditioned to be anergic and non-inflammatory (Zigmond et al., 2012, Bain et al., 2012). Resident CX₃CR1^{hi} macrophages are non-migratory, as indicated by their lack of expression of the chemokine receptor CCR7 (Schulz et al., 2009, Zigmond et al., 2012) that is required for tissue exit (Jang et al., 2006). Accordingly, in steady state conditions, but also during chemical-induced acute colitis, mLN lack CX₃CR1^{hi} cells. Recently, it was suggested that under dysbiosis, antibiotic exposure and *Salmonella* infection facilitate expression of CCR7 by CX₃CR1^{hi} cells and their migration towards mLNs (Diehl et al., 2013). In this study we corroborate this finding by showing that under chronic intestinal inflammation, CX₃CR1^{hi} macrophages display CCR7 expression. Moreover, flow cytometry analysis of the mLN of *IL10*^{-/-} *Cx3cr1*^{gfp/+} mice indeed revealed the presence of CCR7⁺ CD64⁺ CX₃CR1^{hi} cells. Collectively these data suggest that the absence of migratory capacity of intestinal

CX₃CR1^{hi} macrophages, rather than being an inherent epigenetically pre-programmed feature of this cell type requires active enforcement by environmental cues.

The severe spontaneous colitis observed in IL10-deficient animals and most likely also that observed in our newly established *Cx3cr1^{cre}IL10Ra^{fl/fl}* model are driven by the commensal gut microbiota (Rakoff-Nahoum & Medzhitov 2006). This notion is supported by the recent finding that a Myd88 deficiency in macrophages can restore homeostasis in *IL10^{-/-}* mice (Hoshi et al., 2012). Moreover, as opposed to other models of gut inflammation (Elinav et al., 2011), we found no evidence for the selection of a colitogenic microbiota that would affect *IL10Ra^{fl/fl}* littermates co-housed with sick *Cx3cr1^{cre}IL10Ra^{fl/fl}* mice. Interestingly, Maloy and colleagues reported that *Helicobacter hepaticus* (*Hh*) - bearing *WT* mice, but not *Hh*- mice are sensitive to antibody-mediated IL10R neutralization responding with the development of colitis (Kullberg et al., 2006). This finding highlights the importance of IL10 in the maintenance of gut homeostasis. Of note, sentinels in our facility were typed *Hh*+. Our data establish that resident lamina propria macrophages require IL10 to prevent their hyper-activation in the gut. Colonic macrophages also constitutively express IL10 mRNA (Zigmond et al. 2012), and we show that BM culture-derived macrophage are subject to an autocrine regulatory loop that controls their response to LPS *in vitro* and has been previously noted (Pils et al., 2010, Siewe et al., 2006). Surprisingly though, *Cx3cr1^{cre}IL10^{fl/fl}* mice did not develop signs of colitis. Hence, cells other than macrophages must provide the critical homeostatic IL10 that suppresses colonic macrophage hyper-activation. Notably, IL10 can be produced by most hematopoietic cells (Moore et al., 2001). Moreover, even certain non-immune cells, such as intestinal stroma and epithelium have been proposed to express IL10 (Ina et al., 2005, Colgan et al., 1999), although the physiological relevance of this expression remains to be shown. In contrast, several studies have highlighted the critical importance of IL10 production by CD4⁺ T cells. Thus, we had originally shown that mice harboring a CD4⁺ T cell-restricted IL10-deficiency develop spontaneous colitis (Roers et al., 2004), similar to IL10-deficient mice. The main homeostatic IL10 producers in the gut are, aside from CX₃CR1^{hi} macrophages, Foxp3⁻ Type I regulatory (Tr1) cells and Foxp3⁺ T_{reg} cells. IL10-producing T regulatory cells in the colon are mainly of the FoxP3⁺ type (Maynard et al., 2007), suggesting that Foxp3⁺ T_{reg} cells, rather Tr1 cells are the prime IL10 source preventing colitis. Supporting this notion, Rudensky and colleagues established using

Foxp3^{Cre}IL10^{fl/fl} mice that mere impairment of IL10 production by Foxp3⁺ T_{reg} cells is sufficient to cause spontaneous inflammation that was restricted to the large, but not small intestine (Rubstov et al., 2008). Interestingly though, IL10-deficient Foxp3⁺ T_{reg} cells retained the potential to suppress T effector cells, both in *in vitro* assays, as well as the CD45RB T cell transfer model of colitis (Murai et al., 2009, Rubstov et al., 2008). The reason why Foxp3⁺ T_{reg} cell-derived IL-10 is required to maintain gut homeostasis hence remained elusive. Our data suggests that colonic Foxp3⁺ T_{reg} cell-derived IL10 is critical to ensure the homeostatic non-inflammatory gene expression signature of intestinal CX₃CR1^{hi} macrophages (Rivollier et al., 2012, Zigmund et al., 2012). In absence of this regulatory T cell- derived IL10 these mononuclear phagocytes respond to the abundant microbial stimuli in the gut with the production of pro-inflammatory cytokines and chemokines triggering inflammation. Such a scenario is supported by the fact that IL10-deficient mice are protected from colitis by a myeloid cell-restricted Myd88 deficiency (Hoshi et al., 2012). Moreover, a T effector cell-independent regulatory role of T_{reg} cells on macrophages is also supported by the fact that these cells can reverse intestinal inflammation in *H. hepaticus*-infected Rag2^{-/-} mice and the Tbet^{-/-} Rag2^{-/-} mice (Maloy et al., 2005, Garrett et al., 2007).

Of note, the Rudensky group established in collaboration with us that also mice harboring a Foxp3⁺ T_{reg} cell-restricted IL10Ra deficiency develop spontaneous colitis (Chaudhry et al., 2011). Numbers of Foxp3⁺ T_{reg} cells were increased in these *Foxp3^{Cre}IL10Ra^{fl/fl}* mice, however notably, these cells failed to produce IL10. Given the fact that IL10 suppresses TH17 cells (Huber et al., 2011) we had interpreted this colitis phenotype as a failure to suppress TH17 cell-mediated inflammation (Chaudhry et al., 2011). Our results offer an alternative explanation, though not mutually exclusive. Thus, like in *Foxp3^{Cre}IL10^{fl/fl}* mice, the impaired production of IL10 by T_{reg} cells in *Foxp3^{Cre}IL10Ra^{fl/fl}* mice likely compromises the conditioning Ly6C⁺ monocytes and the establishment of non-inflammatory CX₃CR1^{hi} macrophages that is critical for gut homeostasis.

This study highlights the central role CX₃CR1⁺ macrophages play in IBD pathophysiology. IL10Ra-deficient macrophages express a battery of pro-inflammatory cytokines that can trigger deleterious T cell responses, as indicated by the elevated IL17 and IL6 serum levels. Of note, *Rag-deficient IL10^{-/-}* mice develop colitis only upon transfer of T cells (Murai et al., 2009, Liu et al., 2011) and gut

inflammation in this model hence depends on the presence of effector T cells. The gene signature of IL10Ra-deficient macrophages might bear potential targets for future therapeutic IBD intervention. A lead to these approaches could be the prominent impact on lipid and eicosanoid metabolism we observe in macrophages that are blind to IL10. Of note, a link between IL10 and PGE₂ has been previously noted in studies involving cultured human macrophages (Antoniv et al., 2005). Interestingly, also the IL10-dependent bacterial clearance in a meningitis model is associated with the potential of this cytokine to suppress PGE₂ levels (Mittal et al., 2010). Moreover, it was recently reported that inflammatory monocytes could directly inhibit neutrophil activation in a PGE₂-dependent manner in response to commensals (Grainger et al., 2013). However, prostaglandins have pleiotropic functions and can - depending on the receptors they engage and the cellular context - exert both pro- and anti-inflammatory functions (Dey et al., 2006). Successful therapeutic manipulation of the PGE₂ system for IBD management will hence require additional insights into eicosanoid activities in the healthy and diseased gut context.

Collectively, our results establish intestinal CX₃CR1^{hi} macrophages as key drivers of IL10 deficiency-based gut inflammation. The gene expression profiles of IL10R deficient macrophages provided in this study and future epigenetic profiling should provide candidate molecules taking part in the early events of the pathology, that might open new avenues for the research of the pathogenesis of the disease and could serve as potential targets for therapeutic manipulations aiming at restoration of gut homeostasis.

The recent past has seen major advances in our understanding of the functional organization of the mammalian mononuclear phagocyte compartment. Collectively, these cells have become well appreciated to play central roles in the maintenance of tissue integrity during development and after injury, as well as in the initiation and resolution of innate and adaptive immunity. Much remains to be learned about specific cellular interactions in physiological tissue context. However, the pace of the current data accumulation seems to justify cautious optimism that in the not so far future we might be able to add to our medical IBD treatment options strategies that target specific cells or specific functions of these cells. Given their central role in the maintenance of gut inflammation, intestinal macrophages and other monocyte-derived cells have emerged as prime targets for such efforts.

REFERENCES

Ajami, B., Bennett, J.L., Krieger, C., McNagny, K.M., and Rossi, F.M. (2011). Infiltrating monocytes trigger EAE progression, but do not contribute to the resident microglia pool. *Nat Neurosci* 14, 1142-1149.

Alencar H, King R, Funovics M, Stout C, Weissleder R, Mahmood U. A novel mouse model for segmental orthotopic colon cancer. *Int J Cancer*. 2005 Nov 10;117(3):335-9.

Antoniv, T. T., Park-Min, K. H. & Ivashkiv, L. B. Kinetics of IL-10-induced gene expression in human macrophages. *Immunobiology* 210, 87–95 (2005).

Artis, D. (2008). Epithelial-cell recognition of commensal bacteria and maintenance of immune homeostasis in the gut. *Nat. Rev. Immunol.* 8, 411–420.

Atarashi, K., Tanoue, T., Shima, T., Imaoka, A., Kuwahara, T., Momose, Y., Cheng, G., Yamasaki, S., Saito, T., Ohba, Y., et al. (2011). Induction of colonic regulatory T cells by indigenous *Clostridium* species. *Science* 331, 337-341.

Auffray, C., Fogg, D., Garfa, M., Elain, G., Join-Lambert, O., Kayal, S., Sarnacki, S., Cumano, A., Lauvau, G., and Geissmann, F. (2007). Monitoring of blood vessels and tissues by a population of monocytes with patrolling behavior. *Science* 317, 666-670.

Bain, C. C. et al. Resident and pro-inflammatory macrophages in the colon represent alternative context-dependent fates of the same Ly6Chi monocyte precursors. *Mucosal Immunology* 6, 498-510 (2012).

Banerjee, S. et al. MEP1A allele for meprin A metalloprotease is a susceptibility gene for inflammatory bowel disease. *Mucosal Immunology* 2, 220–231 (2009).

Barnden, M.J., Allison, J., Heath, W.R., and Carbone, F.R. (1998). Defective TCR expression in transgenic mice constructed using cDNA-based alpha- and beta-chain genes under the control of heterologous regulatory elements. *Immunol. Cell Biol.* 76, 34–40.

Becker, C. et al. High resolution colonoscopy in live mice. *Nat. Protoc.* 2006, 1, 2900–2904.

- Bevins, C.L., and Salzman, N.H. (2011). Paneth cells, antimicrobial peptides and maintenance of intestinal homeostasis. *Nat Rev Microbiol* 9, 356-368.
- Bogunovic, M., Ginhoux, F., Helft, J., Shang, L., Hashimoto, D., Greter, M., Liu, K., Jakubzick, C., Ingersoll, M.A., Leboeuf, M., et al. (2009). Origin of the lamina propria dendritic cell network. *Immunity* 31, 513-525.
- Boonstra, A. et al. Macrophages and myeloid dendritic cells, but not plasmacytoid dendritic cells, produce IL-10 in response to MyD88- and TRIF-dependent TLR signals, and TLR-independent signals. *J Immunol* 2006;177:7551–7558.
- Bruhl, H., Cihak, J., Plachy, J., Kunz-Schughart, L., Niedermeier, M., Denzel, A., Rodriguez Gomez, M., Talke, Y., Luckow, B., Stangassinger, M., and Mack, M. (2007). Targeting of Gr-1+,CCR2+ monocytes in collagen-induced arthritis. *Arthritis Rheum* 56, 2975-2985.
- Cerovic V, Houston SA, Scott CL, Aumeunier A, Yrlid U, Mowat AM, Milling SW. Intestinal CD103(-) dendritic cells migrate in lymph and prime effector T cells. *Mucosal Immunol.* 2013 Jan;6(1):104-13.
- Céspedes MV, Espina C, García-Cabezas MA, Trias M, Boluda A, Gómez del Pulgar MT, Sancho FJ, Nistal M, Lacal JC, Manges R. Orthotopic microinjection of human colon cancer cells in nude mice induces tumor foci in all clinically relevant metastatic sites. *Am J Pathol.* 2007 Mar;170(3):1077-85.
- Chaudhry, A. et al. Interleukin-10 Signaling in Regulatory T Cells Is Required for Suppression of Th17 Cell-Mediated Inflammation. *Immunity* 34, 566–578 (2011).
- Cheong, C., Matos, I., Choi, J.H., Dandamudi, D.B., Shrestha, E., Longhi, M.P., Jeffrey, K.L., Anthony, R.M., Kluger, C., Nchinda, G., et al. (2010). Microbial stimulation fully differentiates monocytes to DC-SIGN/CD209(+) dendritic cells for immune T cell areas. *Cell* 143, 416-429.
- Cho, J.H. (2008). The genetics and immunopathogenesis of inflammatory bowel disease. *Nat Rev Immunol* 8, 458-466.

Colgan, S. P., Hershberg, R. M., Furuta, G. T. & Blumberg, R. S. Ligation of intestinal epithelial CD1d induces bioactive IL-10: Critical role of the cytoplasmic tail in autocrine signaling. *PNAS*. 96, 813939-43 (1999).

Coombes, J.L., Siddiqui, K.R., Arancibia-Carcamo, C.V., Hall, J., Sun, C.M., Belkaid, Y., and Powrie, F. (2007). A functionally specialized population of mucosal CD103+ DCs induces Foxp3+ regulatory T cells via a TGF-beta and retinoic acid-dependent mechanism. *J Exp Med* 204, 1757-1764.

Cros, J., Cagnard, N., Woollard, K., Patey, N., Zhang, S.Y., Senechal, B., Puel, A., Biswas, S.K., Moshous, D., Picard, C., et al. (2010). Human CD14dim monocytes patrol and sense nucleic acids and viruses via TLR7 and TLR8 receptors. *Immunity* 33, 375-386.

Denning, T.L., Wang, Y.C., Patel, S.R., Williams, I.R., and Pulendran, B. (2007). Lamina propria macrophages and dendritic cells differentially induce regulatory and interleukin 17-producing T cell responses. *Nat Immunol* 8, 1086-1094.

Dey, I., Lejeune, M. & Chadee, K. Prostaglandin E 2receptor distribution and function in the gastrointestinal tract. *British Journal of Pharmacology* 149, 611–623 (2006).

Diehl GE, Longman RS, Zhang JX, Breart B, Galan C, Cuesta A, Schwab SR, Littman DR (2013). Microbiota restricts trafficking of bacteria to mesenteric lymph nodes by CX(3)CR1(hi) cells. *Nature* Feb 7;494(7435):116-20.

Edelmann L, Edelmann W. Loss of DNA mismatch repair function and cancer predisposition in the mouse: animal models for human hereditary nonpolyposis colorectal cancer. *Am J Med Genet C Semin Med Genet*. 2004 Aug 15;129C(1):91-9.

Edelson, B.T., Kc, W., Juang, R., Kohyama, M., Benoit, L.A., Klekotka, P.A., Moon, C., Albring, J.C., Ise, W., Michael, D.G., et al. (2010). Peripheral CD103+ dendritic cells form a unified subset developmentally related to CD8alpha+ conventional dendritic cells. *J Exp Med* 207, 823-836.

Elinav, E. et al. NLRP6 Inflammasome Regulates Colonic Microbial Ecology and Risk for Colitis. *Cell* 145, 745–757 (2011).

Engelhardt, K. R. et al. Clinical outcome in IL-10- and IL-10 receptor-deficient patients with or without hematopoietic stem cell transplantation. *Journal of Allergy and Clinical Immunology* 131, 825–830.e9 (2013).

Farache J, Koren I, Milo I, Gurevich I, Kim KW, Zigmond E, Furtado GC, Lira SA, Shakhar G. Luminal bacteria recruit CD103+ dendritic cells into the intestinal epithelium to sample bacterial antigens for presentation. *Immunity*. 2013 Mar 21;38(3):581-95.

Farré L, Casanova I, Guerrero S, Trias M, Capellá G, Manges R. Heterotopic implantation alters the regulation of apoptosis and the cell cycle and generates a new metastatic site in a human pancreatic tumor xenograft model. *FASEB J*. 2002 Jul;16(9):975-82.

Fiorentino, DF. et al. Two types of mouse T helper cell. IV. Th2 clones secrete a factor that inhibits cytokine production by Th1 clones. *J Exp Med* 1989;170:2081–2095.

Fogg, D.K. et al. A clonogenic bone marrow progenitor specific for macrophages and dendritic cells. *Science*, 2006, 311, 83–87.

Franke, A. et al. Sequence variants in IL10, ARPC2 and multiple other loci contribute to ulcerative colitis susceptibility. *Nat Genet*. 2008 Nov;40(11):1319-23).

Garrett, W. S. et al. Communicable Ulcerative Colitis Induced by T-bet Deficiency in the Innate Immune System. *Cell* 131, 33–45 (2007).

Geissmann, F., Jung, S., and Littman, D.R. (2003). Blood monocytes consist of two principal subsets with distinct migratory properties. *Immunity* 19, 71-82.

Ginhoux, F. et al. Fate Mapping Analysis Reveals That Adult Microglia Derive from Primitive Macrophages. *Science* 330, 841–845 (2010).

Glocker, E. O et al. Inflammatory Bowel Disease and Mutations Affecting the Interleukin-10 Receptor. *N Engl J Med* 2009;361:2033-45.

Grainger, J. R. et al. Inflammatory monocytes regulate pathologic responses to commensals during acute gastrointestinal infection. *Nature Medicine* 19, 713–721 (2013).

Grimm, M.C., Pullman, W.E., Bennett, G.M., Sullivan, P.J., Pavli, P., and Doe, W.F. (1995). Direct evidence of monocyte recruitment to inflammatory bowel disease mucosa. *J. Gastroenterol. Hepatol.* 10, 387–395.

Hadis, U., Wahl, B., Schulz, O., Hardtke-Wolenski, M., Schippers, A., Wagner, N., Muller, W., Sparwasser, T., Forster, R., and Pabst, O. (2011). Intestinal tolerance requires gut homing and expansion of FoxP3⁺ regulatory T cells in the lamina propria. *Immunity* 34, 237-246.

Hapfelmeier, S. et al. Reversible microbial colonization of germ-free mice reveals the dynamics of IgA immune responses. *Science* 328, 1705–1709 (2010).

Hashimoto, D., Miller, J., and Merad, M. (2011). Dendritic cell and macrophage heterogeneity in vivo. *Immunity* 35, 323-335.

Hettinger, J. et al., Origin of monocytes and macrophages in a committed progenitor. *Nat Immunol.* 2013 Aug;14(8):821-30. doi: 10.1038/ni.2638. Epub 2013 Jun 30.

Hoshi N, Schenten D, Nish SA, Walther Z, Gagliani N, Flavell RA, Reizis B, Shen Z, Fox JG, Iwasaki A, Medzhitov R. (2012). MyD88 signalling in colonic mononuclear phagocytes drives colitis in IL-10-deficient mice. *Nat Commun.* 3:1120.

Huber, S. et al. Th17 cells express interleukin-10 receptor and are controlled by Foxp3⁻ and Foxp3⁺ regulatory CD4⁺ T cells in an interleukin-10-dependent manner. *Immunity* 34, 554–565 (2011).

Ina, K. et al. Intestinal Fibroblast-Derived IL-10 Increases Survival of Mucosal T Cells by Inhibiting Growth Factor Deprivation- and Fas-Mediated Apoptosis. 1–11 (2005).

Ivanov, II, Atarashi, K., Manel, N., Brodie, E.L., Shima, T., Karaoz, U., Wei, D., Goldfarb, K.C., Santee, C.A., Lynch, S.V., et al. (2009). Induction of Intestinal Th17 Cells by Segmented Filamentous Bacteria. *Cell*.

Irizarry, R.A., Hobbs, B., Collin, F., Beazer-Barclay, Y.D., Antonellis, K.J., Scherf, U., and Speed, T.P. (2003). Exploration, normalization, and summaries of high density oligonucleotide array probe level data. *Biostatistics* 4, 249–264.

Jaensson, E., Uronen-Hansson, H., Pabst, O., Eksteen, B., Tian, J., Coombes, J.L., Berg, P.L., Davidsson, T., Powrie, F., Johansson-Lindbom, B., and Agace, W.W. (2008). Small intestinal

CD103+ dendritic cells display unique functional properties that are conserved between mice and humans. *J Exp Med* 205, 2139-2149.

Jang, M. H. et al. CCR7 is critically important for migration of dendritic cells in intestinal lamina propria to mesenteric lymph nodes. *J. Immunol.* 176, 803–810 (2006).

Jemal A, Siegel R, Ward E, Murray T, Xu J, Smigal C, Thun MJ. Cancer statistics, 2006. *CA Cancer J Clin.* 2006 Mar-Apr;56(2):106-30.

Johansson-Lindbom, B., Svensson, M., Pabst, O., Palmqvist, C., Marquez, G., Forster, R., and Agace, W.W. (2005). Functional specialization of gut CD103+ dendritic cells in the regulation of tissue-selective T cell homing. *J Exp Med* 202, 1063-1073.

Jostins L et al.(2012). Host-microbe interactions have shaped the genetic architecture of inflammatory bowel disease. *Nature* Nov 1;491(7422):119-24.

Jung, S., Aliberti, J., Graemmel, P., Sunshine, M.J., Kreutzberg, G.W., Sher, A., and Littman, D.R. (2000). Analysis of fractalkine receptor CX(3)CR1 function by targeted deletion and green fluorescent protein reporter gene insertion. *Mol Cell Biol* 20, 4106-4114.

Jung, S., Unutmaz, D., Wong, P., Sano, G., De los Santos, K., Sparwasser, T., Wu, S., Vuthoori, S., Ko, K., Zavala, F., et al. (2002). In vivo depletion of CD11c+ dendritic cells abrogates priming of CD8+ T cells by exogenous cell-associated antigens. *Immunity* 17, 211–220.

Kamada, N., Hisamatsu, T., Okamoto, S., Chinen, H., Kobayashi, T., Sato, T., Sakuraba, A., Kitazume, M.T., Sugita, A., Koganei, K., et al. (2008). Unique CD14 intestinal macrophages contribute to the pathogenesis of Crohn disease via IL-23/IFN-gamma axis. *J. Clin. Invest.* 118, 2269–2280.

Kassiotis, G., and Kollias, G. (2001). Uncoupling the proinflammatory from the immunosuppressive properties of tumor necrosis factor (TNF) at the p55 TNF receptor level: implications for pathogenesis and therapy of autoimmune demyelination. *J Exp Med* 193, 427-434.

- Kobayashi, K.S., Chamaillard, M., Ogura, Y., Henegariu, O., Inohara, N., Núñez, G., and Flavell, R.A. (2005). Nod2-dependent regulation of innate and adaptive immunity in the intestinal tract. *Science* 307, 731–734.
- Kühn, R. et al. Interleukin-10-deficient mice develop chronic enterocolitis. *Cell* 1993;75:263–74.
- Kullberg, M. C. et al. IL-23 plays a key role in *Helicobacter hepaticus*-induced T cell-dependent colitis. *Journal of Experimental Medicine* 203, 2485–2494 (2006).
- Lathrop, S. K. et al. Peripheral education of the immune system by colonic commensal microbiota. *Nature* 478, 250–254 (2012).
- Lauritsen, K., Laursen, L. S., Bukhave, K. & Rask-Madsen, A. J. Use of colonic eicosanoid concentrations as predictors of relapse in ulcerative colitis: double blind placebo controlled study on sulphasalazine maintenance treatment. *Gut* 29, 1316–1321 (2006).
- Lee, S.H., et al. (1985) Quantitative analysis of total macrophage content in adult mouse tissues. *Immunochemical studies with monoclonal antibody F4/80. J Exp Med* 161, 475-489.
- Lin, M.L., Zhan, Y., Proietto, A.I., Prato, S., Wu, L., Heath, W.R., Villadangos, J.A., and Lew, A.M. (2008). Selective suicide of cross-presenting CD8⁺ dendritic cells by cytochrome c injection shows functional heterogeneity within this subset. *Proc. Natl. Acad. Sci. USA* 105, 3029–3034.
- Liu, K., Victora, G.D., Schwickert, T.A., Guemronprez, P., Meredith, M.M., Yao, K., Chu, F.F., Randolph, G.J., Rudensky, A.Y., and Nussenzweig, M. (2009). In vivo analysis of dendritic cell development and homeostasis. *Science* 324, 392-397.
- Liu, B., Tonkonogy, S. L. & Sartor, R. B. Antigen-Presenting Cell Production of IL-10 Inhibits T-Helper 1 and 17 Cell Responses and Suppresses Colitis in Mice. *YGAST* 141, 653–662.e4 (2011).
- Maloy, KJ. et al. CD4⁺CD25⁺T(R) cells suppress innate immune pathology through cytokine-dependent mechanisms. *J Exp Med*;197:111–119. (2003)

Maloy, K. J., Antonelli, L. R. V., Lefevre, M. & Powrie, F. Cure of innate intestinal immune pathology by CD4+CD25+ regulatory T cells. *Immunology Letters* 97, 189–192 (2005).

Maynard, C. L. et al. Regulatory T cells expressing interleukin 10 develop from Foxp3+ and Foxp3- precursor cells in the absence of interleukin 10. *Nat Immunol* 8, 931–941 (2007).

Meredith, M.M., Liu, K., Darrasse-Jeze, G., Kamphorst, A.O., Schreiber, H.A., Guermonprez, P., Idoyaga, J., Cheong, C., Yao, K.H., Niec, R.E., and Nussenzweig, M.C. (2012). Expression of the zinc finger transcription factor zDC (Zbtb46, Btbd4) defines the classical dendritic cell lineage. *J Exp Med* 209, 1153-1165.

Mittal, R. et al. IL-10 administration reduces PGE-2 levels and promotes CR3-mediated clearance of Escherichia coli K1 by phagocytes in meningitis. *Journal of Experimental Medicine* 207, 1307–1319 (2010).

Moore, KW. et al. Interleukin-10 and the interleukin-10 receptor. *Annu Rev Immunol* 2001;19:683–765.

Moser AR, Pitot HC, Dove WF. A dominant mutation that predisposes to multiple intestinal neoplasia in the mouse. *Science*. 1990 Jan 19;247(4940):322-4.

Mukhopadhyay, S., Pluddemann, A., and Gordon, S. (2009). Macrophage pattern recognition receptors in immunity, homeostasis and self tolerance. *Adv Exp Med Biol* 653, 1-14.

Muthuswamy, R. et al. PGE2 transiently enhances DC expression of CCR7 but inhibits the ability of DCs to produce CCL19 and attract naive T cells. *Blood* 116, 1454–1459 (2010).

Murai, M., Turovskaya, O., Kim, G., Madan, R., Karp, C.L., Cheroutre, H., and Kronenberg, M. (2009). Interleukin 10 acts on regulatory T cells to maintain expression of the transcription factor Foxp3 and suppressive function in mice with colitis. *Nat Immunol* 10, 1178-1184.

Neufert C, Becker C, Neurath MF. An inducible mouse model of colon carcinogenesis for the analysis of sporadic and inflammation-driven tumor progression. *Nat Protoc*. 2007;2(8):1998-2004.

Neurath MF et al. Assessment of Tumor Development and Wound Healing Using Endoscopic Techniques in Mice. *Gastroenterology* 2010;139:1837–1843.

Niess, J.H., Brand, S., Gu, X., Landsman, L., Jung, S., McCormick, B.A., Vyas, J.M., Boes, M., Ploegh, H.L., Fox, J.G., et al. (2005). CX3CR1-mediated dendritic cell access to the intestinal lumen and bacterial clearance. *Science* 307, 254-258.

O'Garra, A. et al. Production of cytokines by mouse B cells: B lymphomas and normal B cells produce interleukin 10. *Int Immunol* 1990;2:821–832.

Okayasu, I., Hatakeyama, S., Yamada, M., Ohkusa, T., Inagaki, Y., and Nakaya, R. (1990). A novel method in the induction of reliable experimental acute and chronic ulcerative colitis in mice. *Gastroenterology* 98, 694-702.

Palframan, R.T., Jung, S., Cheng, G., Weninger, W., Luo, Y., Dorf, M., Littman, D.R., Rollins, B.J., Zweerink, H., Rot, A., and von Andrian, U.H. (2001). Inflammatory chemokine transport and presentation in HEV: a remote control mechanism for monocyte recruitment to lymph nodes in inflamed tissues. *J Exp Med* 194, 1361-1373.

Persson EK, Scott CL, Mowat AM, Agace WW. Dendritic cell subsets in the intestinal lamina propria: Ontogeny and function. *Eur J Immunol*. 2013 Aug 21. doi: 10.1002/eji.201343740.

Peterson, D.A., McNulty, N.P., Guruge, J.L., and Gordon, J.I. (2007). IgA response to symbiotic bacteria as a mediator of gut homeostasis. *Cell Host Microbe* 2, 328-339.

Pils MC, Pisano F, Fasnacht N, Heinrich JM, Groebe L, Schippers A, Rozell B, Jack RS, Müller W. Monocytes/macrophages and/or neutrophils are the target of IL-10 in the LPS endotoxemia model. *Eur J Immunol*. 2010 Feb;40(2):443-8.

Platt, A.M., Bain, C.C., Bordon, Y., Sester, D.P., and Mowat, A.M. (2010). An independent subset of TLR expressing CCR2-dependent macrophages promotes colonic inflammation. *J Immunol* 184, 6843-6854.

Poulin, L. F. et al. DNGR-1 is a specific and universal marker of mouse and human Batf3-dependent dendritic cells in lymphoid and nonlymphoid tissues. *Blood* 119, 6052–6062 (2012).

Powrie, F., Leach, M.W., Mauze, S., Caddle, L.B., and Coffman, R.L. (1993). Phenotypically distinct subsets of CD4⁺ T cells induce or protect from chronic intestinal inflammation in C. B-17 scid mice. *Int. Immunol*. 5, 1461–1471.

Rakoff-Nahoum, S., Hao, L. & Medzhitov, R. Role of Toll-like Receptors in Spontaneous Commensal-Dependent Colitis. *Immunity* 25, 319–329 (2006).

Roers, A. et al. T cell-specific inactivation of the interleukin 10 gene in mice results in enhanced T cell responses but normal innate responses to lipopolysaccharide or skin irritation. *J. Exp. Med.* 200, 1289–1297 (2004).

Reddy BS, Ohmori T. Effect of intestinal microflora and dietary fat on 3,2'-dimethyl-4-aminobiphenyl-induced colon carcinogenesis in F344 rats. *Cancer Res.* 1981 Apr;41(4):1363-7.

Rescigno, M., Urbano, M., Valzasina, B., Francolini, M., Rotta, G., Bonasio, R., Granucci, F., Kraehenbuhl, J.P., and Ricciardi-Castagnoli, P. (2001). Dendritic cells express tight junction proteins and penetrate gut epithelial monolayers to sample bacteria. *Nat Immunol* 2, 361-367.

Rivollier, A., He, J., Kole, A., Valatas, V., and Kelsall, B.L. (2012). Inflammation switches the differentiation program of Ly6Chi monocytes from antiinflammatory macrophages to inflammatory dendritic cells in the colon. *J Exp Med* 209, 139-155.

Rubtsov, Y. P. et al. Regulatory T cell-derived interleukin-10 limits inflammation at environmental interfaces. *Immunity* 28, 546–558 (2008).

Satpathy, A.T., Kc, W., Albring, J.C., Edelson, B.T., Kretzer, N.M., Bhattacharya, D., Murphy, T.L., and Murphy, K.M. (2012). Zbtb46 expression distinguishes classical dendritic cells and their committed progenitors from other immune lineages. *J Exp Med* 209, 1135-1152.

Saunders, D., Lucas, K., Ismaili, J., Wu, L., Maraskovsky, E., Dunn, A., and Shortman, K. (1996). Dendritic cell development in culture from thymic precursor cells in the absence of granulocyte/macrophage colony-stimulating factor. *J. Exp. Med.* 184, 2185–2196.

Savage DC. Microbial ecology of the gastrointestinal tract. *Annu Rev Microbiol.* 1977;31:107-33.

Schenk, M., Bouchon, A., Seibold, F., and Mueller, C. (2007). TREM-1— expressing intestinal macrophages crucially amplify chronic inflammation in experimental colitis and inflammatory bowel diseases. *J. Clin. Invest.* 117, 3097–3106.

Schulz, O., Jaensson, E., Persson, E.K., Liu, X., Worbs, T., Agace, W.W., and Pabst, O. (2009). Intestinal CD103+, but not CX3CR1+, antigen sampling cells migrate in lymph and serve classical dendritic cell functions. *J Exp Med* 206, 3101-3114.

Schulz, C. et al. A Lineage of Myeloid Cells Independent of Myb and Hematopoietic Stem Cells. *Science* 336, 86–90 (2012).

Serbina, N.V., and Pamer, E.G. (2006). Monocyte emigration from bone marrow during bacterial infection requires signals mediated by chemokine receptor CCR2. *Nat Immunol* 7, 311-317.

Serbina, N.V., Salazar-Mather, T.P., Biron, C.A., Kuziel, W.A., and Pamer, E.G. (2003). TNF/iNOS-producing dendritic cells mediate innate immune defense against bacterial infection. *Immunity* 19, 59-70.

Shechter, R., London, A., Varol, C., Raposo, C., Cusimano, M., Yovel, G., Rolls, A., Mack, M., Pluchino, S., Martino, G., et al. (2009). Infiltrating blood-derived macrophages are vital cells playing an anti-inflammatory role in recovery from spinal cord injury in mice. *PLoS Med* 6, e1000113.

Sheibanie, A. F. et al. The Proinflammatory Effect of Prostaglandin E 2 in Experimental Inflammatory Bowel Disease Is Mediated through the IL-23. *J. Immunol.* 178, 8138-47 (2007).

Siddiqui, K.R., Laffont, S., and Powrie, F. (2010). E-cadherin marks a subset of inflammatory dendritic cells that promote T cell-mediated colitis. *Immunity* 32, 557-567.

Siewe, L. et al. Interleukin-10 derived from macrophages and/or neutrophils regulates the inflammatory response to LPS but not the response to CpG DNA. *Eur. J. Immunol.* 36, 3248–3255 (2006).

Smythies, L.E., Sellers, M., Clements, R.H., Mosteller-Barnum, M., Meng, G., Benjamin, W.H., Orenstein, J.M., and Smith, P.D. (2005). Human intestinal macrophages display profound inflammatory anergy despite avid phagocytic and bacteriocidal activity. *J. Clin. Invest.* 115, 66–75.

Sun CM, Hall JA, Blank RB, Bouladoux N, Oukka M, Mora JR, Belkaid Y. Small intestine lamina propria dendritic cells promote de novo generation of Foxp3 T reg cells via retinoic acid. *J Exp Med.* 2007 Aug 6;204(8):1775-85.

Swirski, F.K., Nahrendorf, M., Etzrodt, M., Wildgruber, M., Cortez-Retamozo, V., Panizzi, P., Figueiredo, J.L., Kohler, R.H., Chudnovskiy, A., Waterman, P., et al. (2009). Identification of splenic reservoir monocytes and their deployment to inflammatory sites. *Science* 325, 612-616.

Takeda, K, et al. Enhanced Th1 Activity and Development of Chronic Enterocolitis in Mice Devoid of Stat3 in Macrophages and Neutrophils. *Immunity*, 1999; Vol. 10, 39–49. Franke, A.

Thompson-Snipes, L. et al. Interleukin 10: a novel stimulatory factor for mast cells and their progenitors. *J Exp Med* 1991;173:507–510.

Travassos, L.H., Girardin, S.E., Philpott, D.J., Blanot, D., Nahori, M.A., Werts, C., and Boneca, I.G. (2004). Toll-like receptor 2-dependent bacterial sensing does not occur via peptidoglycan recognition. *EMBO Rep.* 5, 1000–1006.

Van der Flier, L. G. & Clevers, H. Stem Cells, Self-Renewal, and Differentiation in the Intestinal Epithelium. *Annu. Rev. Physiol.* 71, 241–260 (2009).

Varol, C., Landsman, L., Fogg, D.K., Greenshtein, L., Gildor, B., Margalit, R., Kalchenko, V., Geissmann, F., and Jung, S. (2007). Monocytes give rise to mucosal, but not splenic, conventional dendritic cells. *J Exp Med* 204, 171-180.

Varol, C., Vallon-Eberhard, A., Elinav, E., Aychek, T., Shapira, Y., Luche, H., Fehling, H.J., Hardt, W.D., Shakhar, G., and Jung, S. (2009). Intestinal lamina propria dendritic cell subsets have different origin and functions. *Immunity* 31, 502-512.

Varol, C., Zigmund, E., and Jung, S. (2010). Securing the immune tightrope: mononuclear phagocytes in the intestinal lamina propria. *Nat Rev Immunol* 10, 415-426.

Waddell, A., Ahrens, R., Steinbrecher, K., Donovan, B., Rothenberg, M.E., Munitz, A., and Hogan, S.P. (2011). Colonic eosinophilic inflammation in experimental colitis is mediated by Ly6C(high) CCR2(+) inflammatory monocyte/macrophage-derived CCL11. *J Immunol* 186, 5993-6003.

Watanabe, N. et al. Elimination of local macrophages in intestine prevents chronic colitis in interleukin-10-deficient mice. *Dig. Dis. Sci.* 48, 408–414 (2003).

Weber, B., Saurer, L., Schenk, M., Dickgreber, N., and Mueller, C. (2011). CX3CR1 defines functionally distinct intestinal mononuclear phagocyte subsets which maintain their respective functions during homeostatic and inflammatory conditions. *Eur J Immunol* 41, 773-779.

White AC, Levy JA, McGrath CM. Site-selective growth of a hormone-responsive human breast carcinoma in athymic mice. *Cancer Res.* 1982 Mar;42(3):906-12.

Worbs, T., Bode, U., Yan, S., Hoffmann, M.W., Hintzen, G., Bernhardt, G., Forster, R., and Pabst, O. (2006). Oral tolerance originates in the intestinal immune system and relies on antigen carriage by dendritic cells. *J Exp Med* 203, 519-527.

Yona, S. et al. Fate Mapping Reveals Origins and Dynamics of Monocytes and Tissue Macrophages under Homeostasis. *Immunity* 38, 79–91 (2013).

Zigmond, E., Halpern, Z., Elinav, E., Brazowski, E., Jung, S., and Varol, C. (2011). Utilization of murine colonoscopy for orthotopic implantation of colorectal cancer. *PLoS One* 6, e28858.

Zigmond E, Varol C, Farache J, Elmaliyah E, Satpathy AT, Friedlander G, Mack M, Shpigel N, Boneca IG, Murphy KM, Shakhar G, Halpern Z, Jung S. (2012). Ly6C hi monocytes in the inflamed colon give rise to proinflammatory effector cells and migratory antigen-presenting cells. *Immunity* 14;37(6):1076-90.

List of Publications during PhD studies

Kim KW, Vallon-Eberhard A, **Zigmond E**, Farache J, Shezen E, Shakhar G, Ludwig A, Lira SA, Jung S.

In vivo structure/function and expression analysis of the CX3C chemokine fractalkine.

Blood. 2011 Nov 24;118(22):e156-67.

Zigmond E, Halpern Z, Elinav E, Brazowski E, Jung S, Varol C.

Utilization of murine colonoscopy for orthotopic implantation of colorectal cancer.

PLoS One. 2011;6(12)

Zigmond E*, Varol C*, Farache J, Elmaliah E, Satpathy AT, Friedlander G, Mack M, Shpigel N, Boneca IG, Murphy KM, Shakhar G, Halpern Z, Jung S.

Ly6C hi monocytes in the inflamed colon give rise to proinflammatory effector cells and migratory antigen-presenting cells.

Immunity. 2012 Dec 14;37(6):1076-90.

*equal contribution

Farache J, Koren I, Milo I, Gurevich I, Kim KW, **Zigmond E**, Furtado GC, Lira SA, Shakhar G.

Luminal Bacteria Recruit CD103(+) Dendritic Cells into the Intestinal Epithelium to Sample Bacterial Antigens for Presentation.

Immunity. 2013 Mar 21;38(3):581-95.

Zigmond E, Bernshtein B, Friedlander G, Walker C, Yona S, Brenner O, Varol C, Krauthgamer R, Jack RS, Muller, Jung S.

Macrophage restricted IL-10 receptor -, but not IL-10 deficiency causes severe spontaneous colitis.

Submitted

Reviews:

Varol C, **Zigmond E**, Jung S.

Securing the immune tightrope: mononuclear phagocytes in the intestinal lamina propria.

Nat Rev Immunol. 2010 Jun;10(6):415-26.

Bar-On L, **Zigmond E**, Jung S.

Management of gut inflammation through the manipulation of intestinal dendritic cells and macrophages?

Semin Immunol. 2011 Feb;23(1):58-64.

Farache J, **Zigmond E**, Shakhar G, Jung S.

Contributions of dendritic cells and macrophages to intestinal homeostasis and immune defense.

Immunol Cell Biol. 2013 Mar;91(3):232-9

Zigmond E, Jung S.

Intestinal macrophages: well educated exceptions from the rule.

Trends Immunol. 2013 Mar 8.

Student declaration

I declare that the thesis summarizes my independent research.

The studies presented in chapter two were performed in collaboration with Dr. Chen Varol, Tel Aviv medical center.

I led all the studies reported in this thesis.

I designed and performed the experiments, summarized the data and wrote the manuscripts.

Acknowledgements

I would like to thank my mentor, Prof. Steffen Jung for accepting me to his lab and showing me the trail to perform basic science in the highest quality there is.

Thank you for sharing your knowledge and exposing me to the amazing immunological field of the mononuclear phagocytes system. Thank you for teaching me how to ask a scientific question and design a plan in order to answer it, how to present data in a clear way and how to conduct yourself in the competitive field of biological science and still to adhere to the highest scientific standards being your own greatest criticizer. I am truly grateful for all of that.

I would like to thank Dr. Chen Varol for being a great collaborator and a friend. Thank you for all the pioneering and brave ideas and for the long nights we have spent together in the lab.

I would like to thank Biana Bernshtein for working with me in the last year of my PhD studies. It was a great pleasure working with you. Your input was crucial to our success.

I would like to thank the members of the Jung laboratory for discussion and for the great atmosphere and friendship.

Finally I would like to thank my family, my wife Maora and our beautiful daughters Mika, Yuli and Gili for the great support, the understanding, the help in difficult times and for your unconditional love.